

Reference

NBS  
PUBLICATIONS



**NBSIR 85-3159**

# **Fire Growth in Combat Ships**

J. G. Quintiere  
H. R. Baum  
J. R. Lawson

U.S. DEPARTMENT OF COMMERCE  
National Bureau of Standards  
National Engineering Laboratory  
Center for Fire Research  
Gaithersburg, MD 20899

June 1985

Supported in part by:

U.S. David Taylor Naval Ship  
Research and Development Center  
Bethesda, DC

QC  
100  
.U56  
85-3159  
1985



NBS REF  
QC  
100  
456  
85-3159  
1985  
C.1

NBSIR 85-3159

**FIRE GROWTH IN COMBAT SHIPS**

J. G. Quintiere  
H. R. Baum  
J. R. Lawson

U.S. DEPARTMENT OF COMMERCE  
National Bureau of Standards  
National Engineering Laboratory  
Center for Fire Research  
Gaithersburg, MD 20899

June 1985

Supported in part by:  
U.S. David Taylor Naval Ship  
Research and Development Center  
Washington, DC



---

U.S. DEPARTMENT OF COMMERCE, Malcolm Baldrige, *Secretary*  
NATIONAL BUREAU OF STANDARDS, Ernest Ambler, *Director*



TABLE OF CONTENTS

|  | <u>Page</u> |
|--|-------------|
| List of Figures .....  | iv          |
| Abstract .....   | 1           |
| Introduction .....   | 1           |
| Motivation .....   | 1           |
| Objectives .....   | 2           |
| Approach .....   | 2           |
| Background .....   | 3           |
| Review of Literature .....                                   | 3           |
| Phenomenology of Fire Growth .....                           | 9           |
| Ignition Event .....   | 9           |
| Post Blast and Ignition .....                                | 14          |
| Non-Blast Related Fire Growth .....                          | 14          |
| Approaching a Deterministic Ship Fire Growth Model.....      | 20          |
| Fire Damage Model (FDM)/Ship Vulnerability Model (SVM) ..... | 20          |
| Recommendations .....  | 21          |
| Acknowledgements .....                                       | 24          |
| References .....   | 24          |
| Appendix A - Post-Explosion Venting Analysis .....           | 27          |
| Appendix B - Slide-Rule Estimates of Fire Growth .....       | 44          |

LIST OF FIGURES

|   | <u>Page</u> |
|---|-------------|
| Figure 1. Illustration of ventilation effects influencing engine room fire fighting .....   | 4           |
| Figure 2. Basic distinction between ship (a) and building (b) fires .....   | 5           |
| Figure 3. Temperatures in a particular ship compartment for different fire loads $q_0$ [9] .....  | 7           |
| Figure 4. Plausible projectile ignition scenarios: (a) small (b) large (c) most likely .....  | 10          |
| Figure 5. Opposed flow flame spread onto a porous medium .....  | 12          |
| Figure 6. Exponential fire growth in a multi-compartmented structure [20] .....   | 13          |
| Figure 7. Compartment mass loss rate (R) dependence on fuel type and compartment where $A_F$ is fuel area, $A_w$ is window area, and H is its height [24] ..... | 18          |
| Figure A1. Simplified Compartment Venting Model .....   | 35          |
| Figure A2. $\theta, \phi$ vs. $\tau$ for various $\gamma$ , 60.0 m <sup>3</sup> volume, 10.0 m <sup>2</sup> vent area, and 15.0 kg of TNT .....                 | 36          |
| Figure A3. $\theta, \phi$ vs. $\tau$ for various $\gamma$ , 60.0 m <sup>3</sup> volume, 0.1 m <sup>2</sup> vent area, and 15.0 kg of TNT .....                  | 37          |
| Figure A4. $\theta, \phi$ vs. $\tau$ for various $\gamma$ , 60.0 m <sup>3</sup> volume, 1.0 m <sup>2</sup> vent area, and 15.0 kg of TNT .....                  | 38          |
| Figure A5. $\theta, \phi$ vs. $\tau$ for various $\gamma$ , 20.0 m <sup>3</sup> volume, 1.0 m <sup>2</sup> vent area, and 15.0 kg of TNT .....                  | 39          |
| Figure A6. $\theta, \phi$ vs. $\tau$ for various $\gamma$ , 100.0 m <sup>3</sup> volume, 1.0 m <sup>2</sup> vent area, and 15.0 kg of TNT .....                 | 40          |
| Figure A7. $\theta, \phi$ vs. $\tau$ for various $\gamma$ , 200.0 m <sup>3</sup> volume, 1.0 m <sup>2</sup> vent area, and 15.0 kg of TNT .....                 | 41          |
| Figure A8. $\theta, \phi$ vs. $\tau$ for various $\gamma$ , 200.0 m <sup>3</sup> volume, 1.0 m <sup>2</sup> vent area, and 50.0 kg of TNT .....                 | 42          |
| Figure A9. $\theta, \phi$ vs. $\tau$ for various $\gamma$ , 200.0 m <sup>3</sup> volume, 1.0 m <sup>2</sup> vent area, and 100.0 kg of TNT .....                | 43          |

|             |   |    |
|-------------|---|----|
| Figure B1.  | Sketch of a wood crib.....  | 46 |
| Figure B2.  | Reduced specific burning rate as a function of the crib porosity for ponderosa pine wood cribs (taken from Heskestad) [2] ..... | 47 |
| Figure B3.  | Rate of mass loss plot for easy chair [3] .....   | 48 |
| Figure B4.  | Rate of mass loss plot for sofa with "California" foam cushions [3] .....   | 48 |
| Figure B5.  | Weight loss for cotton and mixed fiber core specimens [4]...  | 49 |
| Figure B6.  | Fire radiant heat transfer to a target .....  | 51 |
| Figure B7.  | Flame height dependence on heat release parameters [9] .....  | 52 |
| Figure B8a. | For open flames.....  | 53 |
| Figure B8b. | Corner fire scenario .....  | 53 |
| Figure B9.  | Flame length and geometric environment .....  | 54 |
| Figure B10. | Room smoke filling model .....  | 56 |
| Figure B11. | Ceiling layer height versus time and heat input rate [12] ..  | 56 |
| Figure B12. | Compartment example .....   | 59 |
| Figure B13. | Sketch of compartment ventilation problem .....   | 61 |
| Figure B14. | Corridor smoke transport .....  | 64 |
| Figure B15. | Smoke filling by a fire room to a closed adjacent space ....  | 65 |
| Figure B16. | Dimensionless corridor smoke filling time [23] .....  | 66 |
| Figure B17. | Visibility results derived from Rasbash [27], Jin [28] and Lopez [29] .....   | 68 |
| Figure B18. | Smoke production for plywood as a function of ventilation factor from Saito [31] .....  | 70 |
| Figure B19. | Sketch of flame spread model .....  | 71 |
| Figure B20. | Schematic of the flame spreading rate as a function of the liquid temperature of the fuel [33] .....                            | 73 |

|            |   |    |
|------------|---|----|
| Figure E1. | Room Fire Example.....  | 78 |
| Figure E2. | Mass Loss Rate for Fire Growth Example.....                               | 87 |
| Figure E3. | Heat Flux Predictions in Room for Fire Growth<br>Example.....             | 88 |
| Figure E4. | Flame Height and Extension Across Ceiling for Fire<br>Growth Example..... | 89 |
| Figure E5. | Room Temperature Rise for Fire Growth Example.....                        | 90 |
| Figure E6. | Mass Flow Rate into the Room for Fire Growth<br>Example.....              | 91 |
| Figure E7. | Visibility in Corridor for Fire Growth Example.....                       | 92 |

# FIRE GROWTH IN COMBAT SHIPS

by

J. Quintiere, H. Baum and R. Lawson

## Abstract

A discussion of fire phenomenology pertaining to ships is presented. It draws on background from ship fires, combat ship construction characteristics and scientific knowledge developed for building fires.

Its immediate goal is to assess the prospect of developing a deterministic (physics) model for ship fire growth as initiated by explosive weapon effects. A specific analysis of vented explosion flows is given as well as a procedure for computing fire growth phenomena from formulae.

These analyses are presented as stand-alone reports in Appendices A and B, respectively. The main body of the report concludes with a series of specific recommendations for achieving sound methods of predicting fire hazard conditions in combat ships.

Key words: Explosions; fire damage; fire growth; fire models; room fires; shipboard fires.

## Introduction

MOTIVATION. The study was undertaken to help provide and develop an improved analytical framework for fire growth in Navy combat ships. A specific issue was to address the Fire Damage Model (FDM) of the Ship Vulnerability Model (SVM) developed by Hackett and others at the David Taylor Naval Ship Research and Development Center (DTNSRDC) [1]. This model is essentially a probabilistic analysis of the blast and fire consequences of a missile penetration and explosion within a ship. The intention was to examine the prospect of introducing a deterministic basis for some aspects of the FDM. Realizing, of course, that some features of fire growth - ignition location, initial geometry and configuration - are somewhat random and lend themselves to a statistical description. Yet other aspects of fire growth - flame spread, burn rate, smoke transport - are in principle describable by the laws of physics and chemistry. What is currently known and feasible regarding a full probabilistic-deterministic description and prediction of fire growth is the issue.

Over the last 15 years the growth of knowledge for fire predictions has increased enormously. Although key issues of research still remain to be solved, some headway can be made in quantitative predictions. For example, the prediction of the interaction of a burning object and the compartment it is contained in has led to estimations of fire growth (spread and burn rates) and flashover (an event which marks the transition to full-fire involvement of a compartment's contents). Two recent reviews on this work describe the nature of these models and form a basis for inferring other applications [2,3]. Although a first attempt has been made to extend these single room models to predict fire growth in a multi-story, multi-compartment building, no firm basis currently exists to assess its accuracy or completeness [4].

Moreover the prediction of the fire response and involvement of specific materials still is clouded in empirical testing and the lack of complete scientific knowledge. Nevertheless it should still be fruitful to visit this state of knowledge in the context of potential improvements to the SVM/FDM. Indeed, since much of the progress in applications of fire science to fire safety have been motivated and studied in a building structure environment, it would be useful to examine them in a potential shipboard fire environment.

OBJECTIVES. Thus, based on the current state of fire research and knowledge, we sought to examine the SVM/FDM with the intention of improving its predictive fire growth capability. To the extent that its algorithms and structure were clearly documented, we sought to assess the physics of fire growth it currently uses; to identify areas in which its decision points could be enhanced by algorithms based on physics as an alternative to decisions based on statistics or rational guesses; and to identify important fire phenomena that were not considered at all. Based on the level of effort extended to this task, and on the lack of knowledge in predicting fire growth through structures, only a basis and logical framework could result for improving the predictive capability of the SVM/FDM. Nevertheless the process of such an assessment would be expected to address the feasibility and potential of deterministic modeling for ship fires.

Consequently, attempts to improve the SVM/FDM would lead to uncovering of a broader set of issues related to ship fires. Thus a second objective was to lay out these significant issues and needs associated with the general understanding of ship fires. Indeed the pursuit of this understanding cannot be decoupled from improvements for the SVM/FDM since both goals are mutually connected. Incidentally, suppression of fire, the inverse of growth, has not been explicitly stated here nor addressed. It suffers from a more meager knowledge base than fire growth. Thus it is difficult to intelligently address it in predictive terms. As a result we will preclude any indepth discussion of it except to appropriately raise its general needs in this report.

APPROACH. Coming from a background of research motivated by building fires, and being less familiar with marine problems, we sought to improve our perspective on ships and their fire characteristics. Two moderate size combat ships were visited -- the USS Glover at Norfolk, VA and another vessel, open to the general public, at Alexandria, VA. These helped to acquaint us with a ship's environment, its interior geometry, primary structural characteristics, materials of construction, and its distinction from a building structure. Secondly, we visited the Naval Safety Center at Norfolk, VA to gain an orientation of the types of fires and their frequency of occurrence on ships.

Another source of background information was books on the general topic of ship fires, laboratory reports on specific aspects of ship fire problems, and numerous discussions with U.S. Navy staff who were very helpful in improving our understanding of fires in ships.

In addressing the primary issue of improvements for the SVM/FDM, reliance was placed on several discussions and notes for describing the probabilistic fire damage model [5]. It was not our intention to learn every facet of the model, but to gain a solid appreciation for its computer requirements, its current fire growth logic, and the level of modeling sophistication and detail it

could cope with and still operate effectively in the SVM code. Trade-offs would be necessary to avoid computer intolerable fire physics demands at the cost of its probabilistic computational needs, to distinguish between physics at a level that would fit the current structure of the computer code. Yet it would not be our objective to write a fire physics code for the SVM/FDM, only to establish a pathway to accomplishing this goal.

Subsequent to our orientation of ships and the SVM/FDM we set to develop the following results in this report:

- (1) describe plausible shipboard fire phenomenologies,
- (2) solve the problem of a vented explosion in a compartment for the resultant flow and temperature fields,
- (3) provide a set of algebraic formulae for estimating aspects of generic fire growth in structures, and
- (4) provide a plan for needed research to better understand ship fires.

Each of these items will be documented herein, and their relationship to the objective of this task will become more apparent in subsequent elaborations. Moreover our thoughts and ideas provoked by our background education on ship fires will be presented.

### Background

REVIEW OF LITERATURE. Our review of the literature was not meant to be exhaustive, but comprehensive. It sought to capture a knowledge of ship fires and to gain an appreciation of the types of fire problems which have been addressed in research studies. We purport to make no assessment or criticism of current shipboard fire protection codes and practices. These, of course, are relevant to our goal of understanding and predicting fire behavior; but lacking that full capability, society must defer to the judgement and wisdom embodied in the current codes and regulations. A good description of the history and current state of marine fire protection has been presented by Kerlin [6]. It addresses structural fire protection and suppression methods. It closes with a profound comment: "In as much as it is very difficult to relate small tests to what will occur on actual vessels, the Coast Guard established the Fire and Safety Test Detachment in Mobile, AL in 1969" [6]. The need to validate and establish the relevant foundation for small scale fire tests, as well as theoretical predictive models, is a facet of sound fire protection and research that will not diminish in the near future.

Whereas Kerlin's article [6] gives a capsule view of ship fire protection, two books on the subject give a much broader view. Both have particular distinction, and some inferences will be made for each. The first entitled, Fire Aboard [7] by F. Rushbrook, an Edinburgh fire officer (who I am told was a strong advocate for the Fire Science master's degree program at Edinburgh University [8]) addresses a chronical of ship fire disasters, British legislation on fire protection, practices of protection and fire fighting on ships, and a long list of recommendations. The second book is a two volume Soviet text, Fire Fighting Aboard Ships [9], that is somewhat similar in scope to the

first text, but includes a unique attempt at describing a predictive methodology. Although this attempt might be construed by some to be incomplete and perhaps limited in applicability, its value is its example of an engineering design format for addressing fire safety issues in ships. We shall elaborate further on these two books, giving anecdotal reports from both to illustrate their nature.

Anyone interested in fire fighting and ships will find Rushbrook's book fascinating. The drama and lessons learned from shipboard fire disasters is well told. Figure 1, taken from the book [7], illustrates an effective fire-fighting tactic for engine room fires. The tactic involves entering the shaft tunnel (the horizontal tunnel housing the drive shaft) to the engine room and attacking the fire with water hoses such that air flow will have been induced to flow along the tunnel and up through the engine room to the deck skylight above. In contrast the upper plate in Figure 1 shows what would happen if that skylight were closed and the shaft tunnel door to the engine room were opened. He more fully describes the details to accomplish this task safely, recommends the placement of a fire hydrant in the shaft tunnel, and cites the loss of two ships in which insufficient attention was placed on (natural) ventilation control during fire fighting.

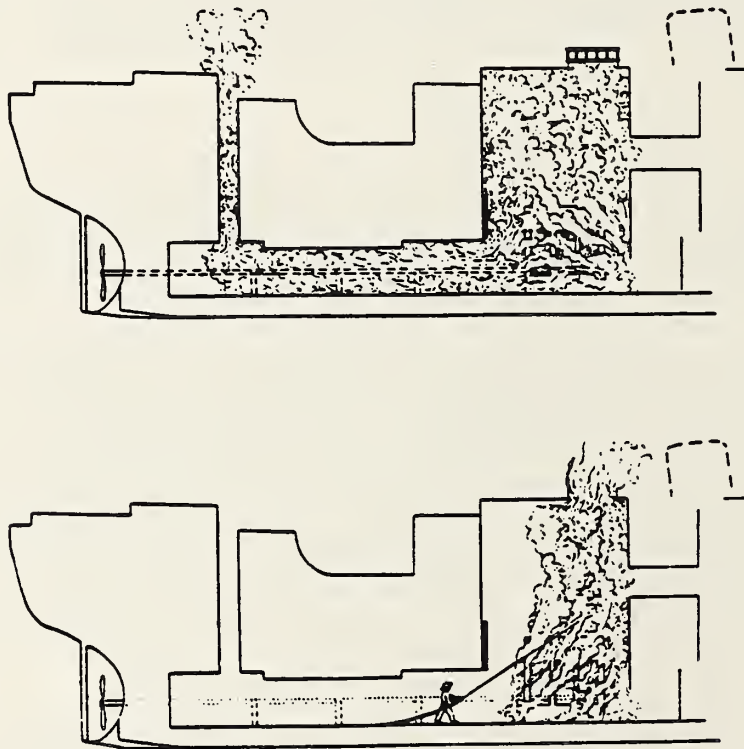


Figure 1. Illustration of ventilation effects influencing engine room fire fighting.

This example of ventilation effects during fire fighting has wider implication to ship fires. A ship is divided vertically into compartmented sections with interconnected horizontal "floors". The only openings, excepting possibly

thick glass portholes, to the outside atmosphere are at the exterior deck levels. Thus at the occurrence of a fire, the hot gases expand and are transported by buoyancy (forced ventilation, while influential, is usually eliminated by shutting down the ventilation system to minimize the spread of smoke), and ambient air is induced toward the fire. As a vertical section of the ship, bounded by hull to deck water-tight bulkheads, fills with smoke, the availability of new ambient air becomes only possible through open deck hatches. Consequently the combustion products and air must both pass through the deck hatches. A similar but different effect occurs in building fires in which the openings to the ambient are typically the windows. But in that case the flow is stratified and the air and combustion products are transported without mixing at the opening (Figure 2). Nevertheless in both cases the growth of the fire beyond a critical early size will be thereafter controlled by the available air flow supply rate to the burning-pyrolyzing fuel region. Simply put: the fire is hot and large enough to produce sufficient fuel vapors so that the air that reaches it all reacts; the resultant chemical energy release rate heats more liquid and solid fuels to volatiles which then react with the air supplied. Hence the air supply rate ultimately governs the burning and volatilization rate.

Indeed, very little study has been made of the burning of fuels in a compartment with only a top opening (the ship case) in contrast to a compartment with a side opening (the building case). An example of the former case was studied by Porter [10] for methanol burning in a 3.64 in. I.D. cylindrical pipe. The burning was oscillatory and the fuel pyrolysis rate was 2 to 8 times that reported for open tank burning conditions. It is obvious to us that the importance of this problem is extremely significant to ship fire behavior, but the current level of research is insufficient to allow suitable extrapolation to real ships. Issues of generality, scale, mechanisms of mixing and burning remain. Nevertheless this small scale study [10] and the few others that exist provide a foundation to develop that understanding into terms comparable to the knowledge known for building fires.

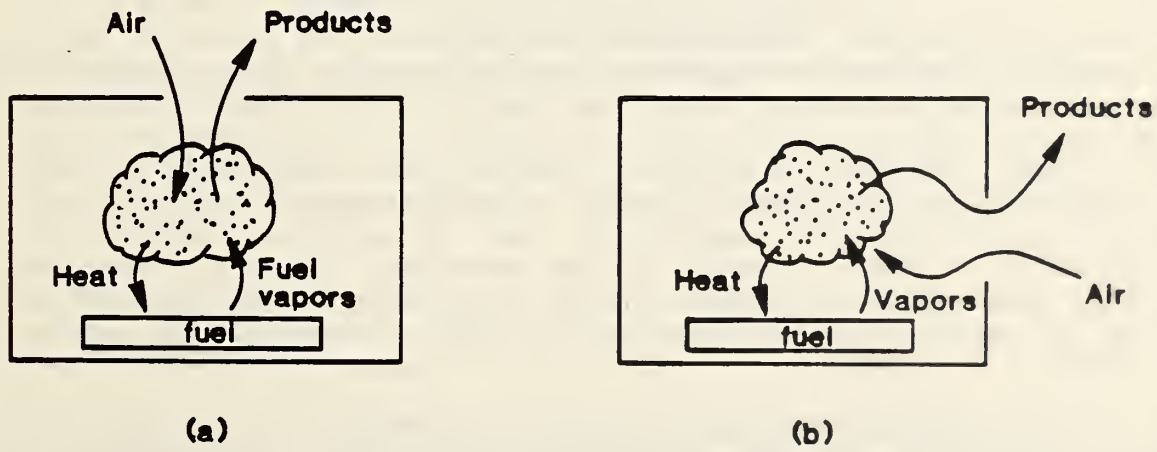


Figure 2. Basic distinction between ship (a) and building (b) fires.

Two other points from Rushbrook [7] should be made. The use of sprinklers on ships can be traced back to a patent specification by John Browne in 1853, but not until 1914 did the Hamburg-Amerika line introduce the automatic sprinkler system into two of its liners [7, pp. 309,310]. While proving their value, it is cited that the Yarmouth Castle fire in 1965 grew because of the inadequacy of its sprinkler system to respond soon enough or effectively to fire in concealed spaces [9, p. 87].

The second point from Rushbrook relates to combustible materials, their use and their evaluation for fire risk. He states with regard to the use of fire resistant materials as barriers to heat conduction and degradation threatened by fire heated steel bulkheads: "Several of the polyurethane rigid foams..... as insulating lining in place of cork, glass wool or similar materials in ship's holds are of great interest to firemen," [9, p. 344]. He goes on to discuss the foam's merits: foamed in place, unaffected by welding, light weight, low flammability rating possible by British Standards B.S.S. 476/1932; but implies the foam should be covered by a "fire-resisting" board. History has demonstrated that such low density foams, as a primary consequence of their density (which roughly correlates with the thermal conductivity for nonconductors), are good thermal insulators and fire barriers; however, this same property allows them to have a rapid surface temperature rise when exposed to heat. Consequently rapid ignition and flame spread rates are possible for these foams and have occurred with dramatic consequences in fires. The message here is that the wisdom embodied in standard flammability tests cannot always respond to the characteristics of newly developed materials. Hence fire safety practitioners must always be vigilant, striving to improve the merits and relevance of test methods.

The significant points from the Soviet book [9] are its character and substance. It truly is an engineering oriented text on the subject. Its first volume traces ship fire and fire fighting experiences, and then addresses test procedures and engineering analyses for addressing the fire risk of materials and construction. Although one may not agree with its standard tests of choice, it is impressive to realize the manner in which they describe their application to engineering methodology. Of course, country and international codes still appear to dominate design practices for ship fire safety. Yet they do provide an engineering approach which..."reflect the requirements of the 1974 International Convention on Life Safety at Sea."... "The 1974 Safety Convention regulations contain detailed fire safety regulations, and the correct and efficient application of these should begin at the design and construction stages." [9, pp. xiii, 251]. A valuable reference guide is their tabulation of physical, chemical, and flammability properties for shipboard materials. These include: density, specific heat, thermal conductivity, decomposition temperatures, heat of combustion, combustibility by calorimetry and surface spread of flame measures. The value is not their particular data set, but the demonstration that rational, useful, relevant data can be assembled for assessing the fire risk of materials and construction designs.

Some anecdotal glimpses of their text will be presented. On material response, they observe that accommodation fires may reach temperatures of 700-900°C whereas fuels involving liquid fuels may reach 1100°C; aluminum melts at 650°C, and brass and copper are destroyed above 900°C. On heat exchange in ship compartment fires, they develop a set of descriptive equa-

tions and relate that model to ship compartment fire experiments [9, ch. 6]. Their experimental results for compartment temperature of typical ship accommodation cabin (8 m<sup>2</sup> floor area, 1.75 x 0.65 m door opening) with various types and levels of fire load  $q_0$ . Here  $q_0$  is defined as the sum of material chemical energy content per unit exposed surface area for linings, or per unit floor for furniture (e.g. Mcal/m<sup>2</sup>). Typical results are shown in Figure 3. They show that the fire load primarily controls the duration of the fire, and in a lesser and envelopic sense affects the temperature level. This is a consequence of ventilation limited fires. The air flow rate through the door opening governs the rate of compartment energy release, and the resulting heat loss rate produces the temperature at each time.

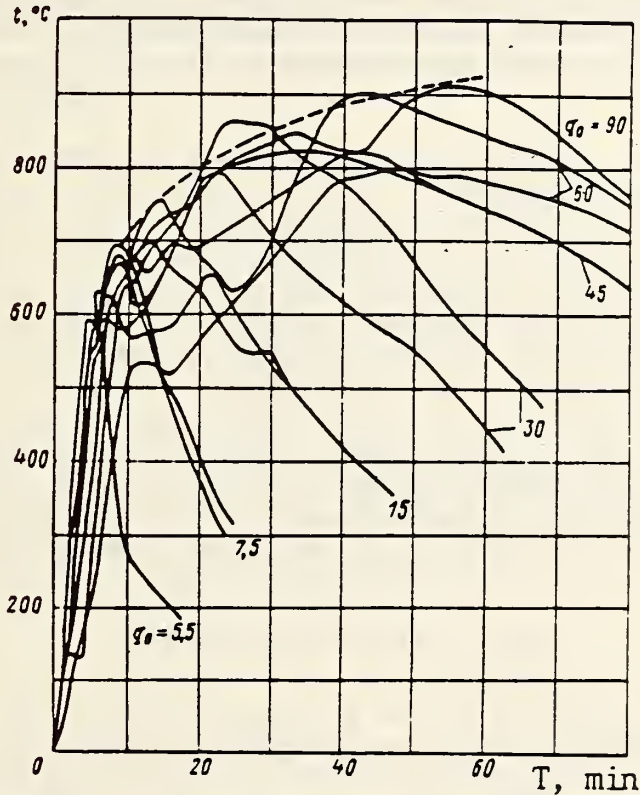


Figure 3. Temperatures in a particular ship compartment for different fire loads  $q_0$  [9].

Although they correlate these results into empirical and potentially useful formulae:

$$\text{active burning time, } t_a = 0.67 q_0 + 2 \text{ (min),} \quad (1)$$

and

$$\text{maximum fire temperature, } t_{\max} = 504 (0.67 q_0 + 2)^{0.148} (\text{°C}) \quad (2)$$

They do not fully account for variations in the compartment opening size, compartment function, and materials of construction. But these can be developed from more complete ship fire experimental analyses, and from extrapolating using current mathematical fire models.

On the subject of fire growth from a compartment along an adjoining corridor, they actually inferred a critical compartment temperature (480°C) below which spread was not possible. The general applicability and limitations of this result of course can be questioned but it is a plausible one. They did try to extend these ideas to spread from compartment to compartment based on experimental results; however, the effect of available air supply (natural ventilation) was clearly obvious to them thereby complicating their conclusions.

Another useful source of understanding the nature of ship fires is the fire incident records reported by the U.S. Naval Safety Center. Their case studies and statistics given in their "Survey" reports are enlightening. These are essentially peacetime records and do not address the ignition scenario of the SVM/FDM. Nevertheless they can be used to establish potential risk levels and priorities for problem solving and research. Some statistics from Survey 4 [11], reflecting reported Navy ship fires between 1973 and June 1980, are summarized as follows:

Compartment Occurrences (greater than 50): Storeroom (86),  
Engineering (70), Quarters (67)

Occurrence by Class:

|                                  |       |
|----------------------------------|-------|
| A (ordinary, solid combustibles) | - 479 |
| B (liquid fuels)                 | - 218 |
| C (electrical equipment)         | - 352 |
| D (metals)                       | - 2   |

Total Cost of Destruction: \$163,599,985

Total Injuries: 266

Total Fatalities: 24

Total Lost Operating Days: 2135

The days lost imply the loss in service of at least one U.S. Navy ship per year!

One might speculate on the value of simulated fire studies of storerooms, enginerooms, quarters (etc.) with their associated fuel loadings and natural ventilation conditions (opening sizes and locations). The results of which might then be correlated as illustrated by Equations (1) and (2). Thus an engineering basis could be established for the fire severity of typical and "most flammable" compartments.

Indicative of attempts to apply technical data and analytic tools to Navy fire problems can be noted from several reports. Benjamin and Gross [12] in 1970 selected shipboard materials based on their relevance to fire hazard potential, and subjected them to three tests: ASTM E-162 spread of flame, potential heat, NFPA 259 (the difference in heats of combustion between the original sample and the remaining sample residue after subjected to 750°C furnace heating for 2 hours), and the Smoke Density Chamber Test (currently ASTM 662-79). Thus they sought to characterize flame spread, energy release and smoke production. The measure of risk derived from these data was based

on criteria levels set by judgment. Later Lee, et al. [13,14] did a similar study of materials, but attempted to include a limited analysis on how to use some of the test data. They also pioneered an alternative approach to predicting compartment fire growth by using scale models. Although the scaling was not complete similitude due to the large number of dimensionless groups needing to be satisfied, they found a remarkable level of success. Found also in reference [13] and other uncited sources are fire load survey results in terms of mass of fuel per (usually floor) area, or its corresponding potential heat per unit area - this latter quantity can be regarded as the fire load  $q_0$  [9]. But in reference [9] the fire severity, after build-up, yields peak temperature variations of 600 to 900°C, while the fire duration is directly proportional to  $q_0$ . Moreover, after full involvement compartment temperatures are more dependent on ventilation than on fuel type or mass (e.g. [9]), while fire duration depends on both ventilation and fuel mass. Our fire growth formulas to be discussed later will more fully recognize these variables.

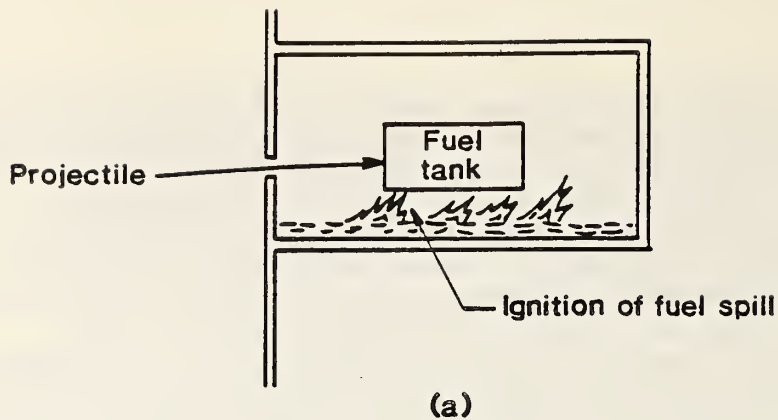
In short, test data, whether it be qualitative rankings or specific physico-chemical properties, cannot alone be used to express the fire hazard of materials in practice. Nor can mathematical models completely address arbitrary fire problems. The state of knowledge is advancing, however, and new test method concepts are providing more meaningful data for engineering analyses [15,16,17]. Only by attacking critical fire problems will progress be made (e.g. the post crash aircraft cabin fire problem, [18]).

Finally, our ship visits triggered thoughts on plausible fire scenarios and relevant fire phenomenology to ships. These will be discussed in the next section. Our observations must, however, be complemented by more scrutiny of the Navy fire data and experts more experienced in the scope of ship fires. We will only address areas in which we could relate our knowledge of and experience gained in the study of building fires.

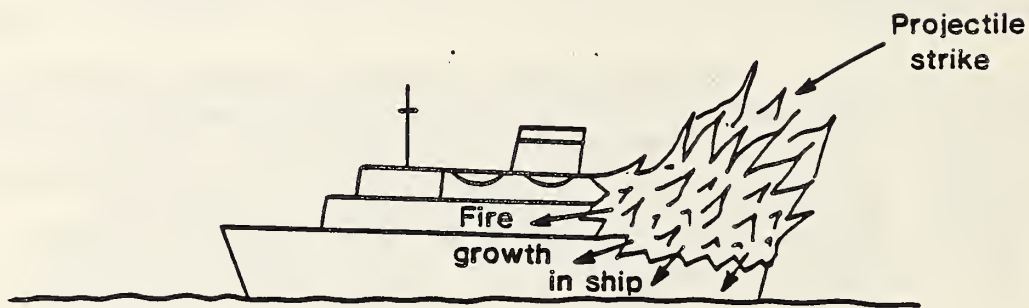
### Phenomenology of Fire Growth

IGNITION EVENT. The particular scenario we are focusing on is that fire growth initiated by a explosive projectile strike to a ship above its water line. We conceptualize this as a projectile penetrating the steel hull, entering a compartment(s), detonating, possibly destroying some structural portion of the ship, and possibly initiating a fire. The strength of the explosive charge and the location of the strike will determine the blast (pressure) and ignition (thermal/fuel) consequences. The scale of these effects will also determine the nature of the fire growth and the outcome of the SVM. These possibilities are illustrated in Figure 4 which shows the limiting cases of (a) small and (b) large effects while (c) depicts the more likely scenario of interest.

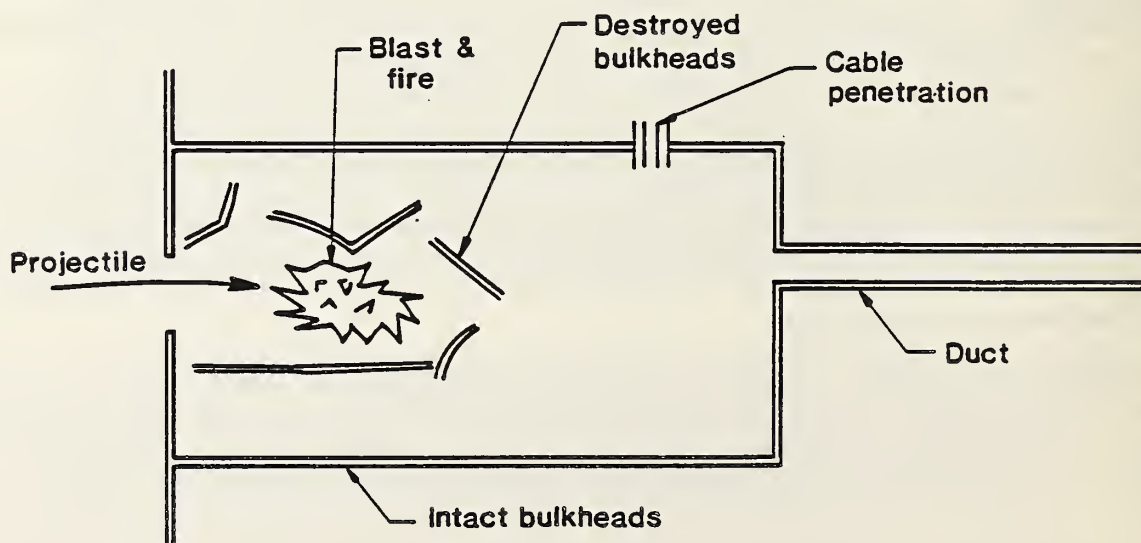
Let us elaborate somewhat on these ignition scenarios. We shall try to present an analytical framework for governing their behavior, but these models should be viewed as qualitative not quantitative. Indeed, it will take more analysis and experimental investigation to develop sound predictive models.



(a)



(b)



(c)

Figure 4. Plausible projectile ignition scenarios: (a) small (b) large (c) most likely.

In case (a) a small projectile is considered to cause a fuel leak which then ignites and fire spreads over the spill. The only essential opening for the compartment is the hole made by the projectile. Therefore the mechanism for fire spread to surrounding compartments is defined to be heat conduction through the enclosure surfaces to cause ignition of objects in contact with these surfaces in the adjoining compartments. Let us consider this to occur at a critical (ignition) temperature  $T_{ig}$ . The critical times are the time to deplete (or reduce to a level of fire extinction) the oxygen in the enclosure and the time for the bounding surfaces to reach  $T_{ig}$ . Let us assume that the spill area is known ( $A_v$ ) and that the evaporation rate of the liquid fuel per unit area can be measured or estimated ( $\dot{m}_v$ ). Then the mass of fuel burned must be in stoichiometric proportion ( $\gamma$ , fuel-oxygen ratio) with the mass of oxygen available. The time to deplete all the oxygen,  $t_o$ , is given by

$$\int_0^{t_o} \dot{m}_v A_v dt = \gamma \cdot (0.233) \rho_\infty V \quad (3)$$

where  $\rho_\infty$  is the initial air density and  $V$  is the volume of the chamber.

The time to heat the metal compartment surfaces to  $T_{ig}$  is found as follows:

- (1) Assume a uniform distribution of heat to the bounding surfaces,  $\dot{q}'' = \dot{m}_v A_v \Delta H/A$  where  $\Delta H$  is the fuel's heat of combustion, and  $A$  is the surface area.
- (2) Assume the heated bounding surfaces of density ( $\rho$ ) and specific heat ( $c$ ) are thermally thin over their thickness ( $\delta$ ).
- (3) Assume a linearized heat loss coefficient ( $h$ ) at the exterior surface to a cold ambient environment ( $T_\infty$ ).

Hence as energy balance yields, the temperature rise as

$$(\rho c \delta) \frac{dT}{dt} = \dot{q}'' - h (T - T_\infty) \quad (4)$$

whose solution is given as

$$\phi = \dot{q}'' e^{-h\tau} \quad (5a)$$

with

$$\phi = \dot{q}'' - h (T - T_\infty), \quad (5b)$$

$$\tau = t / \rho c \delta. \quad (5c)$$

Thus the time ( $t_{ig}$ ) for  $T$  to reach  $T_{ig}$  can be found.

Now, of course, these are only order of magnitude estimates. But if  $t_{ig} \gg t_o$ , then the fire extinguishes and no propagation to the next compartment is likely. If  $t_{ig} \ll t_o$ , then propagation occurs and subsequent growth consequences must be addressed. (Note: Bullen [19] presents a more detailed analysis of fire growth in leaky compartments.)

Let us consider now the large ignition case (b). The scenario considers a large explosion and subsequently large blast damage and fire conditions result. A portion of the deck is blown open and a "submerged-pool fire" condition of burning fuel in a debris laden "porous-bed" is conceptualized. The fire spread below deck into the blast-damaged compartments is opposite to the direction of induced air flow in towards the pool fire. A one-dimensional idealization of this radiation dominated flame spread into a porous bed of fuel and noncombustibles is depicted in Figure 5. The flaming region has a depth of  $L_f$  at a flame temperature  $T_f$ . The porous medium is composed of fuel and inerts of combined bulk density  $\rho_b$  and specific heat  $c$ . A one dimensional radiant flux model is also considered to account for the radiant intensity attenuation in the porous bed with an extinction coefficient  $k\rho_b$  where  $k$  is a constant. For coordinates fixed to the flame front defined by the location of the porous bed temperature to be at the "ignition temperature" for that medium an energy balance yields:

$$\rho_b c (T_{ig} - T_\infty) v_f = \int_0^\infty \dot{q}'' dx \quad (6)$$

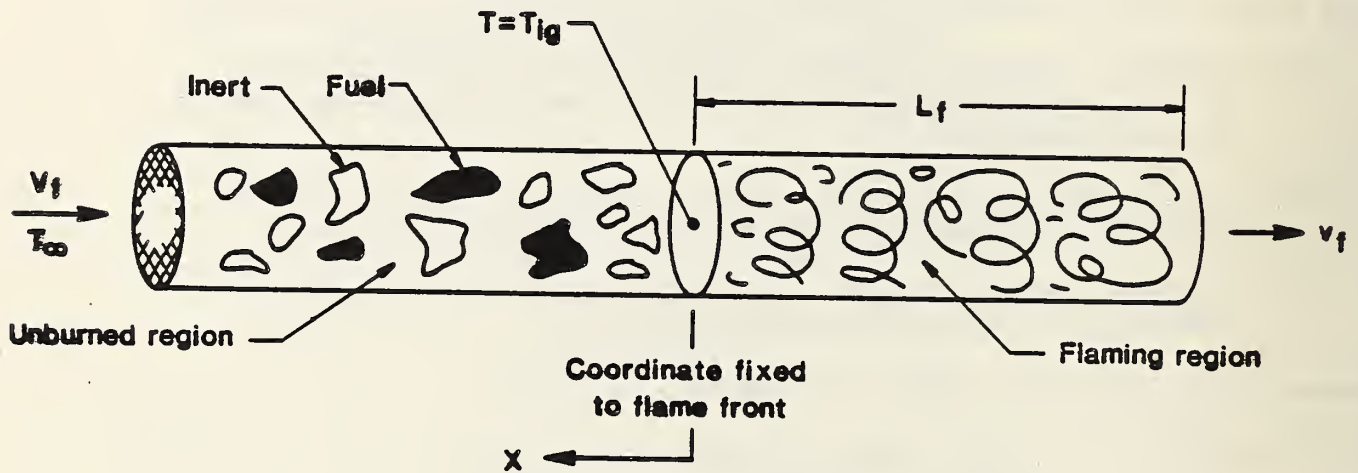


Figure 5. Opposed flow flame spread onto a porous medium.

The forward heat flux is given as

$$\dot{q}'' = \epsilon_f \sigma T_f^4 e^{-k\rho_b x} \quad (7)$$

The flame emissivity is given as

$$\epsilon_f = 1 - e^{-\kappa_f L_f} \quad (8)$$

where  $\kappa_f$  is the extinction coefficient for the flame and depends on the fuel pyrolyzates burning. We shall take the limiting cases of large fires,  $L_f \rightarrow \infty$  or  $\epsilon_f = 1$ ; and smaller fires,  $\epsilon_f \approx \kappa_f L_f$ . Also if we assume no burnout of the fire then its volume  $V_f$  could be given by  $L_f A$  where  $A$  is some appropriately defined flame front area. Hence combining the above into Eq. (6) gives

$$\frac{dV_f}{dt} = \frac{A\sigma T_f^4 \epsilon_f}{\rho_b^2 c k (T_{ig} - T_\infty)} \quad (9a)$$

or for small fires,  $\epsilon_f \rightarrow \kappa_f L_f$

$$\frac{dV_f}{dt} = \frac{\sigma T_f^4 V_f \kappa_f}{\rho_b^2 c k (T_{ig} - T_\infty)}, \quad (9b)$$

and for large fires,  $\epsilon_f \rightarrow 1$ ,

$$\frac{dV_f}{dt} = \frac{A\sigma T_f^4}{\rho_b^2 c k (T_{ig} - T_\infty)}.$$

So that for a given fire, the fire volume will first grow exponentially then reach a constant for a given fuel bed. It is interesting that the only experimental correlation (prediction) of multiple compartment fire growth has been given as  $V_f$  proportional to  $e^{\alpha t}$  where  $\alpha$  is a constant dependent on the fuel arrangement. This is shown in Figure 6 for the Gary, Indiana dwelling experiments conducted by Labes, and also Waterman has developed similar experimental results [20].

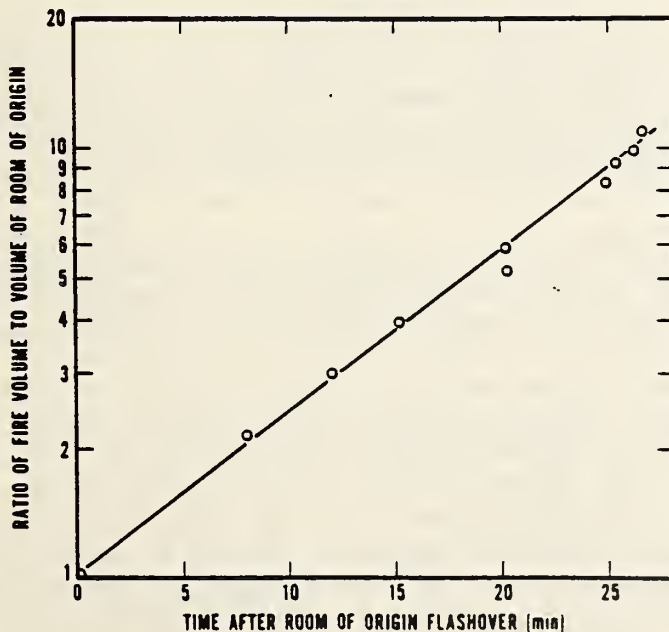


Figure 6. Exponential fire growth in a multi-compartmented structure [20].

Thus some approximate physical insight has been suggested for small and large projectile initiated ship fires. The more general case is (c) and is the one in which the slow steady growth of the fire through the intact ship structure is the crucial one to analyze. Unfortunately we are only at the beginning of such a process. The state of knowledge must expand to fully address this case for buildings and ships. But the lack of such understanding will continue to lead to excessive costs of fire loss and inefficiencies and uncertainties in the practice of fire safety. Let us examine what we know, what we can do, and what we have done.

POST BLAST AND IGNITION. Motivated by case (c) of Figure 4, we conceived of a blast affected area and an intact structural boundary with perhaps ducts or utility penetrations present. The fire in the blast region could then grow to the "intact" region, and then possibly to the next space through the ducts or utility penetrations. The SVM currently describes and predicts the blast damage, giving its extent and the breached bulkhead "openings." It does not address the blast associated pressure driven flows and their thermal characteristics. Since the flows and temperature would influence the extent of the heated region potentially ignited or primed for fire spread, we felt it of importance to pursue this analysis. Its value is not in or of itself but as a first step in a submodel for predicting the fire growth in the SVM/FDM. That algorithm and its description are described in Appendix A. Its incorporation in the FDM can now be carried forward. Yet complicating issues still remain.

One such issue is whether the blast of a fuel rich explosive will ignite the combustibles affected, particularly when they are solids. Of course, temperatures will rise to decomposition levels, but in the absence of sufficient oxygen, depleted by the explosion, ignition might not occur. This suggests needed experiments to examine vented explosions by typical weapon charges and their effect on combustible solids. No evidence of such key, but simple experiments have been found by informally surveying experts in explosion research.

Another issue is whether dust, particularly in the ducts, will be suspended in a hot blast generated flow resulting in a flammable mixture and fire propagation. Again, only carefully designed experiments will bring the correct insight needed. Moreover we have learned that dust-laden duct fires, without blast influence, have occurred.

NON-BLAST RELATED FIRE GROWTH. After a short time (in the order of seconds or so), the blast effects will have decayed and the fire growth environment will revert to that generally experienced by natural fires. In particular, the ambient conditions would be roughly at normal temperature and pressure. Moreover, any forced ventilation devices will have been disabled or intentionally shut down in the fire area. (This precludes smoke control systems that may exist and spring into action.) Hence the fire is in a natural convection environment. Consequently all that is known about freely burning fires in "still air" surroundings can be brought to bear. But as soon as the "air" flow induced by the fire becomes vitiated (reduced in  $O_2$  due to contamination by re-circulating combustion products), or the fire pyrolyzing region grows extensively in size so that all the air supplied is reacted, then we have a "ventilation-controlled" fire. That means that the fuel's mass loss rate will tend to be reduced from the freely burning state. In addition any heat transfer from hot surfaces transmitted through the flames to the fuel surface

will tend to increase the mass loss rate. These "air and heat" feedback effects are well known but are not generally predictable. This, coupled with the lack of general test prescriptions to derive data to predict the spread and burn rate of combustibles in an enclosed free environment, limits fire risk analysis. It does not mean futility, but only that one must work harder to get specific answers. A view on what is known on predictive techniques for compartment fire growth [21] and a review on what is known on fire growth from compartments [19] has already been presented. Let us instead examine what items might be addressed specifically for ships. Also let us examine how current knowledge and experimental techniques might be applied.

In a naval vessel the combustible materials lining the structural bounding surfaces include the following:

- (1) painted surfaces,
- (2) hull insulation,
- (3) floor pads in electrical spaces,
- (4) floor coverings in general,
- (5) aluminum structural components,
- (6) electrical cables and others.

These materials vary in composition, some have been modified by fire retardants, others currently in use may have been regulated out of future use.

These lining materials are significant to fire spread because they have large exposed surface areas and provide continuous pathways to combustibles of higher "fire loadings," (e.g. the mass of combustible per unit area). Although only a thin combustible surface coating may exist, it should be realized that under typical fire heating conditions roughly only 1 mm of the depth into the surface controls its ignition and flame spread [17]. Even retarded materials burn, under realistic fire conditions. Hence, a proper measure of the ignition and flame spread potential, in terms meaningful to modeling, can only lead to improved "decisions" in the SVM/FDM on the role of painted surfaces in fire growth. This applies to the other lining types as well, but painted surfaces certainly should be given priority in a Navy environment. Finally, aluminum structural components are not expected to play a direct role in surface flame spread since the conditions of natural fires are generally insufficient to cause its ignition. However, aluminum melts at approximately 650°C which is easily attainable under severe fire conditions. Thus the possible melting of aluminum could have some mitigating influence on flame spread or promote fire spread into the next compartment. To our knowledge any mitigating influence has not been studied.

The next dominant item prevalent in Navy ships appears to be electrical cables. These may be painted metallic armour-covered or have plastic coated insulation. Our ship visit suggested that these cables run overhead in trays and bundles along the narrow 1-2 m wide corridors. They nearly span the width of the corridor and could be up to 30 cm deep. They, like linings, provide a potential conduit for flame spread and possess a moderate fire load. Indeed when it is realized that energy release rate controls flame length in ceiling fires and therefore flame spread rate, cables are truly a significant potential fire propagation hazard [2]. Much study of cable fires has been done, particularly by utilities and agencies concerned with the fire impact on the control of nuclear reactors or other power generating facilities. Yet no

predictive prescriptions exist for cable fires. Immediate needs in the SVM/FDM might be satisfied by carefully planned experiments of cable type fires in a ship board setting. Thus the potential for propagation and its quantitative conditions of ignition might be deduced for classes of cable type and configuration. Of course more general results and predictive procedures could stem from such experiments. In short, to predict these complex phenomena, first one must observe and quantitatively record them. Then organization of the data and observations may lead to models and improved test procedures. Another issue associated with cables is the fire resistance of their penetration points through bulkheads. This must also be studied experimentally.

A subtle fire possibility is fire growth through ducts due to dust and debris. A more obvious pathway is along the exterior of ducts which are painted or covered by insulating materials.

The most concentrated quantity of combustibles, excluding munitions, is most likely the liquid fuels - diesel oils, hydraulic fluids, aviation fuels - stored in tanks and pumped through pipe lines. Kanury [23] describes some phenomenological characteristics of fire problems related to these fuels and their state. For those fuels exposed to air whose flash or fire point temperatures are below normal ambient temperature (22°C), a flammable mixture will form at the liquid surface and a spark will cause propagation in the pre-mixed fuel/air mixture. Subsequent evaporation could sustain these rapid and extensive fire conditions. But for fuels whose flash points are above 22°C, additional heating must occur for them to be ignited and for flames to propagate. Pool fires of contained liquid spills or spray fires from line and tank ruptures are the possibilities. Some predictive capability exists here but it is meager. Studies of particular Navy liquid fuels would be of value to extend the knowledge base, and more importantly to develop specialized predictive models (correlations) for these fuels.

Munitions and their storage areas are of course critical to a ship's survival when threatened by fire. This problem involves issues of fire heat transfer and bomb "cook-off" phenomena. A complete evaluation of this problem would involve an assessment of the use of available "cook-off" data, and the inclusion of passive and active fire protection measures for magazines. In the level of accuracy anticipated in "deterministic" FDM, a fire close to a magazine will probably constitute a high probability of total ship destruction. Hence it would not be fruitful to refine this problem to great depth at this time.

Let us now address fires in compartments and their likely conditions of spread to adjoining spaces. Certainly a combat ship is highly compartmented. Indeed this may have evolved from early ideas on fire protection as reported by Rushbrook [9, p. 310]:

William Miller, of London, patented a system (No. 1414: June 8th, 1863) of dividing a ship into small cellular watertight compartments:

varying in dimensions into cubic feet or cubic yards or larger, but never very large, which cells may be arranged

in the vessel where found most convenient but they must always be of sufficient number and capacity to float the vessel when filled with water to the required height.

Miller proposed that pipes to admit water "with great liberty" should lead to every compartment, so that any fire could be quickly extinguished. The inventor also included details of a visual alarm system consisting of open-ended tubes leading from each space, from which smoke would issue when a fire occurred.

Miller's system of dividing up a vessel into small compartments has, of course, long since been adopted in The Merchant Marine.

Criteria for fire growth between compartments have not been well developed [20], but we can divide them into two categories: that which is due to hot gas and flame transport through openings, and that which is due to heat transfer through bulkheads, etc. The former involves fluid dynamics and radiant heat transfer, the latter involves heat conduction primarily. Both, however, will depend strongly on the temperature of the fire gases in the compartment and the fire's duration.

For fully-developed (all fuels involved) compartment fires, their temperatures will depend on the size and thermal properties of the compartment, on the ventilation factor (window area,  $A_w$  and its height,  $H$ )  $A_w/\overline{H}$ , and to a lesser extent on the mass of fuel (fire load). Fire duration is then given by the mass loss rate ( $R$ ) and the mass available. These ideas have been well developed and predicted mostly for fires involving wood. They have also been illustrated, albeit incompletely, by the description given in the Soviet work [9]. The symbolism introduced above relates to a work by Bullen and Thomas [24] from which we take the illustrations in Figure 7.

The left illustration in Figure 7 shows how the mass loss rate increases with  $A_w/\overline{H}$  up to the stoichiometric value and follows a downward concave curve above that value. The significance of the stoichiometric line is that the region to its left implies ventilation controlled fires in which all the air entering the compartment is consumed. The subsequent drop in  $R$  with  $A_w/\overline{H}$  is due to decreases in compartment temperatures caused by excesses in the amount of air flow rate over that needed for combustion. As  $A_w/\overline{H}$  gets very large, we approach the freely burning fire case in still air. The enhancement in  $R$  above its free burn value is due to the susceptibility of the particular fuel to radiant heating by the hot compartment. For example, wood cribs have very little enhancements, but liquid fuel pools have high enhancements.

The right illustration in Figure 7 shows a collection of data for different fuel types burned in compartments. The inclined and horizontal lines shown ideally mark the ventilation limited and free burn behavior of wood crib fires in enclosures, respectively. The other fuels (liquid fuels and plastics) tend to have higher  $R/A_F$  (mass loss rate per unit fuel area) due to the radiation enhancement effect. This means that at the scale of these experiments (1/3 of typical conventional rooms), radiant heat transfer from the hot gases and heated surfaces reaches the condensed-phase fuel surfaces and causes more volatilization of fuel. For liquids, this is controlled by their flame optical properties and their latent heats of vaporization. For solids, an effective heat of gasification must be deduced. The paper by Bullen and Thomas [24] lays a foundation and methodology for predicting the mass loss

rates of fuels burning in compartments and their corresponding "window" flame effects. Unfortunately this cannot be accurately extended to arbitrary cases. If the Soviet [9] experiments in ship compartments were designed to be a full-scale extension of the Bullen-Thomas experiments, an improved predictive equation (over Eqns. (1) and (2)) would surely emerge for ship fire safety design applications. It is strongly felt that such experimental analyses are needed to give credence to any first generation deterministic SVM/FDM. Of course this research will only yield results for a compartment burning in normal ambient surroundings. The peculiar but essential configuration of ships should lead to compartment fire combustion products retained by the ship and likely fed back to the fire. This means the overall flow pattern induced by the fire and constrained by the ship's geometry must be understood. Let us examine this aspect of the problem.

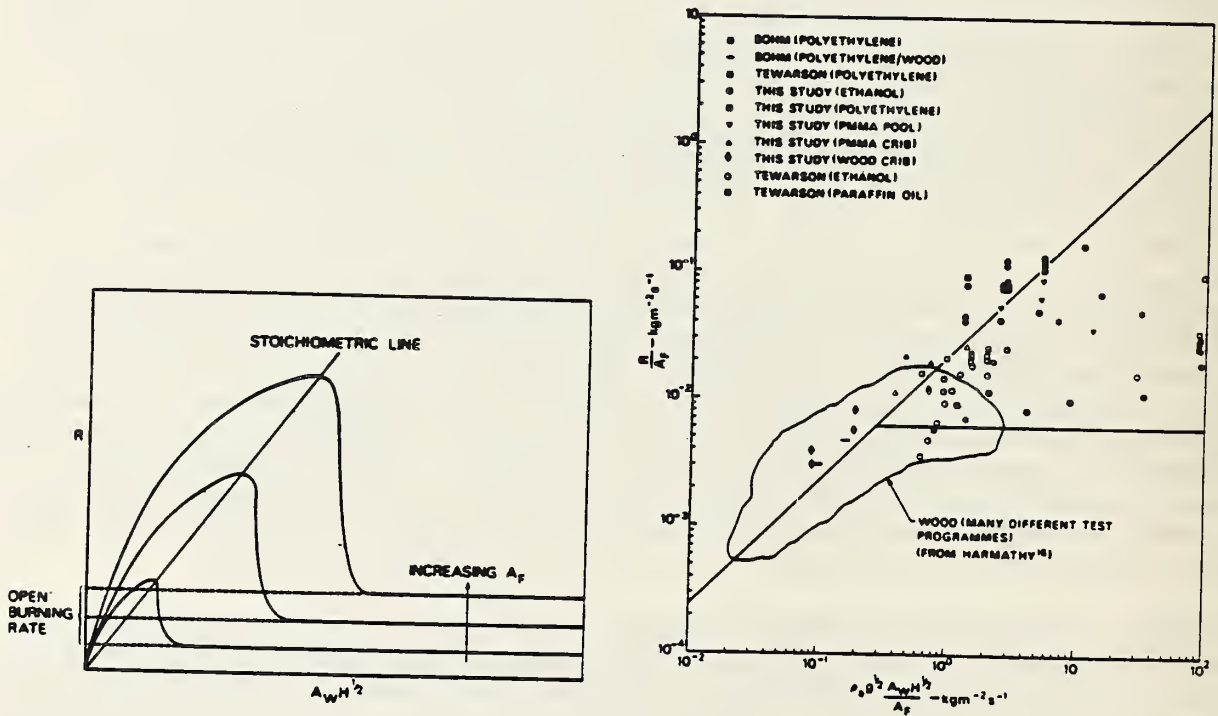


Figure 7. Compartment mass loss rate ( $R$ ) dependence on fuel type and compartment where  $A_f$  is fuel area,  $A_w$  is window area, and  $H$  is its height [24].

A ship is a sealed vessel with inter-connecting internal decks, compartments and passages. The openings to the external atmosphere are at the upper decks, internal decks are connected by floor and ceiling hatches and stair (ladder) accesses. This is very different from a building wherein the openings to the atmosphere are primarily windows in the walls. In contrast we know much about fire induced natural convection flows through window-like openings, but we know nothing about the unstable case of a single opening in a ceiling. This is related to the issues addressed by Porter [10] on combustion in partially closed vessels. Moreover we have been told of considerable full-scale studies on the combustion in roof-opening tanks by Yumoto and others in Japan motivated by a ship fire disaster [25]. Thus this fundamental problem must be addressed in the context of ship fire flows and combustion rates as they are affected by these natural ventilation phenomena.

One aspect of this problem has already been taken by the simulation of natural convection flows resulting from a fire in a ship [26]. This flow-simulation model is in a research state at the National Bureau of Standards at which extensions and refinements are continually being addressed to insure its ultimate accuracy. Flow through a single ceiling opening is one such needed refinement. Moreover, a test of the current model's credibility to ship applications is critically needed now. Such tests would insure its relevance. Jones [26] of NBS is continuing this research. That theoretical effort needs experimental support. Moreover it is too computer intensive at this time for direct inclusion into the SVM/FDM. But that does not preclude its future verified results from being correlated into useful engineering formulae for application in the SVM/FDM.

Experiments in support of this computer simulation research could take different forms. One is to consider full-scale smoke movement studies in ships. Those would be costly, difficult to fully and accurately instrument, and their results would be limited and difficult to assess. An alternative approach would be small scale experiments - commonly called Froude number scaling. This form of similitude scaling attempts to preserve the ratio of inertia to buoyant forces, but ignores viscous (boundary layer effects) forces. This could be done in air with actual smoke and fire simulated sources, or by analogy to a salt water - fresh water system. The latter Froude number modeling technique is described by Zukoski [27] as follows:

Dimensionless velocity ( $v^*$ ), temperature ( $\Delta T^*$ ), and density ( $\Delta \rho^*$ ) change are related to the dimensionless energy source term ( $q^*$ ) where

$$v^* = v/\sqrt{g\ell}$$

$$\Delta T^* = \Delta \rho^* = \frac{T - T_\infty}{T_\infty} = \frac{\rho_\infty - \rho}{\rho_\infty}$$

$$q^* = \frac{\dot{E}}{\rho_\infty \sqrt{g\ell} c_p T_\infty \ell^2}$$

where  $v$  is velocity  
 $g$  is gravitational acceleration  
 $\ell$  is a length scale  
 $T$  is temperature  
 $\rho$  is density  
 $\dot{E}$  is fire energy release rate  
 $c_p$  is specific heat

and  $\infty$  denotes initial or reference states. To relate this to the salt water analog, hot combustion products correspond to salt water and air corresponds to fresh water in an inverted geometrical configuration. The energy source term then becomes

$$q^* = \frac{\Delta\rho_o \dot{V}_o}{\rho_1 \sqrt{g\ell} \ell^2}$$

where  $\Delta\rho_o$  and  $\dot{V}_o$  are respectively the density difference and volumetric flow rate of the salt water plume at its source, and  $\rho_1$  is the fresh water density. Thus a scale model clear plastic ship inverted into a fresh water pond can be used to observe and measure the behavior of fire induced flows in a realistically similar fashion.

Not only would such experiments be useful for model verification, but this approach might lead to a design tool for the fire safety of ships; not to mention the alternative use for existing structural plastic ship models.

The last subject to address is the phenomenonology associated with the suppression of fires. The lack of scientific and engineering design knowledge in suppression dwarfs our limited knowledge of fire growth. Only a systematic program of research in this area will be productive.

#### Approaching a Deterministic Ship Fire Growth Model

FIRE DAMAGE MODEL (FDM)/SHIP VULNERABILITY MODEL (SVM). The primary purpose of this study has been to address the development of a deterministic fire growth model for the SVM. The discussion thus far presented should illustrate that it is not a straight forward exercise; but is it feasible. It will take focused attention, time, and the resolution of several phenomenological fire issues. Some background has been presented on these issues and our current state of knowledge reviewed. Let us now try to contrast that with a current description of the SVM/FDM. The basis of that description is derived from discussions with Hackett [1].

As we understand, the SVM is a probabilistic model that attempts to predict the damage to a ship wrought by a missile strike. It includes the ship geometry, compartment functions, vital components, structural characteristics and other information in computer storage. It considers missile characteristics and a strike location probabilistically. The resulting blast area, opened regions of structural boundaries, and subsequent fire area are computed. The blast-structural effects are assumed to occur instantaneously and are estimated by formulae based on physics (i.e., deterministically). The fire damage estimates (FDM) involve more aspects and are currently computed by a combination of physical formulae, statistical models, and empirical judgment.

Here we will give our inferences and impressions of the features in the current FDM. Each compartment is assigned a probability of fire for each missile hit. The fuels in each are classed as A, B, C, D, i.e. solids, liquids, electrical, metals, respectively. After a missile hit, the blast area is calculated and set equal to the initial fire area. Fuel in that area is reconsidered, (i.e., it could have excess missile propellant), and some fuels may now have vaporized ("fumes") to be "more easily burned." Next, spread to adjoining compartments is assessed based on their fuel state and on their state of flooding. Burning time is estimated from a statistical model and modified by a factor related to the ventilation (openings) state of the compartment. The fire growth time and its time to control based on automatic and manual suppression actions is also estimated from statistics. The nature of the fire growth analysis is to compare and estimate the time for critical fire events to occur. For example, fire burnout time versus fire endurance (of structure) time, fire build-up time (flashover) versus fire fighting response time, and fire control or suppression time versus bomb or magazine cook-off time. The basis of these calculations and their logical incorporation into a physically consistent algorithm set in the FDM is the objective of improvement. To accomplish improvements will require continual interactions among computer scientists, fire researchers, and Navy experts. Here we offer a first step toward this process.

In order to foster improvements in the FDM we took the following approach. This was based on the need to preserve simplicity in the deterministic algorithms for the FDM because it could not currently tolerate the additional computer burden of a large scale fire-physics code. Nevertheless we desired to be comprehensive and generic in our application. Hence we have compiled a series of algebraic equations with which one can make state of the art estimates of fire growth characteristics. Suppression is not included because we do not have comparable knowledge as in fire growth. This approach is constituted in Appendix B. It is founded on building fire research knowledge and may therefore be lacking for complete ship applications. Some items it calculates are as follows: fuel burn rate, radiation to its surroundings, room flashover, room temperature, visibility, and burn time. An examination of Appendix B should provoke refinements and more focused applications to shipboard fires. This is our intent. Thus it can form a basis for more formulae and applications to the FDM.

The concept of the FDM in the SVM is a needed tool. Its feasibility for accurate assessments will always be debated. Yet those knowledgeable in computational fire research and fire safety systems evaluations will concur that it is a reasonable approach which also provides a framework for improvement. The current fire technology is developing at a rate to make improvements feasible and the FDM a sound tool, but it needs focused support or it will not have sufficient credibility in applications to the Navy's unique fire problems. The potential of the SVM/FDM is clear. It needs continued, organized growth and critique to realize its full level of merit. We shall close this report with some specific recommendations to advance that needed growth.

RECOMMENDATIONS. This report already has alluded to or has specified several worthwhile and needed studies. These not only bear on accomplishing an accurate and versatile SVM/FDM, but also can contribute to fire safety design and practices for ships in general. A structured program is needed to pursue

and organize the research into useable tools of practice. There is an opportunity for orchestrating such a program for its purposes as compared to the fire research program for buildings. The latter has benefited from most of the research but its implementation is slow due to a varied arrangement of consensus standards, codes and regulations. Yet no central agency in the Navy appears to have the responsibility for fire research and safety. That kind of focus could have great benefit. Moreover, only through such coordination will the recommendations listed below derive any synergism or overall impact - particularly through system models like the SVM/FDM.

We will simply close by listing a set of recommended needs and studies that relate to our stated objectives herein. The items listed bear on our previous discussions but do not address priority or program completeness exactly. Moreover it is not organized into an integrated plan but could serve as the elements of one. However we shall categorize these elements as follows:

### 1. Blast and Ignition Effects

- a. Characteristics (pressure, temperature, oxygen, heat flux, time) of explosions in vented chambers to simulate typical missile penetration and detonation.
- b. Investigation of the ignition characteristics of typical fuels subject to explosions in vented compartments.
- c. Investigation of the possible propagation in dust and debris laden atmospheres following explosions in confined spaces.

### 2. Fires of Typical Shipboard Contents

- a. Characteristics of flame spread on painted metal.
- b. Characterization and quantification of lining materials on ships - floor pads, insulation, nonstructural panels.
- c. Characterization of liquid fuels burning in spray (ruptured pipe) or pool (spill) configurations.
- d. Research on test methods capable of measuring material fire data needed for predicting performance.
- e. The tabulation of useful data of shipboard materials for predictive and design applications, e.g. thermal properties, decomposition temperatures, thermodynamic properties, flammability properties (flash points, lower flammability limits, etc.), and new fire properties evolving from research.

### 3. Compartment Fires

- a. Studies of fully-developed fires in typical Navy ship compartments characterized by their size and contents. Of particular interest should be the mass loss rate of the contents, its burn duration, its flame extension and heat transfer from the opening. Opening vent size should be varied.

A special facility to weigh all of the room contents continuously during the burning is needed. Subsequent investigation of the fire load survey data for these typical compartment types may then prove valuable - but not before.

- b. Studies on the effect of vent size and location on compartment burn rates. This can be done for idealized burn conditions, e.g. liquid pool fires, or gas burner fires. Of special interest should be the floor and ceiling only vent cases. The latter case ideally portrays the engine room or the entire ship fire.

#### 4. Spread from a Compartment

- a. Characterization of the conditions (heat flux, temperature) to cause spread to the corridor or adjacent compartment.
- b. Prediction of compartment vent flame lengths.
- c. Spread by conduction through metal barriers.
- d. A study of the potential or necessary conditions for fire propagation in ducts.
- e. Conditions, exposure and causative, for the penetration of fire barriers (door seals) or utility "poke-throughs."

#### 5. Overall Ship Fire Dynamics

- a. A study of fire induced flows through ships. Computer models have addressed this and they should be further extended and tested. One experimental technique is the use of analog similitude techniques (i.e., salt water-water tank studies of ship models).
- b. Small (or large scale - possibly from accident records) scale studies of ship fire burn rates and durations involving effect of contents, and external conditions.

#### 6. Suppression

- a. Quantitative studies of agent application rates needed for extinguishment.
- b. Quantitative studies of the effect of burn rate, smoke production and other combustion products by the addition of extinguishment agents.
- c. The effect of diluents and oxygen starvation on combustion.

#### 7. Statistics

- a. Organized study of ship fire records to determine frequency and likely causes of fires.

- b. Statistical predictive correlations of fire growth and suppression features.

## 8. People-Fire Interactions

- a. Quantitative expressions of tolerance and activity levels of humans in fire conditions.
- b. Models to express the response and effectiveness of fire fighting.

In addition to the above recommendations, we should address the performance and limits of vital equipment under fire and smoke conditions. Thus, we offer a suggested course of experimental activities and their analyses to support the sound development of the FDM. Moreover, the results of such a program could have significant benefit to the fire safety design engineer by offering more quantitative capability. Appendix B illustrates the prospect of a design methodology developed from available building fire research.

### Acknowledgements

We wish to express our appreciation to Owen Hackett for his friendly and informative discussions and to Gene Remmers for his support and encouragement -- both of the U.S. David Taylor Naval Ship Research and Development Center.

### References

1. Hackett, O.F., "Fire Modeling to Improve Warship Survivability" presented at The Conference on Fire Propagation Onboard Warships, Ottawa, Canada, 26, 27 Sept. 1983, Final Rept. Ship Damage Control Capabilities Studies, David Taylor Naval Ship Res. Div. Cntr., Oct. 1983.
2. Hathaway, W.T., "Survey of Fire Modeling Efforts with Application to Transportation Vehicles," Rept. No. DOT-TSC-OST-81-4, U.S. Dept. of Trans., Transportation Systems Center, Cambridge, MA 02242, July 1981.
3. Jones, W.W., "A Review of Compartment Fire Models," NBSIR 83-2684, Nat. Bur. Stand., U.S. Dept. of Commerce, April 1983.
4. Tanaka, T., "A Model of Multiroom Fire Spread," NBSIR 83-2718, Nat. Bur. Stand., U.S. Dept. of Commerce, August 1983.
5. Hackett, O.F., Private Communications, David Taylor Naval Ship Res. Dev. Center, 1983/84.
6. Kerlin, D.J., "A Marine View of Fire Protection," SFPE Tech. Rpt. 82-10, Soc. of Fire Protection Engrs., Boston, MA 02110.
7. Rushbrook, F., Fire Aboard, The Technical Press, Ltd., London, 1961.
8. Rasbash, D.J., Private Communications, Edinburgh University, Edinburgh, Scotland, 1984.

9. Stavitskiy, M.G., Kortunov, M.F., Sidorjuk, V.M., Vostryakov, V.I. and Martynenko, V.I., Fire Fighting Aboard Ships, Vol. 1, Gulf Publishing Co., Houston, TX, 1983.
10. Porter, J.W., "Pulsating Combustion of Liquid Fuel in Partially Closed Vessels," Comb. and Flame, 11, 6, p. 501, 1967.
11. Anonymous, "Survey 4 of Selected Shipboard Fires, U.S. Naval Safety Center, Norfolk, VA, 1980.
12. Benjamin, I. and Gross, D., "Naval Shipboard Fire Risk Criteria," NBS Rep. 10159, Nat. Bur. Stands., January, 1970.
13. Lee, B.T. and Parker, W.J., "Fire Buildup in Shipboard Compartments - Characterization of Some Vulnerable Spaces and the Status of Predictive Analysis," NBSIR 79-1714, Nat. Bur. Stand., May 1979.
14. Lee, B.T. and Breese, J.N., "Submarine Compartment Fire Study-Fire Performance Evaluation of Hull Insulation," NBSIR 78-1584, Nat. Bur. Stand., May 1979.
15. Tewarson, A., "Physico-Chemical and Combustion/Pyrolysis Properties of Polymeric Materials," NBS-GCR-80-295, Nat. Bur. Stand., Dec. 1980.
16. Babrauskas, V., "Development of the Cone Calorimeter -- A Bench-Scale Heat Release Rate Apparatus Based on Oxygen Consumption," NBSIR 82-2611, Nat. Bur. Stand., Nov. 1982.
17. Quintiere, J.G. and Harkelroad, M., "New Concepts for Measuring Flame Spread Properties," ASTM STP (Symp. on Applications of Fire Sciences to Fire Engineering) to be pub., Amer. Soc. Testing and Materials, 1984/5.
18. Quintiere, J.G., Babrauskas, V., Cooper, L., Harkelroad, M., Steckler, K., and Tewarson, A., "The Role of Aircraft Panel Materials in Cabin Fires and Their Properties," FAA Tech. Rept. (to be pub.) Fed. Aviation Admin. Tech. Center, Atlantic City, NJ, 1985.
19. Bullen, M.L., "The Ventilation Required to Permit Growth of a Room Fire," CP41/78 Building Res. Estab., Fire Res. Sta., Borehamwood, UK, March 1978.
20. Quintiere, J.G., "The Spread of Fire from a Compartment -- A Review," ASTM STP 685, Amer. Soc. Testing and Materials, p. 139, 1980.
21. Quintiere, J.G., "A Perspective on Compartment Fire Growth," Comb. Sci. Technol., 39, 11, 1984.
22. Quintiere, J.G., "Some Factors Influencing Fire Spread Over Room Linings and in the ASTM E-84 Tunnel Test," Fire and Materials, to be pub., 1984/5.
23. Kanury, A.M., "Limiting Case Fires Arising from Tank/Pipeline Ruptures," Fire Safety J., 3, 2-4, Jan/Mar. 1981.

24. Bullen, M.L. and Thomas, P.H., "Compartment Fires with Non-Cellulosic Fuels," 17th symp (Int.) on Comb., The Combustion Inst., 1978.
25. Koseki, H., Private Communications, NBS Guest Worker from the Fire Res. Inst., Tokyo, Japan, July, 1984.
26. Jones, W.W., "Spread of Smoke in a FFG7, presented at the Conf. on Fire Propagation Onboard Warships," Ottawa, Canada, 26,27 Sept. 1983, Final Rept. Ship Damage Control Capabilities Studies, David Taylor Naval Ship Res. Dev. Cntr., Oct. 1983.
27. Zukoski, E.E., "Convective Flows Associated with Room Fires," Cal. Inst. Technol., NSF Grant No. GI 31891X1, June 1975.

## APPENDIX A

### Post-Explosion Venting Analysis

#### Introduction

The environment in a compartment immediately following an explosion is characterized by extremely high pressures. On the other hand, most fire related phenomena occur at essentially ambient pressure. The connection between these two environments is provided by an analysis of the post explosion venting process. The venting of explosion products may be considered separately from the dynamics of the blast itself, due to the wide disparity in time scales associated with each phenomenon. The blast energy is deposited in the enclosure in  $O(10^{-3})$  seconds for small to medium sized enclosures. The venting time, on the other hand, is  $O(10^{-1})$  seconds or longer, depending on post explosion room geometry, gas properties, and energy release.

The model adopted for the analysis can be described as follows. At time  $t = 0$  the compartment of volume  $V$  is ruptured by an explosion releasing an energy  $E$  together with a mass of gas and suspended particulate matter  $M$ . The energy release causes several ruptures of area  $A_1$  in the compartment boundaries. After the passage and reflection of the initial blast/detonation wave, the velocities in the interior of the compartment will be reduced to low subsonic speeds, while the velocity at each vent will be sonic for enclosure pressures  $P_v$  exceeding the ambient pressure  $P_a$  by the ratio

$$\left(\frac{P_v}{P_a}\right) > \left(\frac{\gamma+1}{2}\right)^{\gamma/\gamma-1}$$

Here  $\gamma$  is the ratio of specific heats for the gas particle mixture. The relative smallness of the velocity in the compartment permits its state to be described by an energy and mass balance. Momentum effects only play a role in determining the flow through the vent, which is assumed to be an adiabatic expansion process. The process inside the compartment cannot be taken as adiabatic, however. The high temperature and particulate content of the post explosion gas imply significant radiative cooling, which must be accounted for in the compartment energy balance. It is represented in the mathematical model as an optically thin gas of emissivity  $\epsilon$ . When the pressure ratio  $(P_v/P_a)$  rises above the value  $[2/(\gamma+1)]^{\gamma/\gamma-1}$ , the vent flow is subsonic. The process continues until the compartment and ambient pressures have equalized.

This model is a simplified version of the one developed by Fairweather and Vasey [A1]. These authors study explosions generated by rapid combustion of flammable mixtures. Since the combustion and venting time scales in their problems are comparable, they include a description of flame spread and energy release in their calculations. They also carry along a realistic thermodynamic model of the gas and a detailed computation of the gas emissivity. The price for this is, of course, increased mathematical complexity. Their analysis requires the numerical solution of a system of differential and algebraic equations, in contrast with the analytical results obtained below. Given the uncertainties and approximations inherent in any analysis of this

type, it is not clear whether the advantages of a numerical approach outweigh the insight gained from the analytical solutions.

### Analysis

The starting point is a statement of the conservation of mass and energy for the idealized model sketched in fig. (A1).

$$\frac{d}{dt} \int \rho dV = - \sum_1 (\rho UA)_1 \quad (1)$$

$$\frac{d}{dt} \int \rho \left( e + \frac{1}{2} U^2 \right) dV = \int \rho Q dV - \sum_1 (\rho U h_v A)_1 \quad (2)$$

Here  $\rho$  is the effect gas density (including the particulate loading),  $U$  the gas speed, and  $e$  the internal energy per unit mass. The quantity  $h_v$  is the total enthalpy of the flow in each vent, defined in terms of the enthalpy per unit mass  $h$  by the relation

$$h_v \equiv h + \frac{1}{2} U^2. \quad (3)$$

The above integrals are taken over the entire enclosure volume and the sums are over all the vent openings (see fig. A1). The quantity  $Q$  is the radiant emission per unit mass.

Several assumptions are needed to make further progress. They are:

- i. The gas can be described as an ideal gas with constant specific heats. The thermodynamic pressure  $p$  is then related to the temperature  $T$  and gas constant  $R$  by the equation of state

$$P = \rho RT \quad (4)$$

- ii. The effective gas is optically thin; with emissivity  $\epsilon$ . The radiant emission per unit mass  $Q$  is then

$$Q = 4\epsilon\sigma T^4 \quad (5)$$

Since the optical depth of any ray is too small to absorb any significant fraction of the emitted flux, eq. (5) represents the appropriate expression to insert into eq. (2).

- iii. The gas in the bulk of the enclosure is at rest and in a spatially uniform state devoted by pressure  $P_v$ , density  $\rho_v$ , and temperature  $T_v$ . The enthalpy  $h_v$  is related to the temperature  $T_v$  by the perfect gas law with a constant specific heat  $C_p$ .

$$h_v = C_p T_v$$

- iv. The vent flows are an isentropic expansion from rest. When the enclosure pressure is high enough the vent speed is sonic.

$$U = \left[ 2 \left( \frac{\gamma - 1}{\gamma + 1} \right) c_p T_v \right]^{1/2} \quad (6)$$

$$P_a / P_v < \left( \frac{2}{\gamma + 1} \right)^{\gamma / \gamma - 1}$$

When the enclosure pressure drops below the value required to maintain a sonic vent speed, the subsonic flow vents isentropically to ambient pressure  $P_a$ . The subsonic vent speed is

$$U = \left\{ 2 c_p T_v \left[ 1 - \left( \frac{P_a}{P_v} \right)^{\frac{\gamma - 1}{\gamma}} \right] \right\}^{1/2}. \quad (7)$$

Using the results implied by the above four assumptions in eqs. (1) and (2) the mass and energy conservation equations respectively can be written for the sonic vent case in the form:

$$V \frac{d\rho_v}{dt} = - \sum_i A_i \left( \frac{2}{\gamma + 1} \right)^{1/\gamma - 1} \rho_v \left[ 2 \left( \frac{\gamma - 1}{\gamma + 1} \right) c_p T_v \right]^{1/2} \quad (8)$$

$$V \left\{ \frac{dT_v}{dt} + 4 \frac{(\gamma - 1)}{R} \epsilon \sigma T_v^4 \right\} =$$

$$- (\gamma - 1) \sum_i A_i \left( \frac{2}{\gamma + 1} \right)^{1/\gamma - 1} T_v \left[ 2 \left( \frac{\gamma - 1}{\gamma + 1} \right) c_p T_v \right]^{1/2} \quad (9)$$

These equations are supplemented by initial conditions which ensure that the average density and pressure account for the energy  $E$  and mass  $M$  added instantaneously to the enclosure at the initial instant.

$$\rho_v(0) = \rho_a + M/V$$

$$P_v(0) = P_a + (\gamma - 1) E/V \quad (10)$$

$$T_v(0) = P_v(0) / \rho_v(0) R$$

The solution to the mathematical problem specified by eqs. (8) - (10) is obtained in the following form:

$$T_v = \left\{ \frac{P_a + (\gamma - 1) E/V}{R [\rho_a + M/V]} \right\} \Theta(\tau, \beta) \equiv T_o \Theta$$

$$\tau = \left\{ (\gamma - 1) \left( \frac{2}{\gamma - 1} \right)^{1/\gamma - 1} \sum_i A_i \left[ 2 \left( \frac{\gamma - 1}{\gamma + 1} \right) c_p T_o \right]^{1/2} / V \right\} t$$

$$\beta = \frac{4 \epsilon \sigma T_o^3 V}{R \sum_i A_i \left( \frac{2}{\gamma + 1} \right)^{1/\gamma - 1} \left[ 2 \left( \frac{\gamma - 1}{\gamma + 1} \right) c_p T_o \right]^{1/2}}$$

$$P_v = [P_a + (\gamma - 1) E/V] \theta \left\{ \frac{(1 + \beta) \theta^{5/2}}{1 + \beta \theta^{5/2}} \right\}^{2/5(\gamma-1)}$$

$$\tau = 2 \int_{\sqrt{\theta}}^1 \frac{dU}{U^2 + \beta U^7} \quad (11)$$

The quantity  $T_o$  is the initial enclosure temperature consistent with the prescribed energy and mass deposition. The parameter  $\beta$  is a dimensionless ratio of the pressure relief time by convection to the radiative cooling time. When  $\beta = 0$ , there is no radiative cooling. As  $\beta$  increases, the role of radiative cooling is enhanced.

The quantity  $\tau$  is the dimensionless time, normalized with respect to a pressure relief time scale. Note that the quadrature relating  $\tau$  to the dimensionless temperature  $\theta$  contains the parameter  $\beta$  in the denominator. Hence, as  $\beta$  increases, the time required to cool to a given fraction of the initial temperature is decreased.

When the enclosure pressure  $P_v$  reaches the lowest value at which sonic velocity can be sustained in the vents, the pressure and temperature at that instant are determined from the formulae

$$P_v = \left(\frac{\gamma + 1}{2}\right)^{\gamma/\gamma-1} P_a$$

$$T_v \equiv T_s = T_o \theta_s \quad (12)$$

$$\theta_s \left\{ \frac{(1 + \beta) \theta_s^{5/2}}{1 + \beta \theta_s^{5/2}} \right\}^{2/5(\gamma-1)} = \left(\frac{\gamma + 1}{2}\right)^{\gamma/\gamma-1} [1 + (\gamma-1) E/P_a V]^{-1}.$$

In order to analyze the subsonic phase of the cooling process, it is more convenient to work with dimensionless pressure and temperature variables, defined as:

$$(P_a/P_v) \equiv \phi(s, \lambda)$$

$$(T_v/T_s) \equiv \theta(s, \lambda)$$

$$s \equiv \left\{ (\gamma-1) \sum_i A_i (2 C_p T_s)^{1/2} / V \right\} (t-t_s) \quad (13)$$

$$\lambda \equiv 4 \epsilon \sigma T_s^3 / R \sum_i A_i (2 C_p T_s)^{1/2}$$

Here,  $s$  is the dimensionless time measured on a pressure relief time scale appropriate for subsonic flow. Note that the origin of the  $s$  time scale is at the time  $t_s$  when the vent flow becomes subsonic. The parameter  $\lambda$  is the dimensionless ratio of pressure relief time to radiative cooling time appropriate to subsonic flow conditions. In these variables the mass and energy form conservation equations can be manipulated into the form

$$\frac{1}{\phi} \frac{d\phi}{ds} = \lambda \theta^3 + \frac{\gamma}{\gamma - 1} (\phi)^{1/2} [\theta \{1 - (\phi)^{\gamma-1/\gamma}\}]^{1/2}$$

$$\frac{1}{\theta} \frac{d\theta}{ds} = -\lambda \theta^3 - (\phi)^{1/2} [\theta \{1 - (\phi)^{\gamma-1/\gamma}\}]^{1/2} \quad (14)$$

$$\theta(0) = 1 ; \phi(0) = \left(\frac{2}{\gamma + 1}\right)^{\gamma/\gamma-1}$$

Unlike the sonic vent case, the subsonic venting equations cannot be solved exactly in closed form. An approximate solution can be obtained, however, by taking advantage of the fact that by the time the vent flows become subsonic, the role of radiation will be greatly diminished. Mathematically, this implies small values of  $\lambda$ . Note that if  $\lambda = 0$ , the venting is isentropic.

$$\theta = \left(\frac{2}{\gamma + 1}\right) (\phi)^{-(\gamma-1)/\gamma} \quad (15)$$

We anticipate that for small non-zero values of  $\lambda$ , the relation between  $\theta$  and  $\phi$  will not differ too much from that given by eq. (15). To this end, it is convenient to introduce a new variable  $Z$ ,

$$\theta \equiv \left(\frac{2}{\gamma + 1}\right) (\phi)^{-(\gamma-1)/\gamma} (Z)^{2/5} \quad (16)$$

Substitution of eq. (16) into eq. (14) and elimination of the time variable  $s$  yields

$$\frac{2}{5} \frac{\phi}{Z} \frac{dZ}{d\phi} = -\frac{(\lambda/\gamma) Z}{\lambda Z + g(\phi)}$$

$$g(\phi) = \left(\frac{\gamma}{\gamma - 1}\right) \left(\frac{\gamma + 1}{2}\right)^{5/2} (\phi)^{5(\gamma-1)/2\gamma} + \frac{1}{\gamma} [1 - (\phi)^{(\gamma-1)/\gamma}]^{1/2} \quad (17)$$

The solution must satisfy the initial condition

$$Z(\phi_0) = 1 ; \phi_0 = \left(\frac{2}{\gamma + 1}\right)^{\gamma/(\gamma-1)} \quad (18)$$

The solution satisfying eqs. (17) and (18) may be obtained by noting that if  $\lambda$  is small,  $Z$  varies slowly. The denominator of eq. (17) is then dominated by the function  $g(\phi)$  until  $1 - \phi$  is  $O(\lambda^2)$ . At this point the pressure is nearly ambient and the venting process is over. We therefore approximate eq. (17) by

$$\frac{2}{5} \frac{\phi}{Z} \frac{dZ}{d\phi} = \frac{-(\lambda/\gamma) Z}{\lambda + g(\phi)} \quad (19)$$

Since  $1 - Z$  is  $O(\lambda)$ , the error in  $Z$  computed from this formula is formally  $O(\lambda^3)$ . Eq. (19) can be readily solved to yield

$$Z = \left\{ 1 + (5\lambda/2\gamma) \int_{\phi_0}^{\phi} \frac{dX}{X[\lambda + g(X)]} \right\}^{-1} \quad (20)$$

Thus,  $\theta$  can be expressed in terms of  $\phi$  as

$$\theta = \left( \frac{2}{\gamma + 1} \right) (\phi)^{-(\gamma-1)/\gamma} \left\{ 1 + (2\lambda/5\gamma) \int_{\phi_0}^{\phi} \frac{dX}{X[\lambda + g(x)]} \right\}^{-2/5}$$

$$\phi_0 = \left( \frac{2}{\gamma + 1} \right)^{\gamma/\gamma-1} \quad (21)$$

$$g(X) = \frac{\gamma}{\gamma - 1} \left( \frac{\gamma + 1}{2} \right)^{5/2} (X)^{(5\gamma-3)/2\gamma} [1 - (X)^{(\gamma-1)/\gamma}]^{1/2}$$

Given this relation, the time scale  $s$  can be expressed in terms of  $\phi$  as follows:

$$s = \int_{\phi_0}^{\phi} dX \left\{ \left( \frac{2}{\gamma + 1} \right)^3 (X)^{(3-2\gamma)/\gamma} [Z(X)]^{1/5} [\lambda + g(X)] \right\}^{-1} \quad (22)$$

### Results

Figures A2 through A9 contain a sampling of the results that can be extracted from the above formulae. There are so many parameters that a systematic presentation is impossible. It is precisely for this reason that an analytic approach yielding simple, easily evaluated solutions, has been employed. Four parameter variations were investigated: the enclosure volume, the energy yield (and associated mass loading) of TNT explosive, the vent area, and the specific heat ratio. The first three of these are obviously quantities whose effects are of interest. Their inclusion requires no discussion. The dependence upon  $\gamma$  is displayed because it is less obvious (but true) that the thermophysical properties of the effective gas are also of crucial importance. The values of  $\gamma$  chosen correspond to successively increasing the number of internal degrees of freedom excited in the gas. The gas constant  $R$  is chosen to be that for air; while the value of the emissivity  $\epsilon$  is taken as unity. Clearly, more realistic values are needed, based on the properties of actual explosion products.

The plots show the time history of the dimensionless pressure  $\phi$  and temperature  $\theta$  in terms of the sonic vent time variable. However, all plots show both the sonic and subsonic branches of the venting process. The effective initial pressure and temperature are displayed for each case. Note that these pressures do not correspond to the peak pressures behind either the incident or reflected blast waves in an enclosure of the same volume. It is easy to show that such a choice of initial pressure would lead to an estimate that much more energy was initially deposited in the enclosure than is released in the blast. At the end point of each of these calculations, the pressure inside the vent is ambient but the temperature is elevated with respect to the environment. This situation is similar to that encountered in room fires. The further history of the fire growth and spread can then be treated by methods developed for these scenarios.

In order to use these formulae conveniently it is best not to rely on figures A2 thru A9. Rather, a computer program designed to evaluate equations (10) - (12) for the sonic vent case and equations (13), (21) and (22) for the subsonic vent case should be written. Nothing more than numerical evaluation of a few simple integrals and one algebraic root-finding (eq. 12) is required. The computer time required for an individual run is a fraction of a second, even on a minicomputer.

Given the existence of such a program, a calculation would be performed in the following sequence. First, the structural damage inflicted by a blast must be determined. This information must be obtained from an analysis of blast theories and data. The output should be a prediction of vent area created by the blast. If the temperature and post explosion particle loading can be obtained, the specific heat ratio  $\gamma$  and emissivity  $\epsilon$  can be estimated. Otherwise, an emissivity  $\epsilon = 1$  and values of  $\gamma$  in the range  $7/5 \geq \gamma \geq 9/7$  should be used. This corresponds to a perfectly emitting gas/particle mixture whose gaseous components are air with the vibrational degrees of freedom unexcited ( $\gamma = 7/5$ ) and fully excited ( $\gamma = 9/7$ ). Using the mass and energy released in the explosion, together with the appropriate value of  $\gamma$ , eqs. (10) yield the effective initial density, pressure, and temperature associated with the venting process. Equations (11) then follow the pressure and temperature relief down to the point where the pressure ratio is no longer sufficient to maintain sonic flow at the vents. The pressure at this point is given by the first of eqs. (12). The last of eqs. (12) then given the dimensionless temperature ratio  $\theta_s$  consistent with that pressure and the initial conditions.

Solution of this equation for  $\theta_s$  requires use of the root-finder mentioned above. The easiest way to carry out the procedure is to test each value of  $\theta$  used in the evaluation of the integral in eq. (11) as a possible solution of the last of eqs. (12). When the zero crossing is found, the last sonic vent state has been reached and this branch of the solution terminates. The absolute temperature at this point is then given by the second of eqs. (12) and the first of eqs. (11). The time elapsed is given by the last of eqs. (11) and the second of eqs. (11).

Given the pressure, temperature, and elapsed time, dimensionless pressure, temperature, and time scale appropriate to the subsonic branch are determined by eqs. (13). The solutions in dimensionless form are given by eqs. (21) and (22). The final state is given in dimensionless form by the value  $\theta = 1$ . This determines the dimensionless time  $S$  and temperature  $\theta$  such that the

pressure inside the explosion chamber has equilibrated with the ambient atmosphere. Dimensional values are then obtained by using these values back in eq. (13).

#### References

- A1. Fairweather, M and Vasey, M.W., A Mathematical Model for the Prediction of Overpressures Generated in Totally Confined and Vented Explosions, Proc. Nineteenth Symposium (International) on Combustion, the Combustion Institute, Pittsburgh, p. 645, (1982).

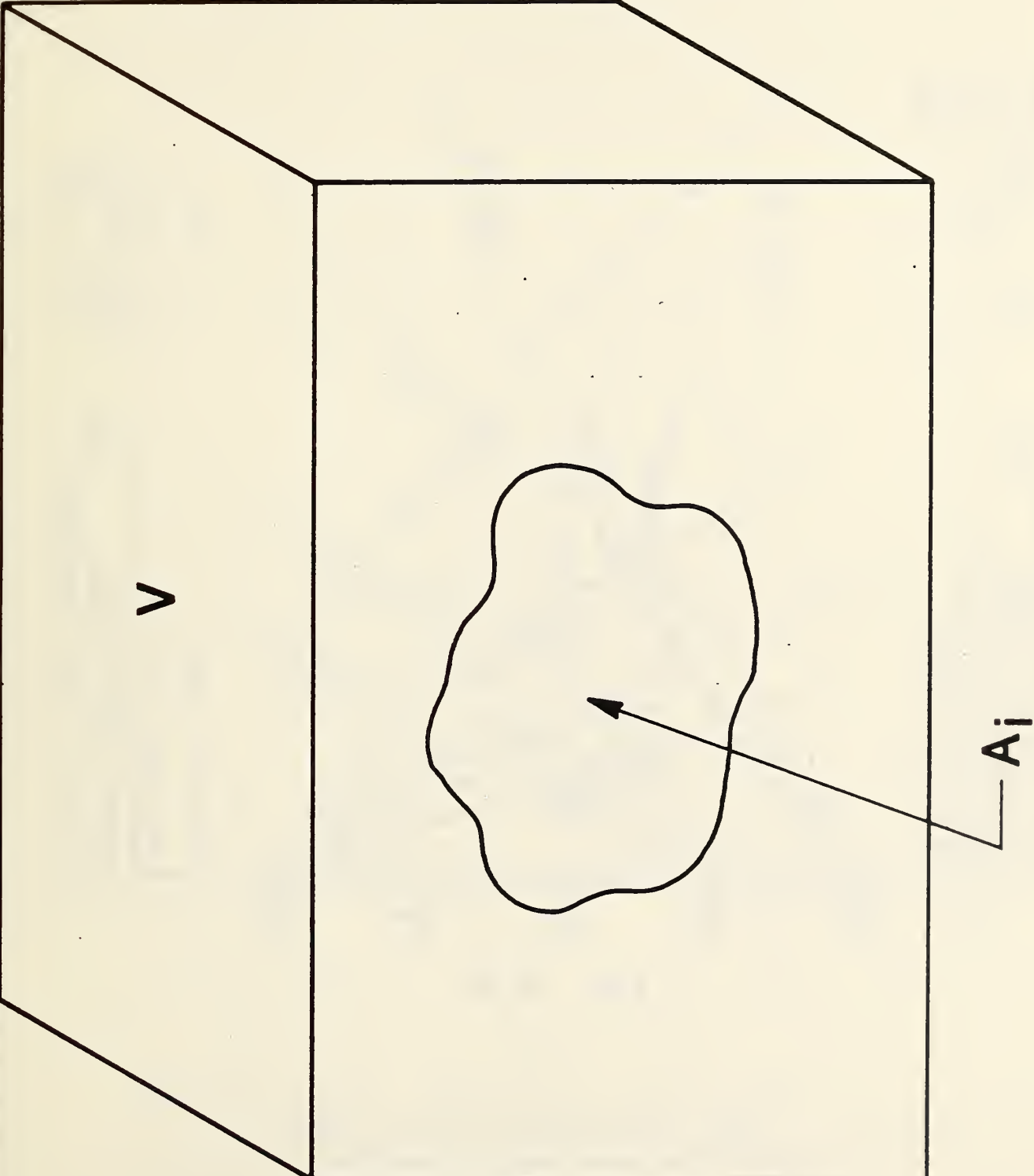


Figure A1. Simplified Compartment Venting Model

| $\gamma$  | $\bar{Y}$ |
|-----------|-----------|
| —         | 11/9      |
| - - -     | 9/7       |
| - · - · - | 7/5       |
| - - - - - | 5/3       |

$\theta, \phi$  VS.  $\tau$  FOR VARIOUS  $\gamma$

Volume = 60.0 m<sup>3</sup>

Vent area = 10.0 m<sup>2</sup>

15.0 kg of TNT

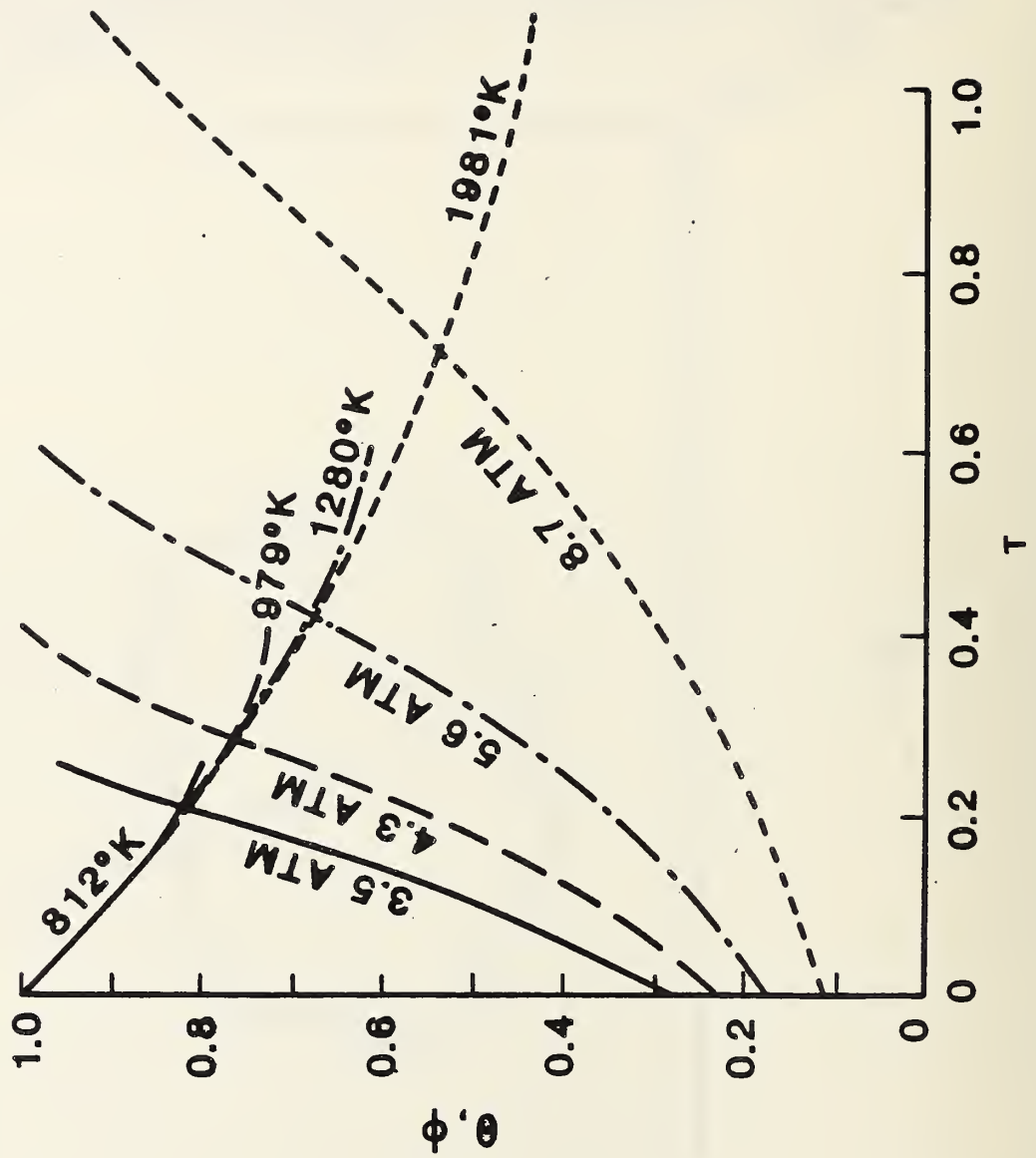


Figure A2.  $\theta, \phi$  vs.  $\tau$  for various  $\gamma$ , 60.0 m<sup>3</sup> volume, 10.0 m<sup>2</sup> vent area, and 15.0 kg of TNT

$\theta, \phi$  VS.  $\tau$  FOR VARIOUS  $\gamma$   
 Volume = 60.0 m<sup>3</sup>  
 Vent area = 0.1 m<sup>2</sup>  
 15.0 kg of TNT

|          |           |      |
|----------|-----------|------|
| $\gamma$ | —         | 11/9 |
|          | - - -     | 9/7  |
|          | - · - · - | 7/5  |
|          | - - - - - | 5/3  |

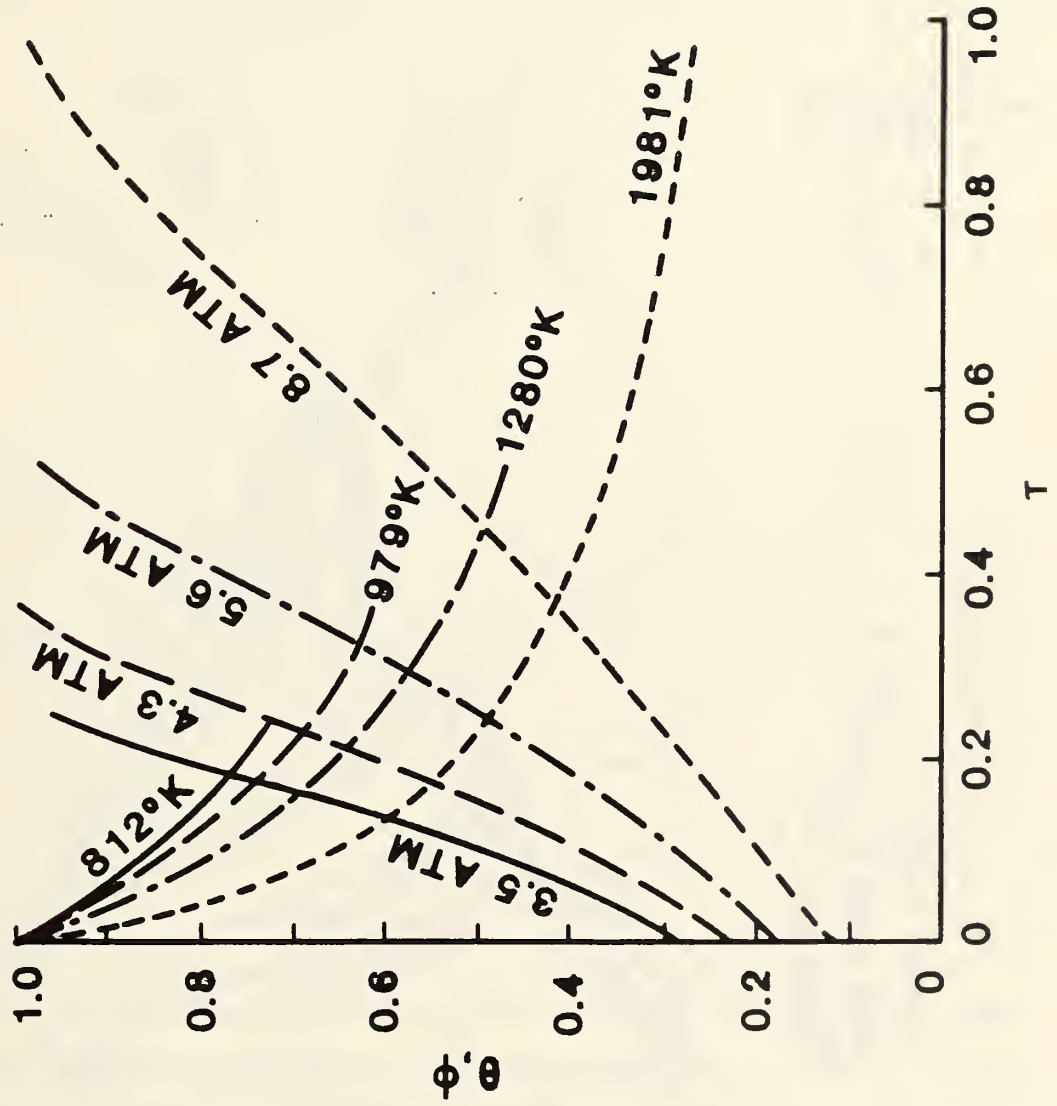


Figure A3.  $\theta, \phi$  vs.  $\tau$  for various  $\gamma$ , 60.0 m<sup>3</sup> volume, 0.1 m<sup>2</sup> vent area, and 15.0 kg of TNT.

$\gamma$   
 — 11/9  
 - - - 9/7  
 - · - · 7/5  
 - - - - 5.3

**$\theta, \phi$  VS.  $\tau$  FOR VARIOUS  $\gamma$**

**Volume = 60.0 m<sup>3</sup>**

**Vent area = 1.0 m<sup>2</sup>**

**15.0 kg of TNT**

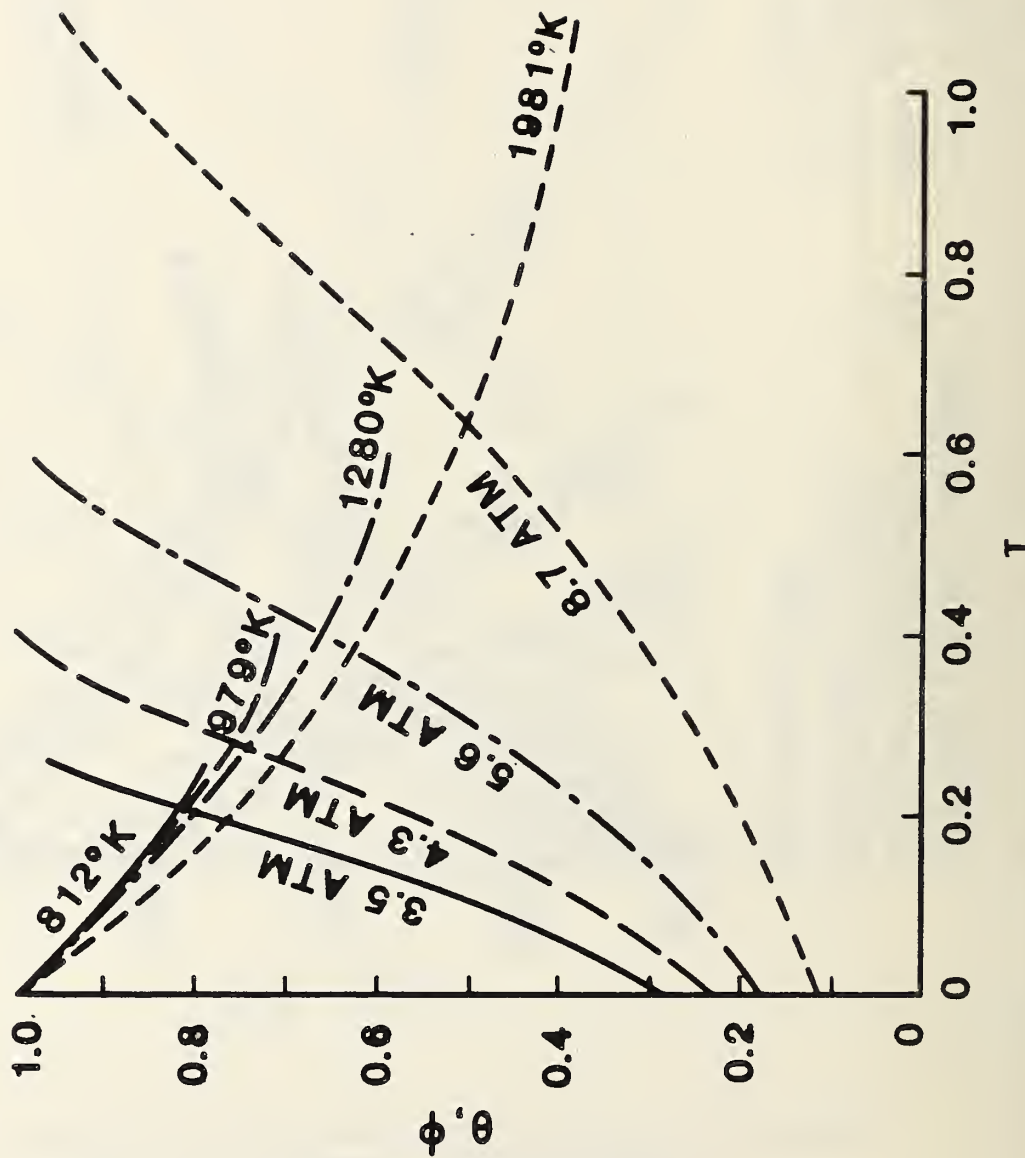


Figure A4.  $\theta, \phi$  vs.  $\tau$  for various  $\gamma$ , 60.0 m<sup>3</sup> volume, 1.0 m<sup>2</sup> vent area, and 15.0 kg of TNT.

$\theta, \phi$  VS.  $\tau$  FOR VARIOUS  $\gamma$   
 Volume = 20.0 m<sup>3</sup>  
 Vent area = 1.0 m<sup>2</sup>  
 15.0 kg of TNT

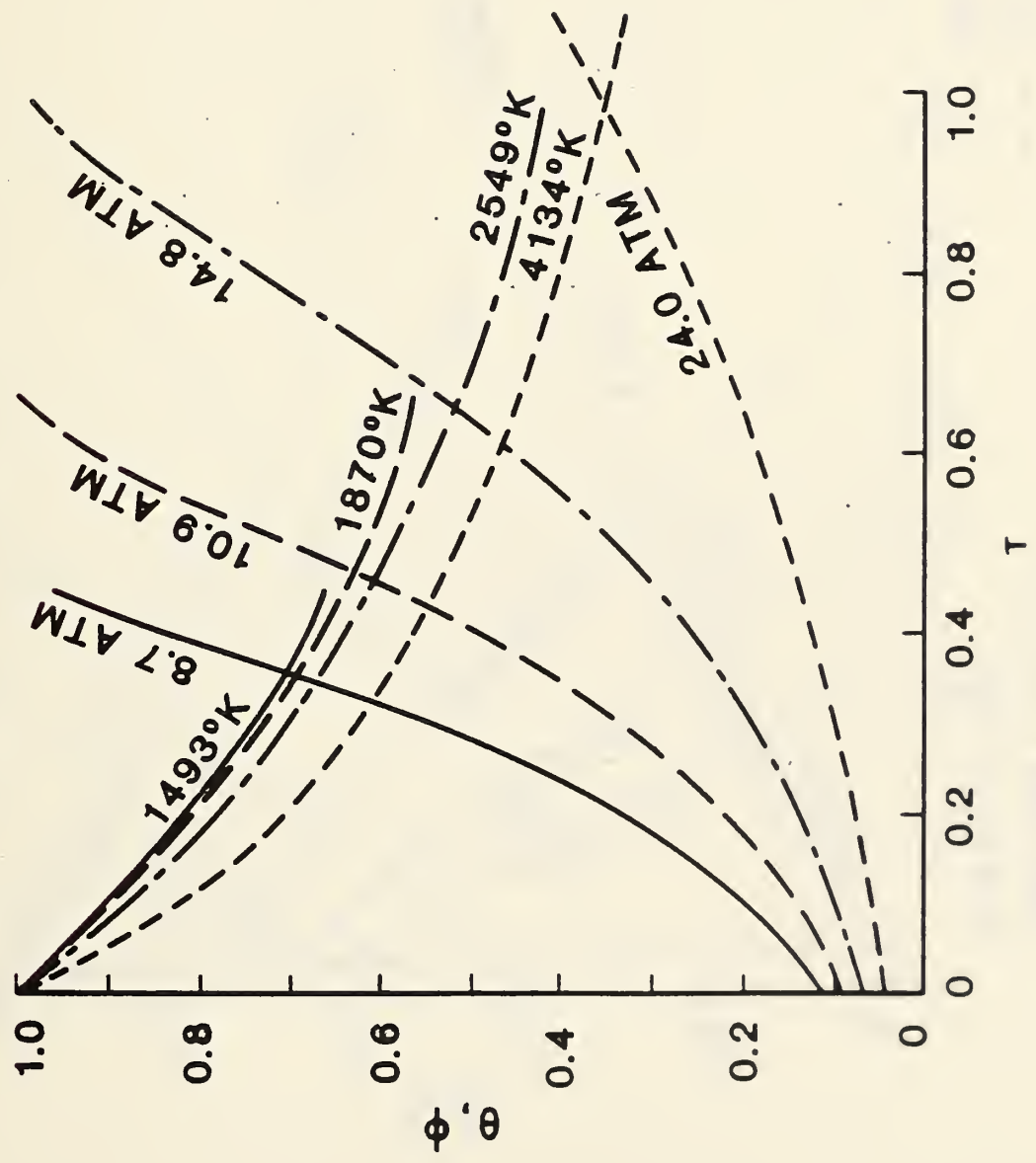


Figure A5.  $\theta, \phi$  vs.  $\tau$  for various  $\gamma$ , 20.0 m<sup>3</sup> volume, 1.0 m<sup>2</sup> vent area, and 15.0 kg of TNT.

$\gamma$   
 — 11/9  
 - - 9/7  
 - · - 7/5  
 - - - - 5/3

$\theta, \phi$  VS.  $\tau$  FOR VARIOUS  $\gamma$

Volume = 100.0 m<sup>3</sup>

Vent area = 1.0 m<sup>2</sup>

15.0 kg of TNT

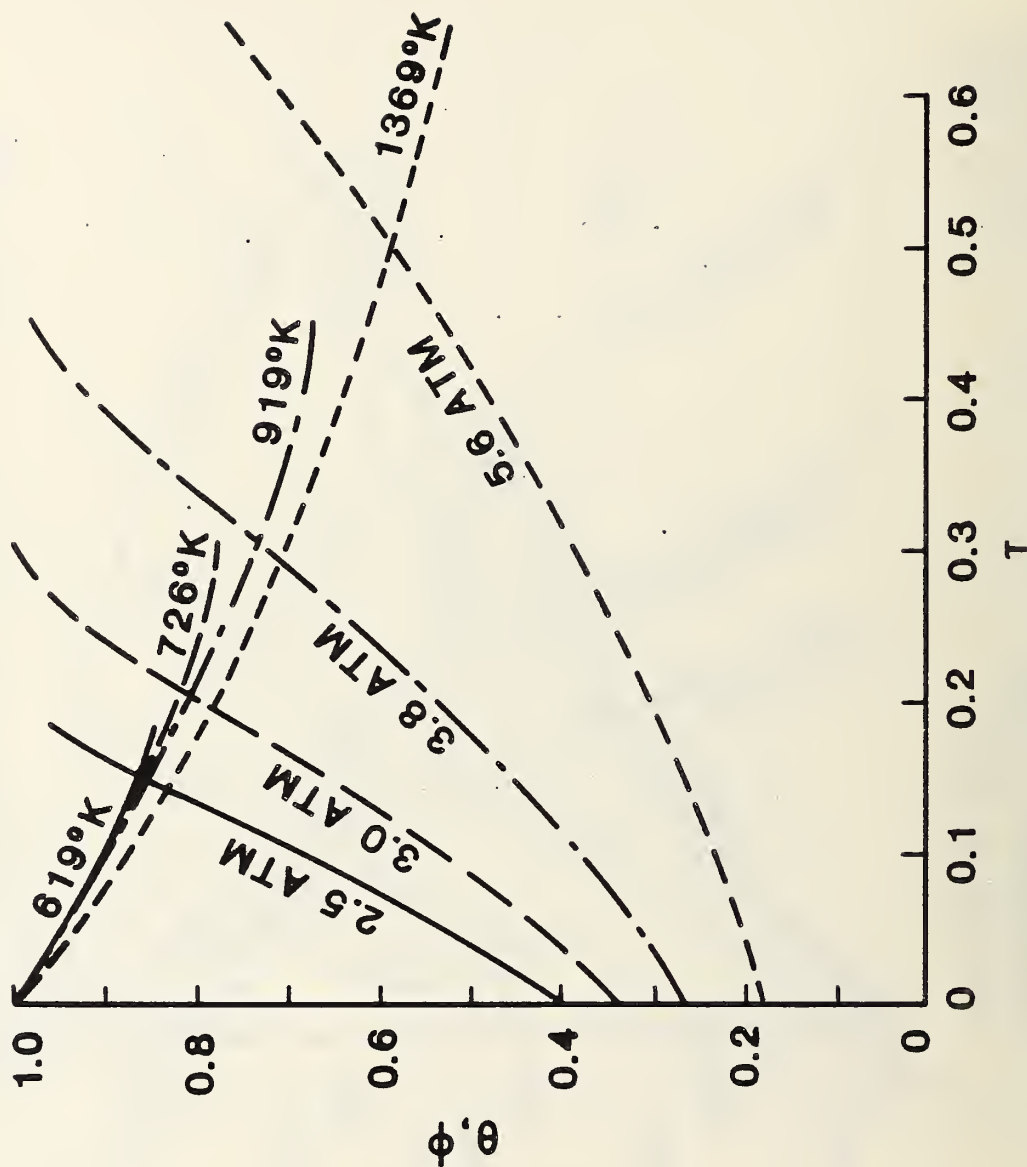


Figure A6.  $\theta, \phi$  vs.  $\tau$  for various  $\gamma$ , 100.0 m<sup>3</sup> volume, 1.0 m<sup>2</sup> vent area, and 15.0 kg of TNT.

$\theta, \phi$  vs.  $\tau$  FOR VARIOUS  $\gamma$   
 Volume = 200.0 m<sup>3</sup>  
 Vent area = 1.0 m<sup>2</sup>  
 15.0 kg of TNT

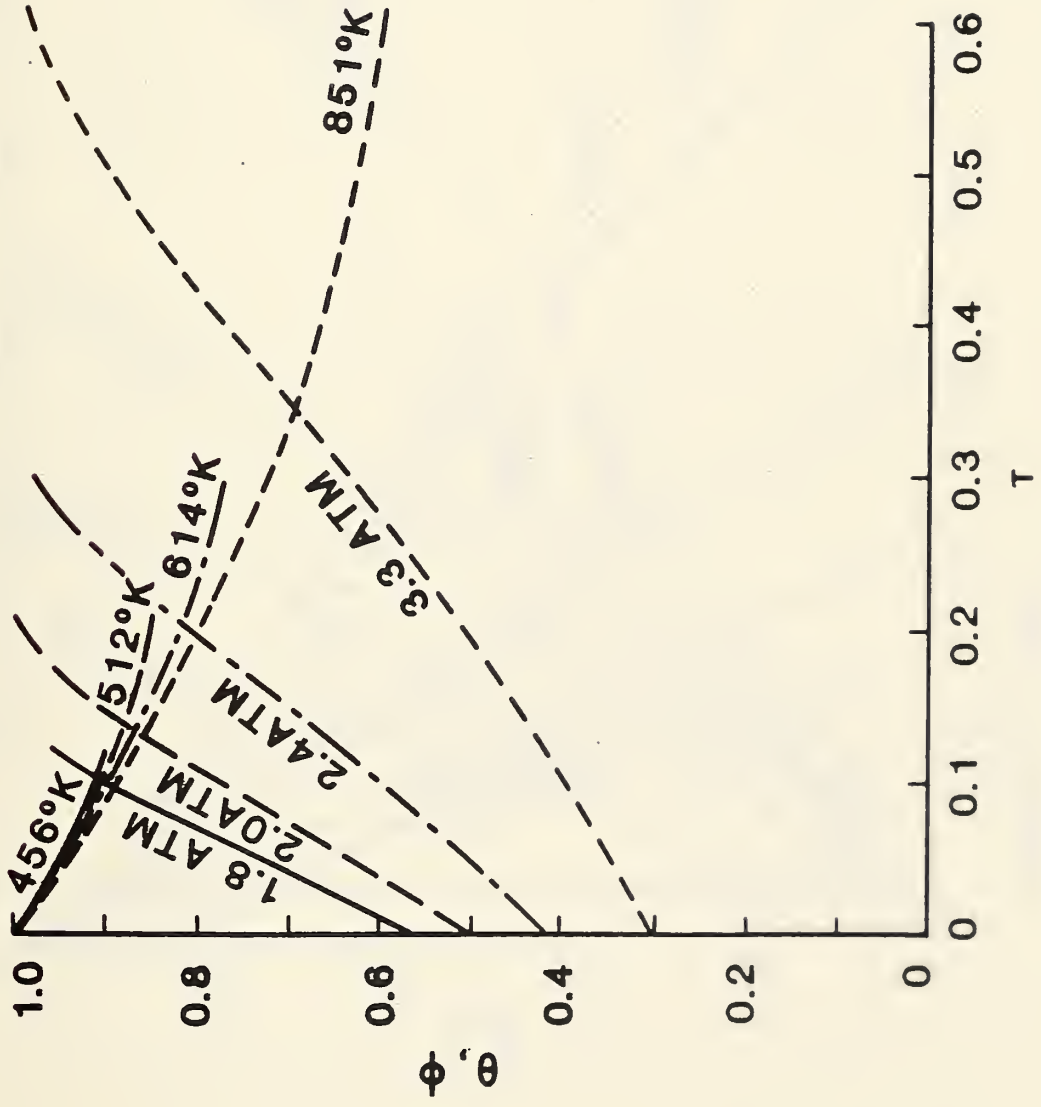


Figure A7.  $\theta, \phi$  vs.  $\tau$  for various  $\gamma$ , 200.0 m<sup>3</sup> volume, 1.0 m<sup>2</sup> vent area, and 15.0 kg of TNT.

$\bar{Y}$   
 11/9  
 9/7  
 7/5  
 5/3

$\theta, \phi$  VS.  $\tau$  FOR VARIOUS  $\bar{Y}$

Volume = 200.0 m<sup>3</sup>

Vent area = 1.0 m<sup>2</sup>

50.0 kg of TNT

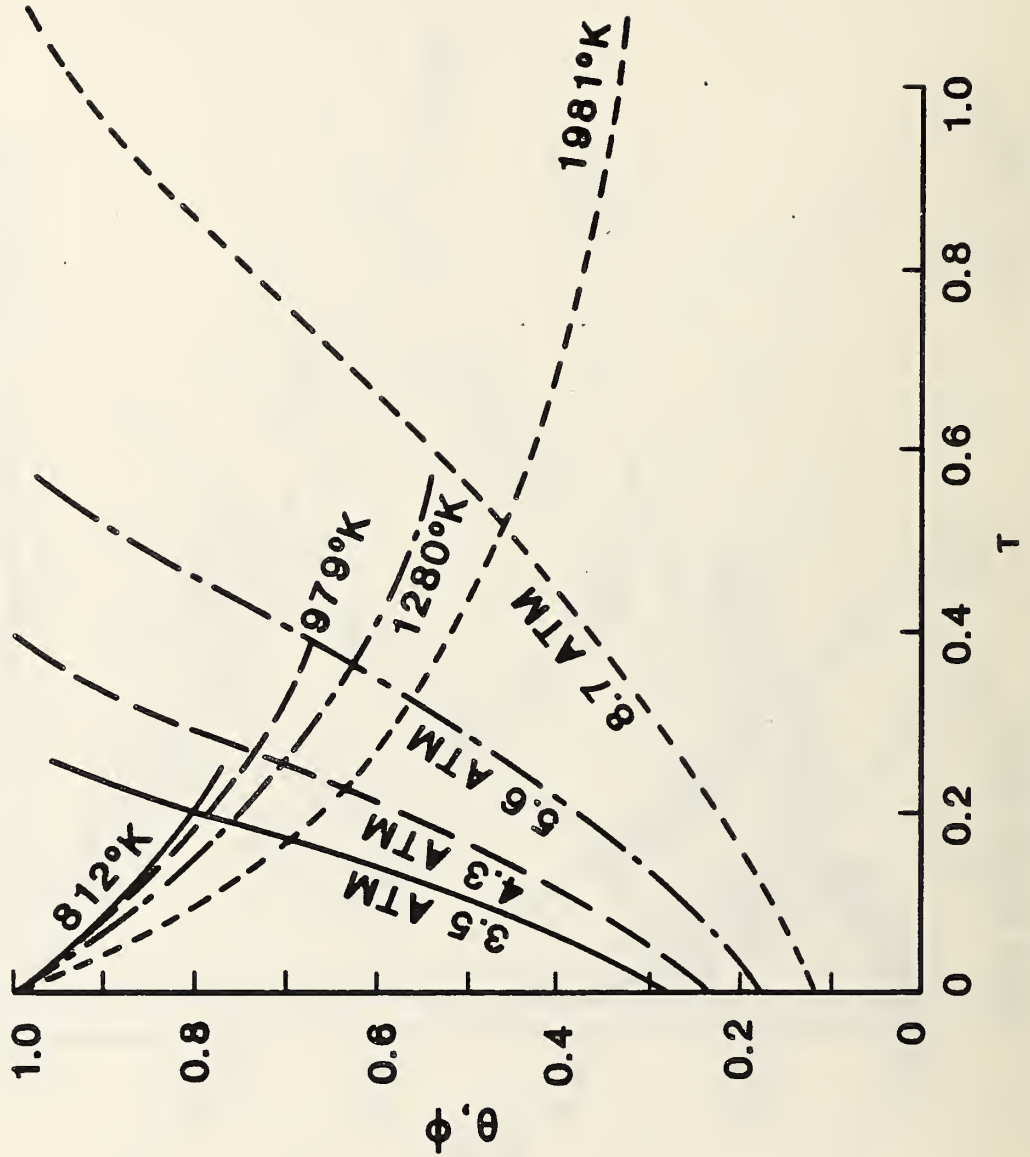


Figure A8.  $\theta, \phi$  vs.  $\tau$  for various  $\bar{Y}$ , 200.0 m<sup>3</sup> volume, 1.0 m<sup>2</sup> vent area, and 50.0 kg of TNT.

$\theta, \phi$  vs.  $\tau$  FOR VARIOUS  $\gamma$   
 Volume  $\approx 200.0 \text{ m}^3$   
 Vent area  $\approx 1.0 \text{ m}^2$   
 100.0 kg of TNT

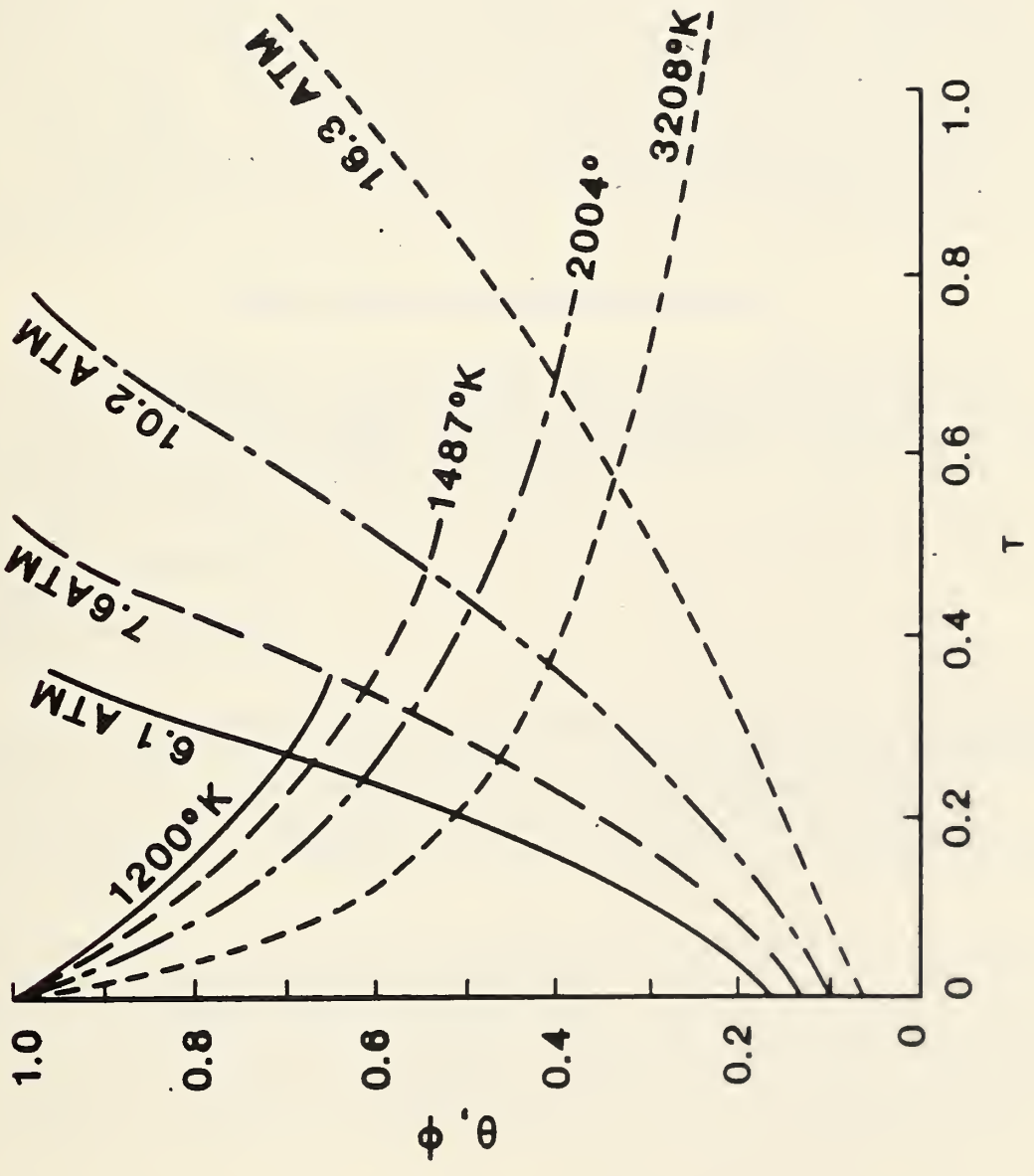


Figure A9.  $\theta, \phi$  vs.  $\tau$  for various  $\gamma$ ,  $200.0 \text{ m}^3$  volume,  $1.0 \text{ m}^2$  vent area, and  $100.0 \text{ kg}$  of TNT.

APPENDIX B

SLIDE-RULE ESTIMATES OF FIRE GROWTH

by

J.R. Lawson and J.G. Quintiere

## 1. Introduction

The purpose of this paper is to provide an analytical basis for estimating the growth of fire in compartments and its consequences. All prediction methods have been selected to allow for solutions to be made using programmable scientific calculators or pocket computers. The paper consists of a series of equations or data each of which describes a particular process in a fire's growth. Only minor discussions of theory are presented to provide some understanding of concepts related to the problem in question. For more information on each process discussed, refer to the appropriate reference materials. The equations presented will apply only to specific fuels or conditions and hence will be approximate when used for more complex or different situations. Also, any consideration of these equations as constituting a dynamic interacting fire system will be filled with inconsistencies. Nevertheless, this series of equations can provide a reasonable sense of the quantitative features of fire growth. It will relate to material type - solids or liquids - not specific materials. For specific materials other than those addressed in the text, one would have to acquire data that is unique to the materials being studied. Moreover, the state-of-the-art does not fully allow for fire predictions of specific materials.

## 2. Fire Size and Growth Rates

In order to make fire growth predictions, one must make a basic assumption about what material is burning. This assumption is used to calculate an estimated burning rate for the model and is a key factor for calculating other fire characteristics associated with fire growth. The four basic types of fuels identified with fire are usually classed as:

- A. Solids (non-metals)
- B. Liquids
- C. Electrical Equipment
- D. Metals

In this paper we shall consider only some representative ways of estimating Class A and Class B materials. For Class A we will consider first a wood crib as representative of a complex structure; then a solid surface like a mattress, chair or slab of material. For Class B materials, a method for estimating burning rates is suggested and input data will be provided for some common liquid fuels.

In 1976, Delichatosios reported work accomplished on the study of fire growth in wood cribs [1]. In his work, it was shown that a simple model could be used to predict fire growth rates for wood cribs. This model is put to use in this report for the same purpose. The model pays particular attention to crib geometry, surface area exposed for burning, and the wood's thermal properties. The equation used for estimating burning rate,  $\dot{m}_f$ , for cribs ignited in the center is,

BURNING RATES FOR WOOD CRIBS.

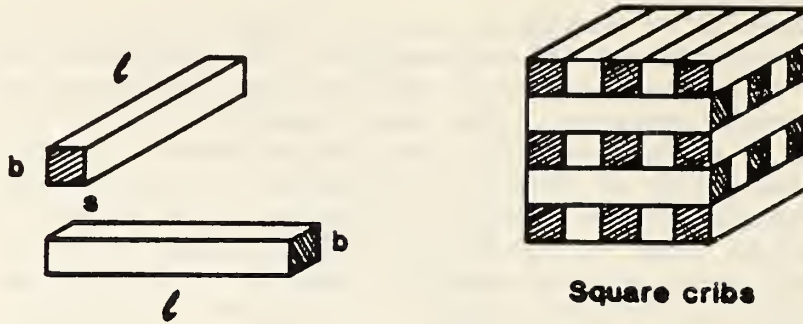


Figure B1. Sketch of a Wood Crib.

$$\dot{m}_f = \dot{m}'' A_s \frac{\pi}{2} \cdot \frac{t}{t_0}^2 \text{ for } t \leq t_0 \quad (1)$$

$\dot{m}''$  - specific burning rate found by:  $\dot{m}'' = cb^{-1/2} f(P)$  where

$$c \sim 10^{-3} \text{ g/cm}^{3/2} \cdot \text{s}$$

$b$  - wood stick thickness (cm)

$f(P)$  - found in Figure B2

$$P = A_v s^{1/2} b^{1/2} A_s$$

$A_s$  - total exposed surface area of wood in the crib =  $4lbnN$  where

$l$  - stick length (cm)

$s$  - stick spacing (cm) =  $l - nb$

$n$  - sticks per crib layer

$N$  - layers of sticks in crib

$A_v$  - total shaft cross-sectional area =  $s^2 \cdot (\text{number} = (n-1)^2)$  of shafts)

$t$  - time in seconds

$t_0$  - time for flames to spread to the outer edge of crib =  $n/(\sqrt{2} \xi)$

$$\xi \sim 0.045 \text{ s}^{-1}$$

$$\dot{m}_f = A_s cb^{-1/2} f(P) \text{ for } t > t_0 \quad (2)$$

where  $f(P)$  is plotted in Figure B2 and when  $P > 0.07$ ,  $f(P) = 1$ .

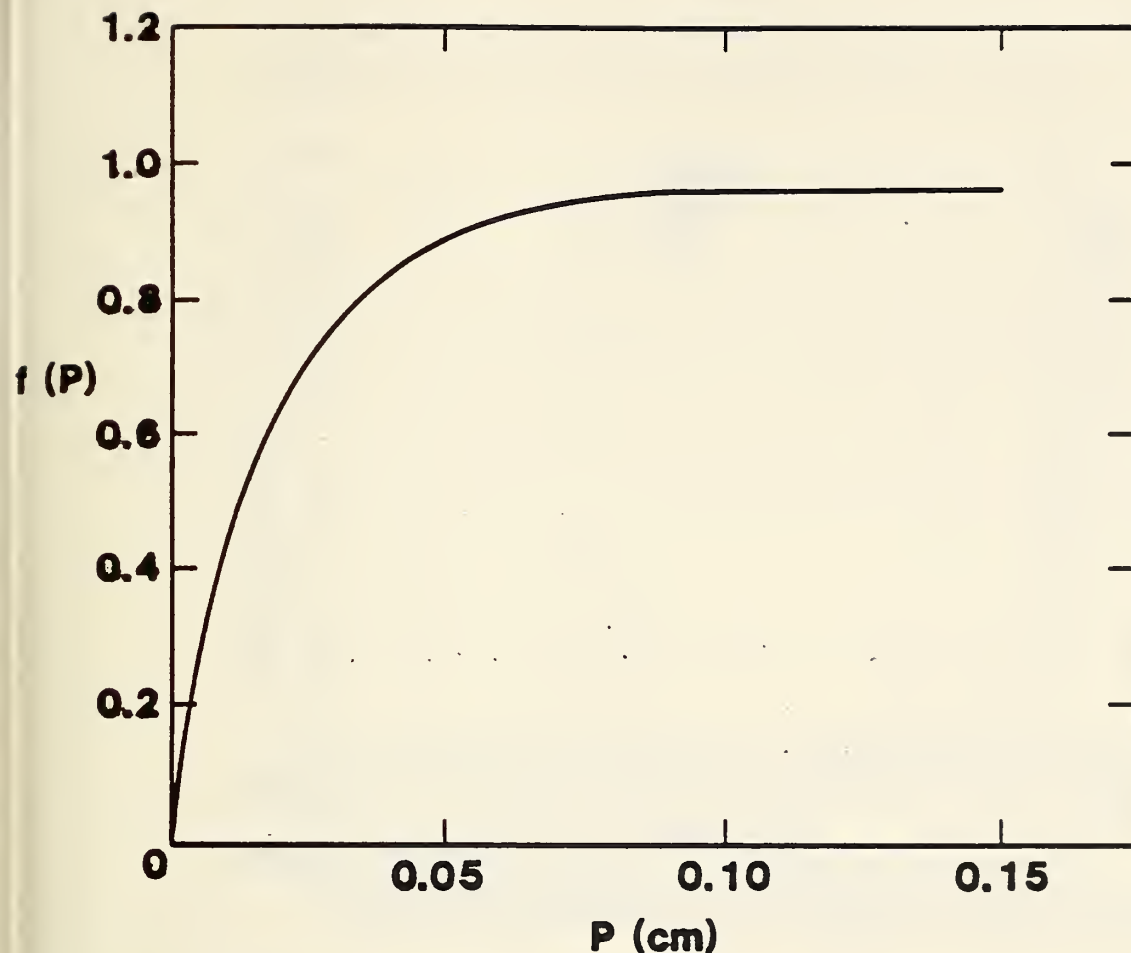


Figure B2. Reduced specific burning rate as a function of the crib porosity for ponderosa pine wood cribs (taken from Heskestad) [2].

BURNING RATES FOR FURNISHINGS. With more complex solids like furnishings, representative data is drawn from a report by Lawson, et al. [3]. Figure B3 exhibits the mass loss rate for a typical stuffed chair and Figure B4 provides data on a typical three seat sofa. Mass loss rate data for burning mattresses is obtained from a report published in 1977 by Babrauskas [4]. Figure B5 presents data for cotton and mixed fiber core mattress specimens. Data from these and other reports can be substituted in for calculations on burning rates for furnishings. Furnishings are complex solids that do not currently lend themselves to simple fire modeling, other common solid materials do.

BURNING RATES FOR PLASTIC POOL FIRES. The burning rate for polyurethane foam was estimated with the following pool fire model developed by Orloff [5].

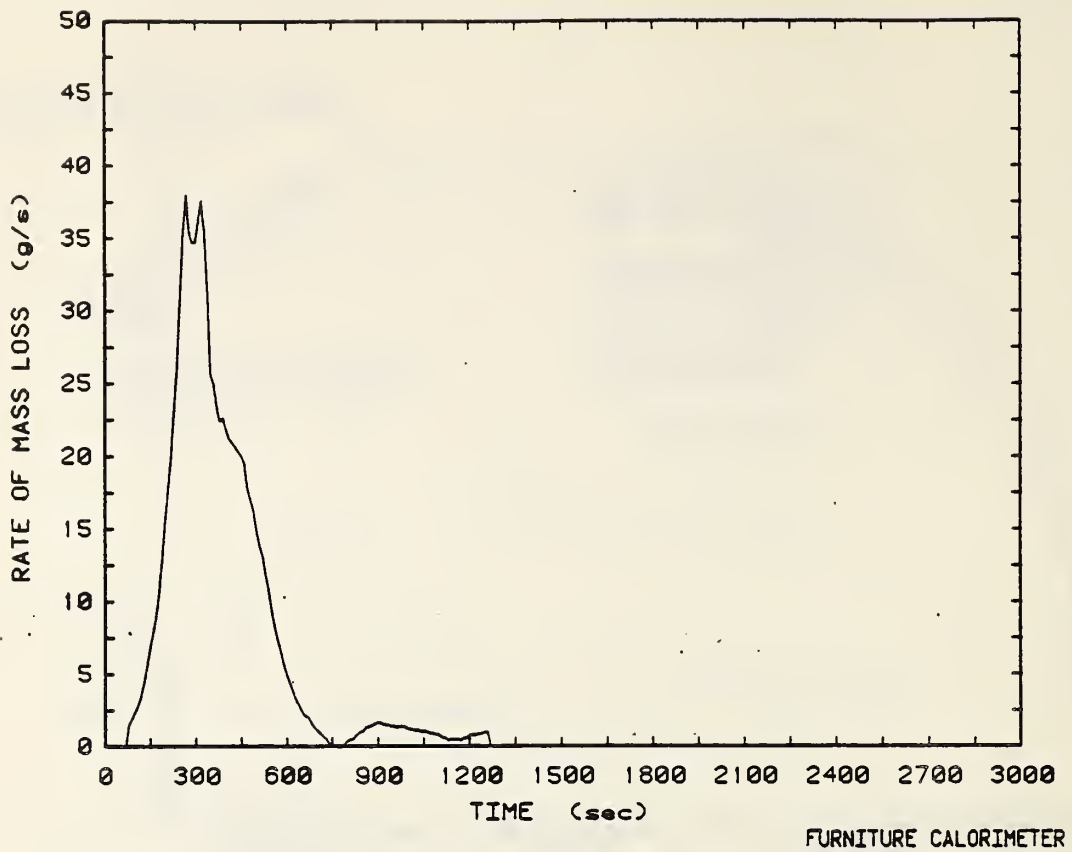
$$\dot{m}_f = \alpha e^{(\alpha t - \beta)} \text{ g/s} \quad (3)$$

where  $\alpha = 0.033 \text{ s}^{-1}$

$\beta = 1.29$  (corresponds to a time shift of 30.35 which accounts for a particular ignition character in this experiment)

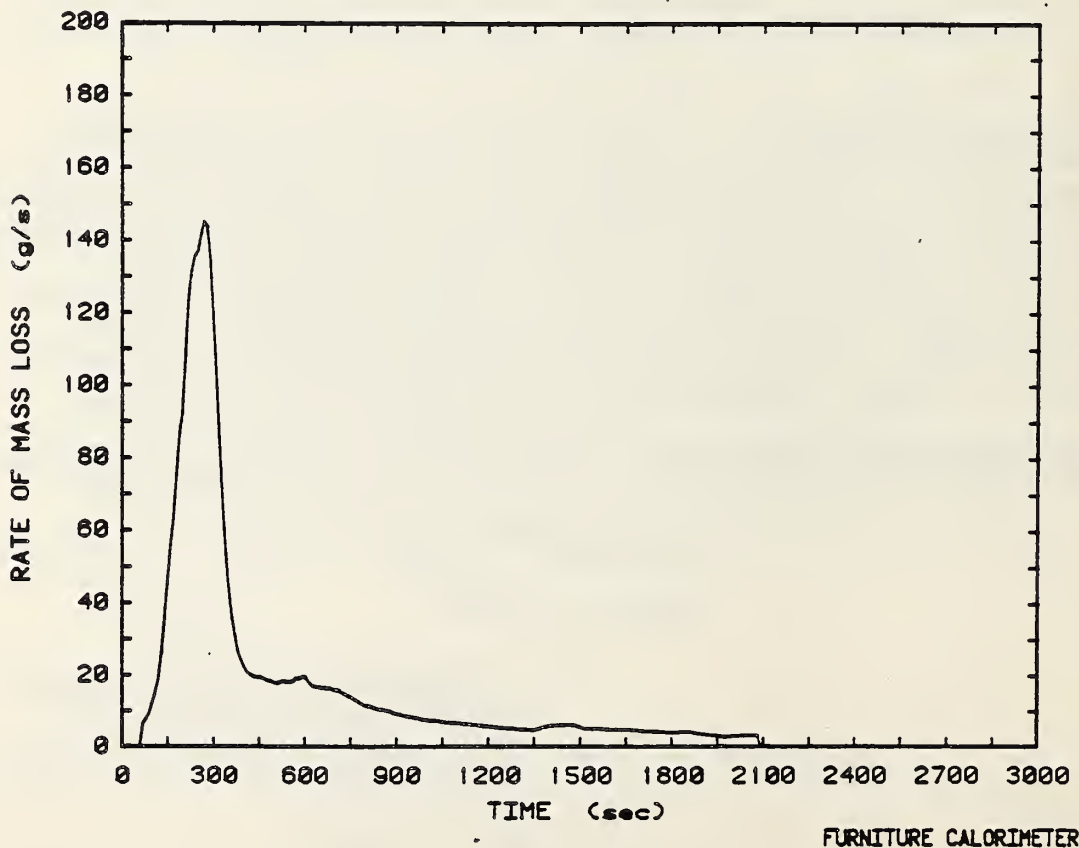
$t =$  time in seconds

for the period  $80 < t < 170 \text{ s}$ .



FURNITURE CALORIMETER

Figure B3. Rate of mass loss plot for easy chair [3].



FURNITURE CALORIMETER

Figure B4. Rate of mass loss plot for sofa with "California foam" cushions [3].

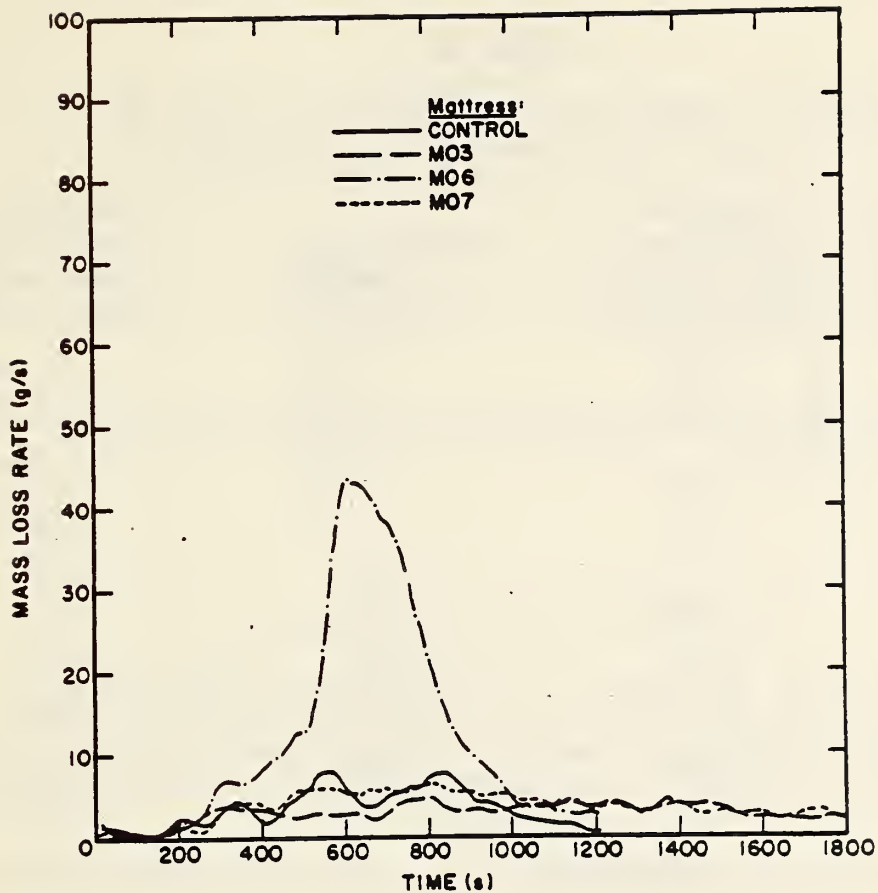


Figure B5. Weight loss for cotton and mixed fiber core specimens [4].

A review of data from furniture fires [3] indicates that for polyurethane foam chairs, Eq. (3) may also produce useful estimates for  $t > 170$  s.

Modak and Croce [6] studied the burning of polymethyl methacrylate (PMMA) plastic pool fires and found that experimentally measured burning rates per unit area,  $\dot{m}''(t)$ , at time  $t$  after ignition were correlated by the equation:

$$\frac{\dot{m}_s'' - \dot{m}''(t)}{\dot{m}_s'' - \dot{m}_i''} = e^{-t/\tau} \quad (4)$$

Therefore  $\dot{m}''(t)$  can be estimated by,

$$\dot{m}''(t) = - [e^{-t/\tau}(\dot{m}_s'' - \dot{m}_i'') - \dot{m}_s''] \quad (5)$$

where  $\dot{m}_i'' \approx 4 \text{ g/m}^2\text{s}$  is the average burning rate per unit area;  $\dot{m}_s''$  is the steady burning rate, and  $\tau$  is the characteristic "gasification time" to reach steady state.

Table B1 contains data that can be used for calculating  $\dot{m}''(t)$  for various size pools of PMMA.

Table B1

Results for PMMA Pool Fires of Varying Scale [6]

| Pool area<br>m <sup>2</sup> | Measured<br>steady<br>burning rate<br>per unit area<br>$\dot{m}''_s$<br>(g/m <sup>2</sup> s) | Gasification<br>time<br>parameter <sup>b</sup><br>$\tau$<br>(s) | Radiative<br>fraction of<br>total heat<br>release rate<br>$\chi$<br>(-) |
|-----------------------------|--|---|---|
| 2.58 x 10 <sup>-3</sup>     | 4.6  | NA  | 0.28 <sup>c</sup>   |
| 5.81 x 10 <sup>-3</sup>     | 5.6  | NA  | 0.32 <sup>c</sup>   |
| 0.0232                      | 7.7 <sup>b</sup>   | 3448  | 0.32 <sup>c</sup>   |
| 0.0523                      | 9.0 <sup>b</sup>   | 1587  | 0.42  |
| 0.0929                      | 17.4 <sup>b</sup>  | 1136  | 0.42  |
| 0.3716                      | 18.0   | 500   | 0.42  |
| 0.5806                      | 18.25  | 357   | 0.42  |
| 1.4865                      | 20.0   | 118   | 0.42  |

<sup>b</sup>Best fit.<sup>c</sup>Varied with time.

NA not available.

BURNING RATES FOR LIQUID POOL FIRES. In order to estimate burning rates for liquid pool fires, data were taken from a report by Burgess, et al. [7]. Their study shows the burning rate for a number of liquid fuels is a function of pool diameter. But for large diameter pools, flame radiation dominates and a maximum burning rate is achieved. Empirically they suggest that this maximum burning rate can be found by

$$\dot{m}''_{\max} = \left( 6.5 \times 10^{-3} \frac{\text{cm}}{\text{min.}} \right) \rho \Delta H_c / \Delta H_v \quad (6)$$

where  $\rho$  is the liquid density

$\Delta H_c$  is the heat of combustion, and

$\Delta H_v$  is the heat of vaporization.

Some specific results are given below in Table B2 for pool diameters greater than 1.5 m.

Table B2

Burning Rates for Liquid Pool Fires.

| Liquid      | $\dot{m}_{\max}''$<br>(g/m <sup>2</sup> s) | $\chi_r$ , flame radiation fraction<br>(%) |
|-------------|--|--|
| n-Hexane    | 76.9                                       | 42   |
| Benzene     | 87.9                                       | 35   |
| UDMH        | 44.3                                       | 24   |
| Methanol    | 15.8                                       | 15   |
| Gasoline    | 45.  | -  |
| Diesel fuel | 43.  | -  |

3. Radiant Heat Flux to a Target

After the initial fire has been defined, it is important to know something about the heat radiated from the source that could cause secondary ignitions. A technique discussed by Modak [8] will be used to estimate radiant flux. This method is depicted in the sketch below and is detailed in Eq. (7).

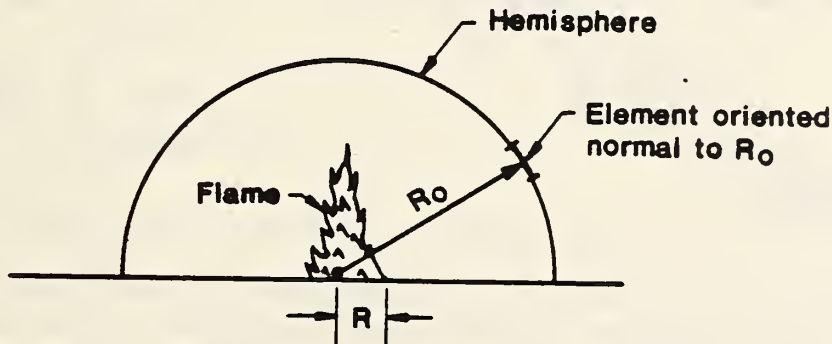


Figure B6. Fire radiant heat transfer to a target.

The incident heat flux at a target can be approximated as

$$\dot{q}_0'' \approx P/4\pi R_0^2 \quad (7)$$

where P is the total radiative power output of the flame. P can be represented as  $\chi_r Q$  where  $\chi_r$  is the radiative fraction and Q is total energy release rate. Usually  $\chi_r$  ranges from 20 to 45 percent for many fuels. For a typical pool fire Modak [8] finds that the above formula is > 90 percent accurate when  $R_0/R > 4$ . At  $R_0/R = 2$ , the approximation is about 80 percent correct.

#### 4. Flame Height

Since burning rates and thermal radiation to targets have been defined, a third physical phenomenon relating to flame geometry must be considered. Flame height is an important characteristic which provides information needed for estimating heat transfer to a room's ceiling and other structures that may be located above a fire. It has been shown by McCaffrey [9] that flame height,  $Z_f$ , is related to the total energy release rate,  $Q$ , and the diameter,  $D$ , of the fire base. This is illustrated in Figure B7 which is taken from a report by Zukoski, et al. [10].

For flame heights where  $(Z_f/D) > 2$ , Zukoski suggested the following equation which provides a reasonable estimate:

$$Z_f = [0.23 \text{ m/kW}^{2/5}] Q^{2/5}, \quad (8)$$

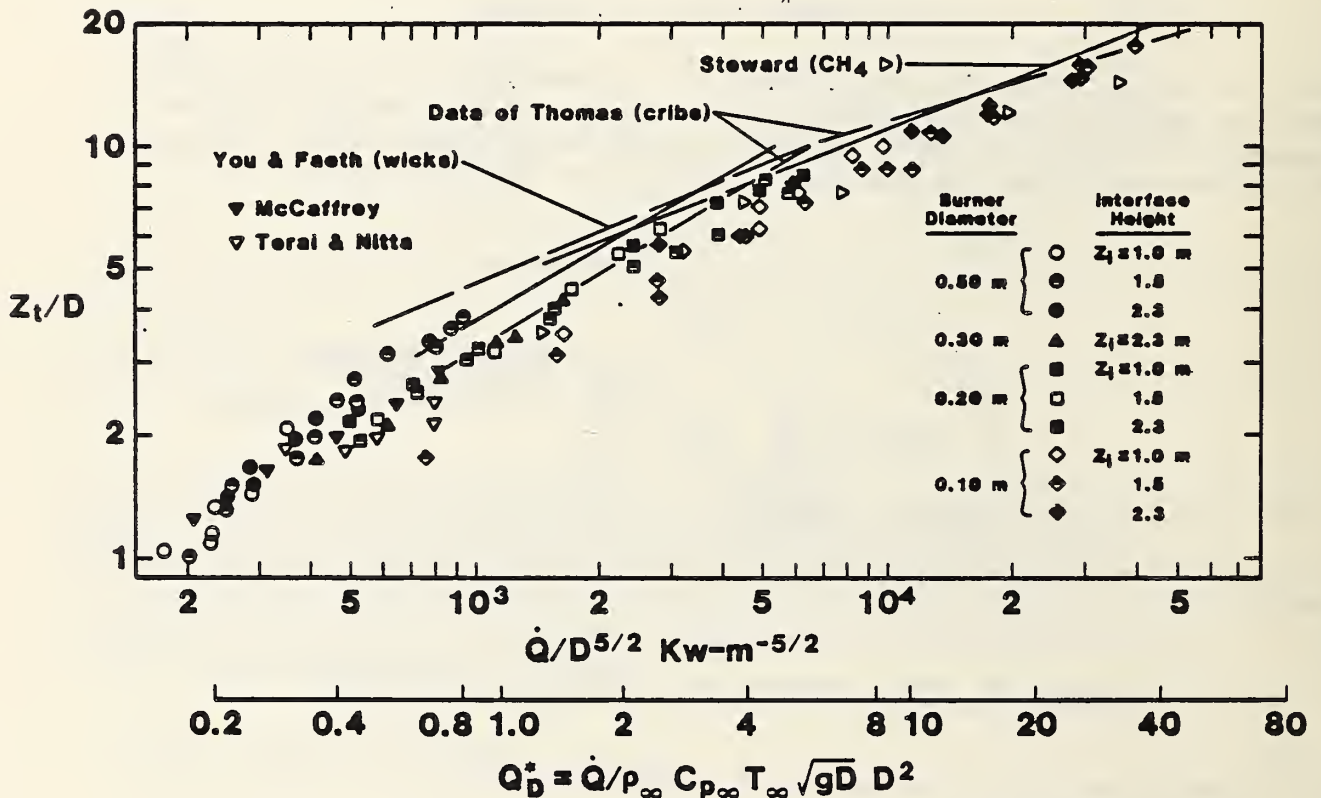
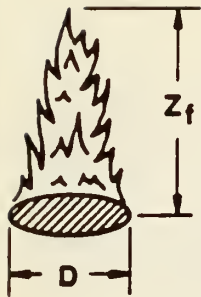


Figure B7. Flame height dependence on heat release parameters [10].

or use Figure B7 directly.

In addition, work reported by Hasemi and Tokunaga [11] for a 0.5 m diameter burner showed that the height of the continuous flame region could be estimated by



$$Z_{f \text{ min}} = (0.11 \text{ m/kW}^{2/5}) \dot{Q}^{2/5} \quad (9)$$

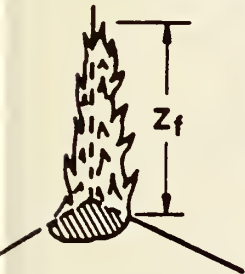
and the height to the flame tip could be estimated by

$$Z_{f \text{ max}} = (0.21 \text{ m/kW}^{2/5}) \dot{Q}^{2/5} \quad (10)$$

Figure B8a. For Open Flames.

These results are consistent with Eq. (8) and Figure B7, but explicitly address the variation of the flame structure from a continuous luminous region to a region above which is intermittent flames terminating at the flame "tip".

Their work also provides equations that are useful in estimating flame heights in a corner fire scenario. See Figure B8b. Equations (11) and (12) provide these estimates.



$$Z_{f \text{ min}} = (0.075 \text{ m/kW}^{2/5}) \dot{Q}^{3/5} \text{ for the continuous flame} \quad (11)$$

$$Z_{f \text{ max}} = (0.118 \text{ m/kW}^{2/5}) \dot{Q}^{3.5} \text{ for the flame tip} \quad (12)$$

Fig. B8b. Corner Fire Scenario.

### 5. Radial Flame Impingement and Heat Flux to a Ceiling

Now that flame height has been estimated, it is possible to estimate radial flame impingement on a ceiling and heat flux at a ceiling using equations offered in a report by You and Faeth [12]. When the height of a free burning flame exceeds the height of the ceiling, flame impingement would occur for that fire burning in a confined geometry. That effect is shown in Figure B9 where  $H_R$  gives the radial flame impingement length.

It has been found [12] that the height ( $H_f$ ) of a free burning fire in the open generally exceeds the sum of the ceiling height ( $H$ ) and impingement length ( $H_R$ ) under these conditions. Thus, for a given fire energy release rate  $\dot{Q}$ , once  $H_f$  exceeds the ceiling height, the radial flame extension can be estimated from the following formulae.

For a ceiling with no side walls,

$$\frac{H_R}{D} = 0.5 [(H_f - H)/D]^{0.96}; \quad (13)$$

and for a ceiling with side walls,

$$\frac{H_R}{D} = 0.69 [(H_f - H)/D]^{0.89} \quad (14)$$

where  $D$  is the fire base diameter and  $H_f$  can be found from Eq. (8). (Here  $Z_f$  and  $H_f$  are the same; since we have not attempted to unify our notation but have retained the notation of the original source.)

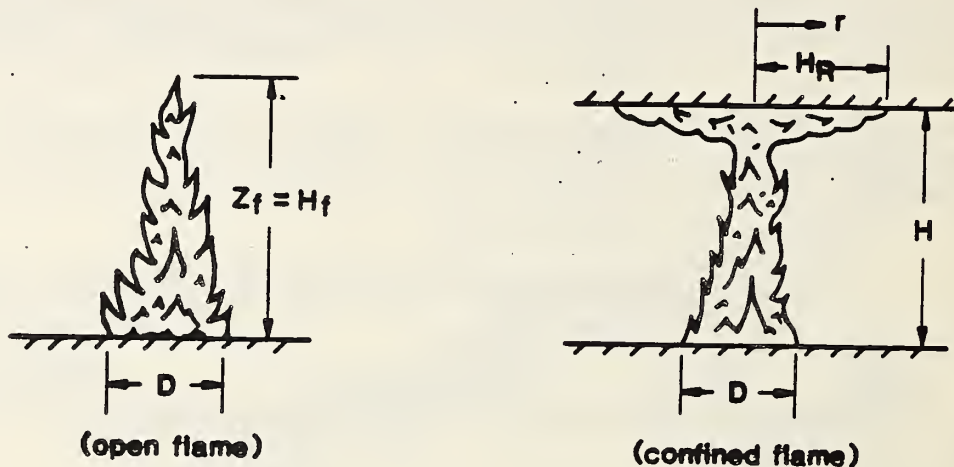


Figure B9. Flame length and geometric environment.

From the work of You and Faeth [12] an estimate of the incident (primarily convective) heat flux to the ceiling just above the fire can be found. This stagnation point heat flux  $\dot{q}''$  is determined from the correlation:

$$\dot{q}'' H^2 / Q = 31.2 Pr^{-3/5} Ra^{-1/6} \quad (15a)$$

where  $H$  is the ceiling height and  $Q$  is the fire energy release rate. The equation was established for a Prandtl number of,  $Pr = 0.7$ ,  $H_f/H < 1.5$ ,  $10^9 < Ra < 10^{14}$ , and where flame radiative heat flux is small. The Rayleigh number,  $Ra$ , is defined as  $(g\beta/\rho c_p \nu^3) = 7.9 \times 10^{12} \text{ kW}^{-1} \text{ m}^{-2}$ .

$$\dot{q}'' = 0.28 Q^{5/6} H^{-7/3} \quad (15b)$$

where  $Q$  is in kW and  $H$  is in m. Much of the data correspond to low  $Ra$ , or small scale so this formula may yield perhaps low estimates on extrapolation to large scale. For  $H_f/H > 1.5$ , they found the stagnation point heat flux to decrease significantly from the above formula. For large flames, flame radiation should be added, and also hot layer gas and surface radiation should be included after the room becomes hot ( $> 300^\circ\text{C}$ ).

## 6. Smoke Filling of a Room

At this point in the calculation process, the basic fire has been characterized, and it is time to direct attention to changes in environmental conditions which result from the fire. In this section, estimates will be made on smoke filling time for a room. The "filling time",  $t_f$ , can be estimated as follows, i.e.,  $t_f$  = time for the layer to reach a door soffit (see Figure B10) or a floor leak as in the case examined by Zukoski [13]. Figure B11 illustrates the dependence of ceiling layer height on time and heat input rate. For these results, heat loss from the smoke layer is neglected, and the room filling times are somewhat shorter than would be expected in a real fire. The governing equation and notation from Zukoski's analysis [13] are described below.

### Smoke Filling Time

$$\frac{dy}{dt} + Q^* + \alpha (Q^*)^{1/3} y^{5/3} = 0 \quad (16)$$

where

$$y = Z/H \quad \text{nondimensional height of smoke layer interface} \quad (17)$$

$$\tau = t \sqrt{g/H} \quad (H^2/S) \quad \text{nondimensional time} \quad (18)$$

$t$  = time

$g$  = acceleration of gravity  $9.8 \text{ m/s}^2$

$H$  = room height

$S$  = floor area of the room

$$Q^* \equiv Q / (\rho_\infty T_\infty C_p \sqrt{gH} H^2) \quad \text{which is a nondimensional fire heat input parameter.} \quad (19)$$

$Q$  = energy release rate of the fire

$\rho_\infty$  = density of the air in room

$C_p$  = specific heat at constant pressure for air

$\alpha$  =  $1/5.4$ , the mass entrainment coefficient

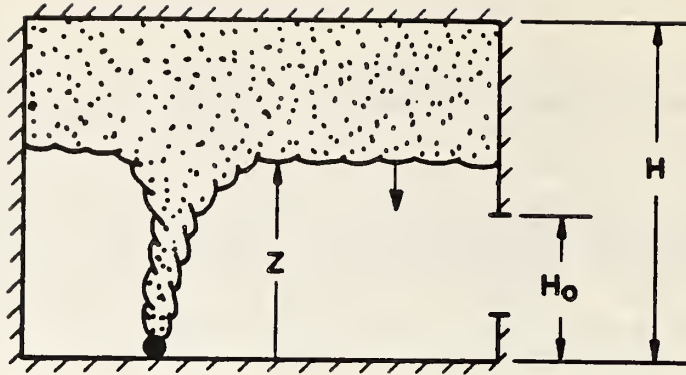


Figure B10. Room smoke filling model.

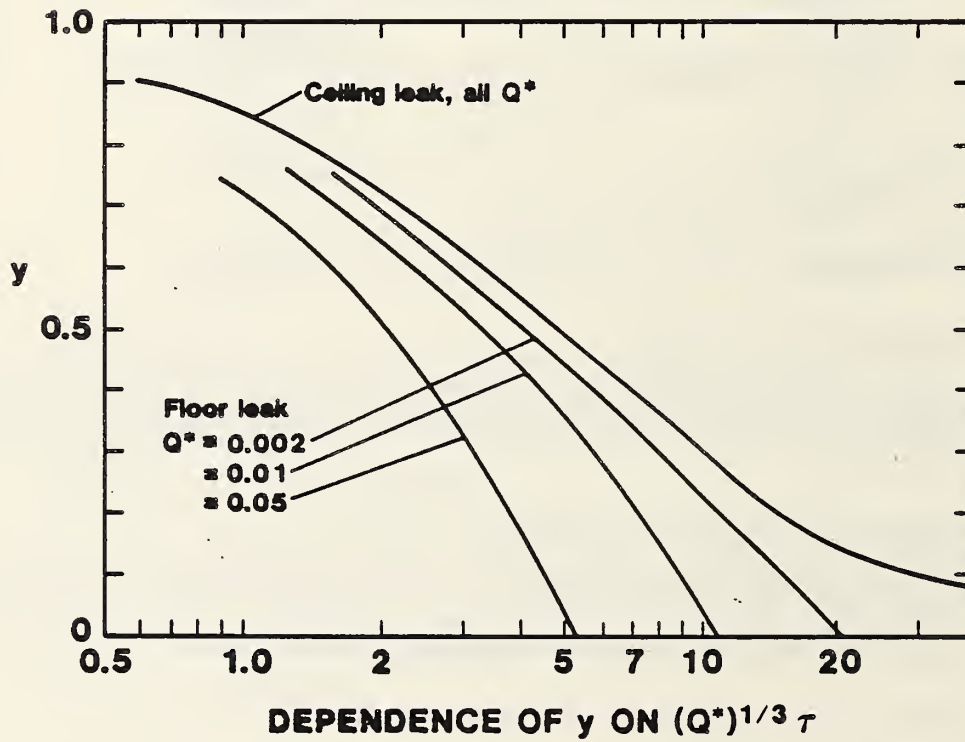


Figure B11. Ceiling layer height versus time and heat input rate [13]

In Eq. (16), if  $Q^*$  is small,  $< 0.01$

$$y = [1 + \frac{2\alpha}{3}(Q^*)^{1/3} \tau]^{-3/2} \quad (20)$$

and if  $Q^*$  is large,  $> 0.4$ ,

$$y \approx 1 - Q^* \tau \quad (21)$$

To solve for  $t_f$  when  $Q^* < 0.01$ , Eq. (20) is solved for  $\tau$ ,

$$\tau \approx \frac{\left(\frac{1}{y}\right)^{2/3} - 1}{\left(\frac{2\alpha}{3}\right) (Q^*)^{1/3}} \quad (22)$$

The time  $t_f$  to fill to a specific position  $y$  is then found by inverting Eq. (18) as follows:

$$t_f = \frac{\tau}{\sqrt{g/H} (H^2/s)} \quad (23a)$$

Smoke layer height from the floor,  $Z$ , can be calculated by Eq. (23b)

$$Z = H \left[ 1 + \left(\frac{2\alpha}{3}\right) \left( \frac{\dot{Q}}{\rho_\infty T_\infty C_p \sqrt{gH} H^2} \right) \left( t \sqrt{g/H} \frac{H^2}{s} \right) \right]^{-3/2} \quad (23b)$$

To solve for  $t_f$  when  $Q^* > 0.4$ , Eq. (21) is solved for  $\tau$ ,

$$\tau \approx \frac{1 - y}{Q^*} \quad (24)$$

and then solved for  $t_f$  again using Eq. (23).

In cases where  $0.01 < Q^* < 0.4$  one must integrate the ordinary differential Eq. (16) or use Figure B10.

## 7. Time to Carbon Monoxide Hazard With Smoldering Fires

The previous section presented a method for estimating smoke filling in a room when an opening is present in a wall or a leak is near the floor. This section uses smoke filling time and other data to estimate hazard time related to carbon monoxide exposure which results from a smoldering chair. Equations used in this estimate are taken from a report by Quintiere et al. [14]. In that analysis the smoke filling time is calculated using Eqs. (16) through (23) where the value of  $\dot{Q}$  is estimated by

$$\dot{Q} = \dot{m} \Delta H \quad (25)$$

where  $\dot{m}$  is the rate of mass loss due to smoldering and  $\Delta H$  is the heat of reaction for the smoldering process. Here we adopt a simpler procedure based on that study to allow ease in making first order estimates.

It is shown that  $\dot{m}$  could be approximated for a smoldering fire in polyurethane or cotton using

$$\dot{m} = ct \quad (26)$$

where  $c = 0.206 \text{ gm min}^{-2}$  for polyurethane and  $c = 0.33 \text{ gm min}^{-2}$  for cotton, and  $t$  represents time in minutes. The heat of reaction for polyurethane is  $\Delta H = 15 \pm 8 \text{ kJg}^{-1}$  and cotton is  $\Delta H = 11 \pm 1 \text{ kJg}^{-1}$ . These results were only for slabs of particular samples of cotton and polyurethane. Moreover the smoldering rate of an upholstered chair composed of cotton and polyurethane initially grew quadratically with time, then remained constant for the next hour. Thus, Eq. (26) with the constants given can only be taken as a rough estimate for  $\dot{m}$ . It was, however, found that the mass generation rate of CO could be taken as proportional to the mass loss rate in smoldering, and that constant  $\gamma$  was estimated as about  $0.1 \text{ g CO/g fuel lost}$  for both the polyurethane and cotton samples discussed above. Thus for those cases the CO generation rate was estimated as

$$\dot{m}_{\text{CO}} = \gamma ct. \quad (27)$$

As a first estimate we will use Eq. (27) and consider a well-mixed closed volume ( $V$ ) in which the smoldering takes place. The more general stratified case with "filling" was discussed in ref. [14], but in actuality the dispersal of smoldering products is not so well defined. Consequently a uniformly mixed volume is reasonable alternative. For this case the mass fraction of CO in the volume defined to be  $Y$  is given by

$$\frac{dY}{dt} = \frac{\gamma \dot{m}}{\rho V} \quad (28)$$

where  $\rho$  is the gas density. Finally adopting a critical dose of 4.5% CO-min for human incapacitation as suggested by the work of Stuart et al [14], and since the dose  $D$  can be expressed as  $D = \int_0^t Y dt$  it follows from Eqs. (26-28) that

$$D = \frac{c \gamma t^3}{6 \rho V} . \quad (29)$$

where  $D = 0.045 \text{ min}$  for the critical dose, the hazard time can be estimated.

Rewriting this equation to solve for  $t$

$$t = \left( \frac{6 D \rho V}{c \gamma} \right)^{1/3} \quad (30)$$

where  $V$  = volume of the room  
 $\rho$  = density of the gas  
 $c$  = values shown above for polyurethane and cotton  
 $\gamma$  = the mass fraction of CO produced per smoldering mass loss of fuel

For example, with a cotton sample  $t = 25.3 \text{ V}^{1/3}$  where  $t$  is in minutes and  $V$  is  $\text{m}^3$ . The time to critical dose is finally calculated using Eq. (30).

It should be emphasized that the above analysis is very approximate and not generally applicable to all smoldering conditions. It is only offered as a first-order of magnitude estimate.

## 8. Temperature Rise of Hot Gases in a Compartment

A second environmental condition that requires consideration in a room fire is the resulting temperature rise. This has been studied and correlated by several different investigations. The method for estimating temperature rise,  $\Delta T$ , here comes from reports by Quintiere [15] and McCaffrey, et al. [16]. This model considers temperature rise in compartments containing single or multiple wall vents, and the venting action is created only by natural convection. Figure B12 describes a compartment example and defines some parameters.

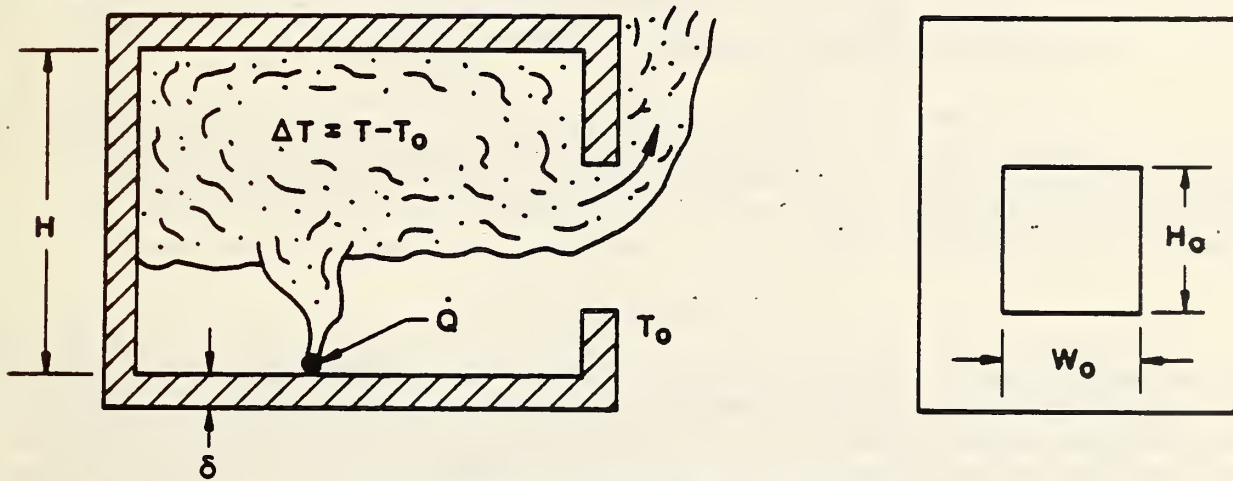


Figure B12. Compartment example.

The equation used for making this estimate of compartment gas temperature rise is

$$\frac{\Delta T}{T_0} = 1.6 \frac{\dot{Q}}{\sqrt{g} C_p \rho_0 T_0 A_0 \sqrt{H_0}}^{2/3} \frac{h_k A}{\sqrt{g} C_p \rho_0 A_0 \sqrt{H_0}}^{-1/3} \quad (31)$$

where  $T_0$  = initial or ambient air temperature

$\dot{Q}$  = rate of energy release

$g$  = acceleration of gravity  $9.8 \text{ m/s}^2$

$C_p$  = specific heat of air at constant pressure

$\rho_0$  = density of ambient air

$A_0 = W_0 H_0$ , vent area

$W_0$  = horizontal vent dimension

$H_0$  = vertical vent dimension

$$h_k = \begin{cases} \sqrt{k\rho c/t}, & t \leq t_p \text{ effective enclosure} \\ k/\delta, & t > t_p \text{ conductance} \end{cases}$$

$k$  = thermal conductivity of the enclosure structure

$\rho$  = density of the enclosure structure

$c$  = specific heat of the enclosure structure

$\delta$  = enclosure material thickness

$$t_p = \left(\frac{\rho c}{k}\right)\left(\frac{\delta}{2}\right)^2, \text{ thermal penetration time}$$

$A$  = total surface area

Both  $h_k A$  and  $A_0 \sqrt{H_0}$  should be summed for multiple structural materials and openings, respectively. The procedure for addressing multiple features is elaborated on in reference [15].

## 9. Ventilation Flow Rate

Now that methods have been presented for estimating burning rates and  $\Delta T$  in a fire compartment, it is time to consider ventilation flow rates in the fire. It was pointed out by Steckler, et al. [17] that the flow of air and gases in room fires has a significant influence on the development of a fire. As a fire develops, the air and gas flow rates control compartment temperature and heat transfer which then affects the rate of fire growth. When a compartment fire reaches a fully involved state, the air flow rate usually controls the fire, and the fire is then considered to be ventilation controlled. The mass flow rate of air and gases will be estimated first in this section, and ventilation limit conditions will be examined later.

In order to further understand the terminology of vent flow refer to Figure B13. Under natural convection conditions and after the hot gases fill the compartment and spill out of the vent, the flow will be countercurrent at the vent. Air will enter at a rate  $\dot{m}_1$  and combustion products will flow out at a rate  $\dot{m}_0$ . These flows result from pressure differences ( $\Delta p$ ) set up at the vent due to the differences in compartment and ambient gas temperatures. At the flow reversal point in the vent, the  $\Delta p$  is zero and this position is termed the neutral plane. The flow rates depend on the fuel mass release rate  $\dot{m}_f$ , the height of the neutral plane  $x_2$ , the height of the hot gas layer  $x_1$ , its temperature  $T$ , and the vent dimensions  $H_0$  and  $W_0$ . In general the vent equations are coupled nonlinear algebraic equations which we will avoid solving, but suggest the approximate procedure below.

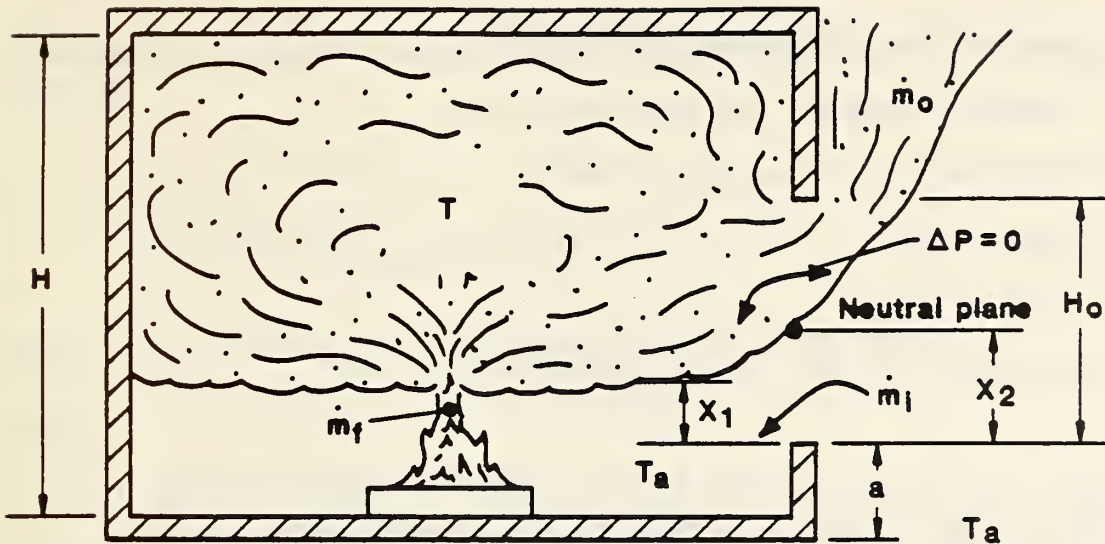


Figure B13. Sketch of compartment ventilation problem.

To make this ventilation flow rate estimate, it is necessary to assume a free burning condition. The first step in making this estimate is to calculate a fuel mass burning rate,  $\dot{m}_f$ , with one of the methods found in section 2, and then calculate the compartment gas temperature by the formula presented in section 8. At this point the dimensionless mass flow rate  $M_o$  can be calculated [18] using,

$$M_o = [\psi^{1/2}/(1 + \psi)] (1 - y_2)^{3/2} \quad (32)$$

where 
$$\psi \equiv \frac{T - T_a}{T_a}$$

and  $y_2 = x_2/H_o$  can be estimated as 0.5 to 0.6 for  $\psi \leq 1$  and for well-ventilated fires where  $\dot{m}_f/\dot{m}_i$  is small as found in reference [18]. For the case of larger  $\psi$  and  $\dot{m}_f/\dot{m}_i$  not small, the neutral plane can be estimated from the work of Kawagoe and Sekine [19] or from reference [18] in which  $x_1 = 0$ :

$$y_2 = \frac{1}{1 + \frac{T}{T_a}^{1/3} \left(1 + \frac{\dot{m}_f}{\dot{m}_i}\right)^{2/3}} \quad (33)$$

This will yield the lower limit for  $y_2$  when the hot layer tends to the floor and the enclosure tends toward a uniform gas temperature. Then mass flow rate out,  $\dot{m}_o$ , can be calculated using,

$$\dot{m}_o = \frac{2}{3} M_o C_{p_a} \sqrt{2g} W_o H_o^{3/2} \quad (34)$$

where  $C$  = opening flow coefficient which is  $\sim 0.7$

$\rho_a$  = density of ambient gas surrounding area

$g$  = acceleration of gravity ( $9.8 \text{ m/s}^2$ )

$W_o$  = opening width

$H_o$  = opening height

The mass inflow rate of air,  $\dot{m}_1$ , can be calculated by,

$$\dot{m}_1 = \dot{m}_o - \dot{m}_f \quad (35)$$

for which steady flow conditions have been assumed. Of course if  $\dot{m}_f/\dot{m}_1$  is found to be large, then iteration is required in the above computations. Moreover the ratio  $\dot{m}_f/\dot{m}_1$  should be compared with the mass stoichiometric fuel to air ratio to examine whether the fire is ventilation limited. We will return to this point shortly.

#### 10. Does Flashover Occur?

The methods presented have provided a basis for predicting the fire environment up to the point of rapid transition in fire behavior. This critical point is called "flashover", and it has been defined in many different ways. A paper by Thomas, et al. [20] describes five different processes or combinations of processes that could lead to flashover. It is pointed out that flashover usually results in a sharp increase in room temperature and rate of energy release. Thomas shows that flashover is typically associated with compartment gas temperatures which range between  $300\text{--}650^\circ\text{C}$ . For the flashover estimates calculated in this paper it is suggested that a critical gas temperature rise of  $500^\circ\text{C}$  be selected. Thus for a given  $\dot{Q}(t)$  the formulae for  $\Delta T$ , given by Eq. (31), can be solved to find the time,  $t$ , at which  $\Delta T = 500^\circ\text{C}$  or the "flashover" time.

Alternatively, the condition for flashover with a constant energy release rate  $\dot{Q}$  follows from Eq. (31) in which  $\Delta T$  is set equal to  $500^\circ\text{C}$ . That result is given as

$$\dot{Q} = 610 (h_k A A_o \sqrt{H_o})^{1/2} \quad (36)$$

for which  $\dot{Q}$  is in kW,  $h_k$  is in  $\text{kW}/(\text{m}^2\text{K})$ ,  $H_o$  in m, and  $A$  and  $A_o$  are in  $\text{m}^2$ . This result says that the energy release rate to cause "flashover" depends on the compartment thermal properties, its surface area, and the vent size.

#### 11. Mass Burning Rate in Ventilation Limited Fires

After "flashover" or in fires where small openings restrict ventilation, the fire will probably become "ventilation limited." That is the supply of air to the room is less than that amount needed for stoichiometric burning of the available gasified fuel. It can also be defined as the point when the oxygen level in the compartment reaches a low value (ideally zero) such that the reaction between fuel and oxygen ceases to produce products or proceeds very slowly.

In general, the energy release rate of the fuel burning in the compartment, is given as

$$\dot{Q} = \begin{cases} \dot{m}_f \Delta H & \text{for } \dot{m}_f/\dot{m}_a \leq \gamma \\ (0.233) \dot{m}_a \Delta H_{\text{ox}} & \text{for } \dot{m}_f/\dot{m}_a \geq \gamma \end{cases} \quad (37)$$

where  $\gamma$  is the mass stoichiometric fuel to air ratio

$\Delta H$  is the fuel heat of reaction

$\dot{m}_a$  is the air flow rate through the vent

and  $\Delta H_{\text{ox}}$  is the heat of combustion per unit mass of oxygen and is taken as 13 kJ/g.

The fire is termed "fuel-controlled" for  $\dot{m}_f/\dot{m}_a < \gamma$ , and the energy release rate depends on the fuel pyrolysis rate. Since the air flow rate is primarily controlled by vent size, the available air supply will reach the limit for combustion as  $\dot{m}_f$  increases. Thus as the fire grows, the rate of energy release within the compartment will be governed solely by the air supply rate. The excess fuel will exit the compartment with combustion continuing in the vent flame. This limit condition in which the maximum possible energy release rate is achieved in the compartment roughly occurs when  $\dot{m}_f/\dot{m}_a = \gamma$  and the fire is termed "ventilation-controlled" as long as  $\dot{m}_f/\dot{m}_a \geq \gamma$ . Fires are generally fuel-controlled before the occurrence of flashover, and ventilation-controlled afterwards [20].

In order to estimate the point of transition to ventilation control, both the fuel mass loss rate and the air supply rate must be known. The mass loss rate  $\dot{m}_f$  depends on the enclosure conditions as illustrated qualitatively below:

$$\dot{m}_f \approx \dot{m}_{fo} \left( \frac{Y_{O_2}}{0.233} \right) + \frac{\dot{q}_e}{L} \quad (38)$$

where  $\dot{m}_{fo}$  - is the free burning value

$Y_{O_2}$  - is the local oxygen concentration around the combustion region within the enclosure

$\dot{q}_e$  - is the net heat transfer rate from the enclosure to the fuel

and  $L$  - is the fuel "heat of vaporization"

There is some evidence from full-scale experiments [14] that up to flashover or shortly before, the mass loss rate in an enclosure is nearly equal to its free burn value. After flashover, the mass loss rate will differ distinctly from its free-burn value. As a first estimate to assess whether the ventilation limit has been reached, the free burn mass loss rate should be compared with the maximum vent air flow rate. The latter can be estimated by using

Eqns. (32 and 33) for  $\dot{m}_f/\dot{m}_1 = 0$  (i.e., small). Thus, the maximum possible vent air flow rate is for  $T/T_a > 2$ :

$$\dot{m}_{a, \max} = 0.5 W_a H_o^{3/2} \text{ (kg/s)} \quad (39)$$

with  $W_o$  and  $H_o$  in m. Hence the ratio of the free burn mass loss rate and maximum air supply rate can be compared with the stoichiometric ratio ( $\gamma$ ).

After ventilation-limited conditions prevail, the mass loss rate of the fuel can not be directly computed. Nevertheless, results for wood crib fires have been empirically correlated [19,21] to yield:

$$\dot{m}_f \approx 0.09 W_o H_o^{3/2} \text{ (kg/s)} \quad (40)$$

with  $W_o$  and  $H_o$  in m. An estimate of the corresponding compartment gas temperature rise might also be made by computing the energy release rate from the maximum possible air flow rate Eq. (39). The result follows [15]:

$$\Delta T = 896 [A_o \sqrt{H_o} / (h_k A)]^{1/3} \text{ (}^\circ\text{C)} \quad (41)$$

where  $A_o$  is the vent area ( $\text{m}^2$ ),  $H_o$  is the vent height (m),  $h_k$  is the enclosure structure conductance ( $\text{kW/m}^2\text{k}$ ) and  $A$  is the structure surface area ( $\text{m}^2$ ).

## 12. Corridor Smoke Transfer and Filling

Much work is currently being done to develop meaningful correlations and models for smoke transfer and filling in corridors. The interest in this subject springs from the need to predict changes in environmental conditions which occur throughout a building as a fire develops. This is of great importance to life safety. An estimate made for the smoke front velocity,  $V_f$ , will be taken from work in progress by Zukoski and Kubota [22]. Figure B14 displays the phenomenon of a smoke layer progressing along a corridor.

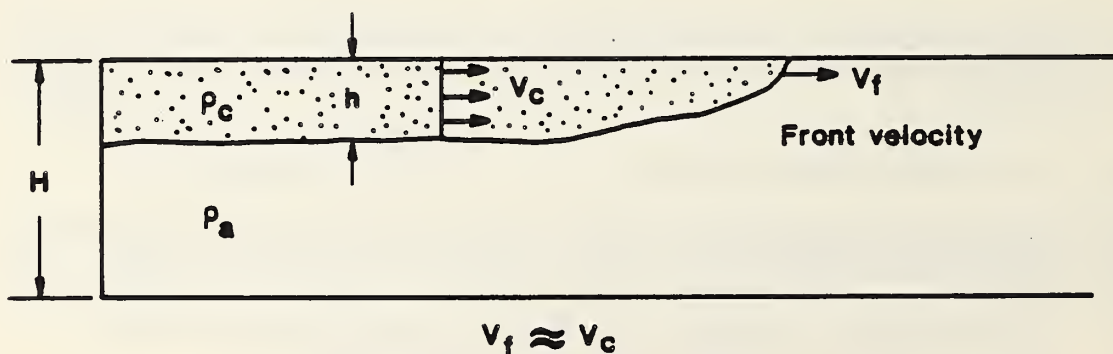


Figure B14. Corridor smoke transport.

From their preliminary analysis, we have extracted a result that represents an upper limit to the front velocity. This corresponds to the limiting case of the smoke layer filling half the corridor height and does not consider viscous effects which would retard the front speed. Thus a simple order of magnitude estimate is given below.

$$v_f = 1/2 \left[ g \left( \frac{\rho_a - \rho_c}{\rho_a} \right) H \right]^{1/2} \quad (42)$$

where  $g$  = acceleration of gravity,  
 $\rho_a$  = density of ambient air,  
 $\rho_c$  = density of the corridor fluid,  
 $H$  = corridor height.

Density can be related to the fire room temperature provided no heat loss occurs. Thus from the ideal gas law:

$$\frac{\rho_a - \rho_c}{\rho_a} = 1 - \frac{T_a}{T}$$

where  $T_a$  = ambient temperature,  
and  $T$  = gas temperature in fire room.

Subsequently the time ( $t_f$ ) for velocity front movement through a corridor is estimated by

$$t_f = \frac{L}{v_f} \quad (43)$$

where  $L$  = corridor length

Smoke filling time for a closed corridor or adjacent space to a room can be estimated using the appropriate formulas selected from section 6. But that approach would ignore the geometrical aspects of the room and corridor and their connecting doorway. It necessitates treating the corridor and room space as a single volume. Alternatively, work by Jones and Quintiere [23] suggest another approach. Figure B15 illustrates this smoke filling from a room fire to a closed adjacent space.

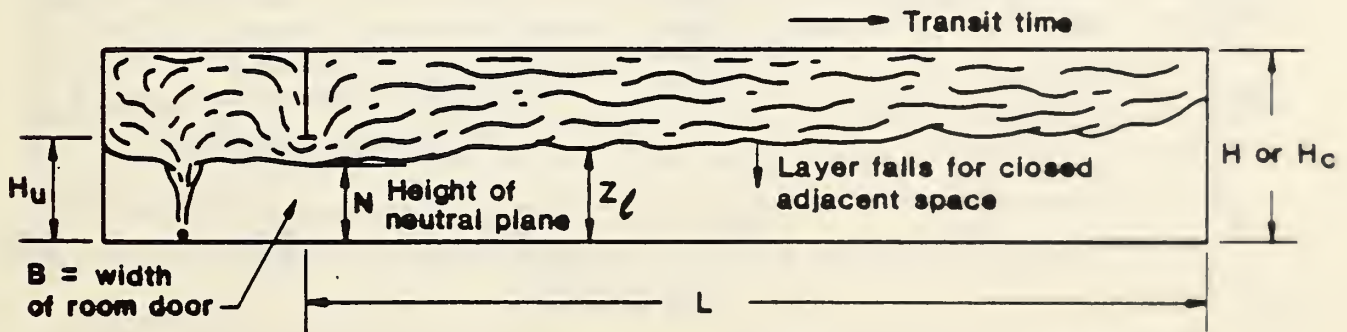


Figure B15. Smoke filling by a fire room to a closed adjacent space.

In this method a scaling parameter,  $\bar{P}^*$ , for the room door is considered, where

$$\bar{P}^* = B(H_u)^{3/2}/(H_c)^{5/2} \quad (44)$$

where  $B$  = width of the connecting door,

$H_u$  = height of connecting door,

$H_c$  = height of corridor.

A correlation based on dimensionless variables was developed using both experimental and computational results. The conditions examined were a room and closed corridor of equal height ( $H_c = 2.32$  m), a fixed room door height ( $H_u = 2.0$  m), variable door widths ( $0.13 \leq B \leq 1.07$  m); and varying heat release rates ( $25 \leq Q \leq 225$  kW). These conditions are representative of many building and developing fire conditions. The correlation is presented in Figure B16 which gives the dimensionless filling time  $\tau$  as a function of the fire and door parameters,  $\bar{Q}^*$  and  $\bar{P}^*$ , respectively. The time for filling was selected as the time for the smoke layer to descend to 1 m above the corridor floor. The dimensionless parameters are defined as follows:

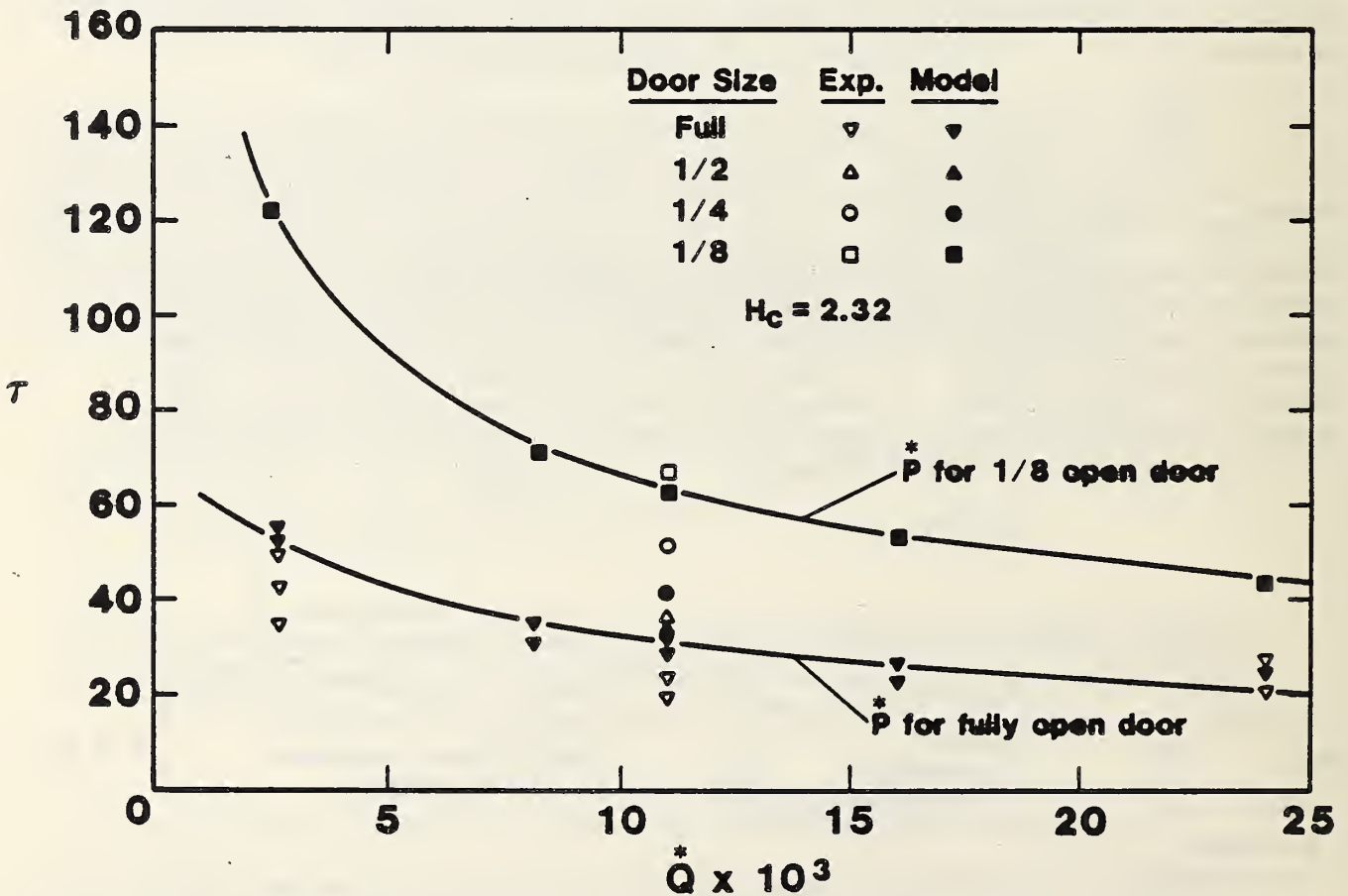


Figure B16. Dimensionless corridor smoke filling time [23]

$\dot{Q}^*$  represents dimensionless heat release rate and is defined by the equation

$$\dot{Q}^* = \dot{Q} / (C_p T_a \dot{m}^*) \quad (45)$$

where  $\dot{Q}$  = net heat release rate

$C_p$  = specific heat of air

$T_a$  = ambient temperature

and

$\dot{m}^*$  = a dimensionless characteristic mass flow which is defined as

$$\dot{m}^* = \rho_a (g H_c)^{1/2} H_c^2 \quad (46)$$

where  $\rho_a$  = ambient density

$g$  = acceleration of gravity

$H_c$  = height of corridor.

The dimensionless time  $\tau$  in Figure B16 is given as

$$\tau = t (\dot{m}^* / \rho_a A H_c) \quad (47)$$

where  $t$  = time (s)

and  $A$  = floor area for the corridor or adjoining space

To make an estimate for filling time  $t$ , a  $\dot{Q}^*$  is selected from which  $\dot{Q}$  is calculated. Using this  $\dot{Q}$ ,  $t$  can be determined from Figure B16. Rearranging Eq. (47) to solve for  $t$  yields

$$t = \frac{\tau}{(\dot{m}^* / \rho_a A H_c)} \quad (48)$$

### 13. Smoke Concentration and Visibility

The production of smoke in fires is an important feature in evaluating life safety. Technically smoke might be considered to include particles, hot combustion products, and toxic gases. Here we will only address the particulate nature of smoke and its effect on visibility. Smoke obscures vision by the reduction of light transmission. Smoke may also reduce vision by irritating the eyes. In this section estimates for smoke concentration and visibility will be calculated for a closed system which consists of a room and adjacent space.

The production rate of smoke particles ( $\dot{m}_s$ ) in a fire can be expressed as

$$\dot{m}_s = \chi_s \dot{m}_f \quad (49)$$

where  $\chi_s$  = fraction of particulate mass to fuel mass loss

$\dot{m}_f$  = fuel mass loss rate

The objective is to compute this production rate and relate it to visibility. Some background on needed data and applications can be found in reports by Quintiere [24], Babrauskas [25] and Tewarson [26]. An approximate relationship to predict visibility, defined to be  $L_v$  the length one can see through smoke when no eye irritation is present, is given as

$$L_v = k_v / (D/L) \quad (50)$$

where  $D/L$  is the optical density per unit path length  
 $k_v$  is a constant selected from Figure B17.

This relationship is derived from the results shown in Figure B17 [24] and is merely an approximate fit to those data. Of course the selected value for  $k_v$  should be consistent with those results but could also represent a conservative design value. To apply Eq. (50) to a particular situation we must compute  $(D/L)$  for that fuel and the configuration it burned in.

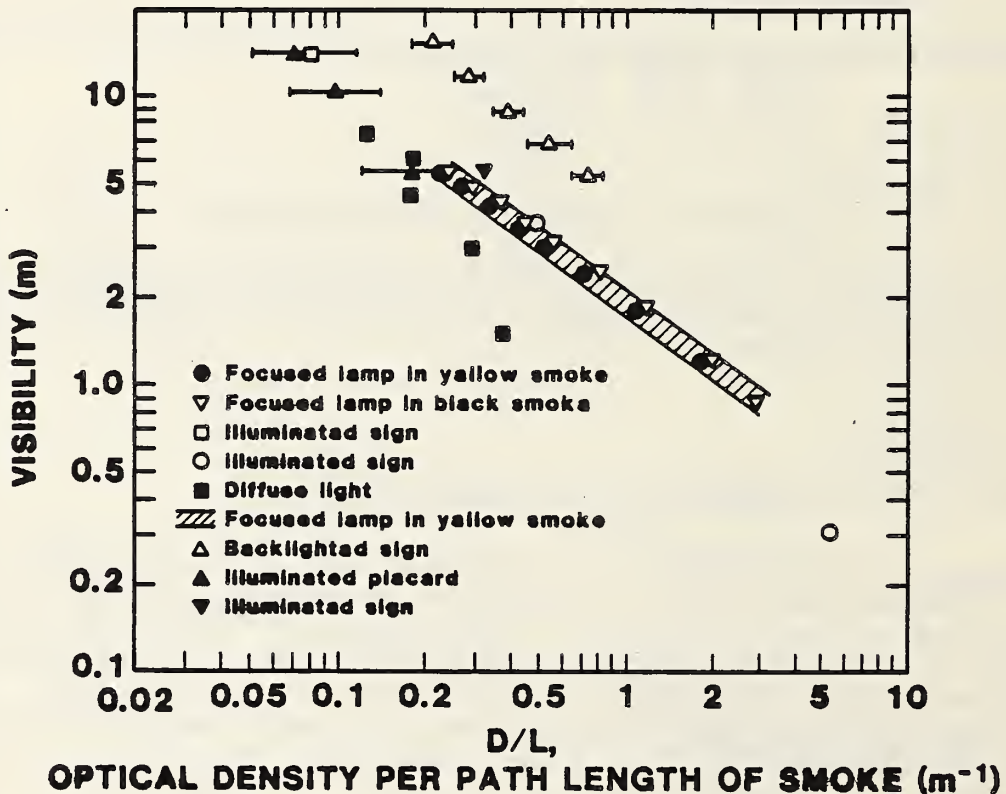


Figure B17. Visibility results derived from Rasbash [27], Jin [28] and Lopez [29].

To compute (D/L) for a closed system, for example a room and adjacent space, the following relationship must be integrated over time:

$$\frac{d(D/L)}{dt} = \frac{\alpha \chi_s}{V} \dot{m}_f \quad (51)$$

where  $t$  is time  
 $\alpha$  is the particle optical density  
 and  $V$  is the volume of the enclosed space.

The mass loss rate  $\dot{m}_f$  should be initially estimated from free burn analysis as before. This will be valid in the early stages of the fire. Data on  $\alpha$  and  $\chi_s$ , properties of the burning fuel, are needed for each fuel. Seader and Ou [30] suggest  $\alpha \approx 3300 \text{ m}^2/\text{kg}$  for fuels burning in air, and these results for a wide range of fuels are given by Tewarson [26]. (However Tewarson defines  $\chi_s$  and  $Y_s$  and reports  $\sigma$ , which is related to  $\alpha$ , as  $\alpha = \sigma / (2.303 Y_s)$ .) Also  $\alpha \chi_s$  can be estimated from the Smoke Density Chamber Test Method described in ASTM E-662. It can be shown that

$$\alpha \chi_s = \frac{D_{s, \max}}{m''} \quad (52)$$

where  $D_{s, \max}$  is the maximum specific optical density measured in ASTM E-662  
 and  $m''$  is the mass of sample consumed per unit of exposed surface area.

Of course the values of  $\alpha$  and  $\chi_s$  for a given material will depend on the exposure conditions during the burning of those samples. For first order estimates these effects are ignored, but judgment must be used in the application of such data.

The estimate based on Eq. (51) assumes that the volume of interest is well mixed and here the filling time has been ignored. Table B3 gives some representative values for  $\alpha$  and  $\chi_s$ .

An important point that should be noted in the discussion above is that in ventilation limited conditions,  $\dot{m}_f$  depends on air flow and  $\chi_s$  has been shown to increase. The ventilation parameter  $A_0 \sqrt{H_0}$  is reduced. This is shown in Figure B18 from the work of Saito [31] for plywood burning in an enclosure of floor area  $A$ .

Table B3

Smoke properties for selected materials burning in air [26]

| <u>Material</u>                       | Particle Optical<br>Density<br>$\alpha$<br><u>(<math>10^3 \text{m}^2/\text{kg}</math>)</u> | Fraction of Particulate<br>Mass to Fuel Mass Loss<br>$X_g$<br><u>(-)</u> |
|---------------------------------------|--|--|
| Oak                                   | 3.17   | 0.013  |
| PMMA                                  | 4.65   | 0.021  |
| Polyurethane foam<br>flexible (GM-25) | 0.426  | 0.32   |
| Granular Polystyrene                  | 2.11   | 0.15   |

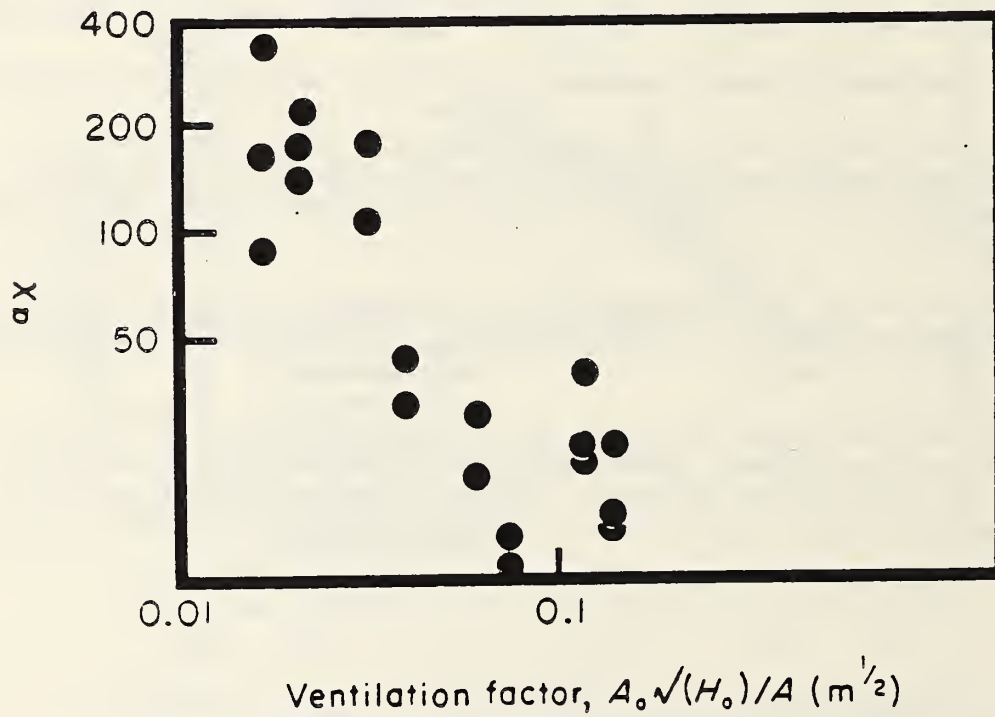


Figure B18. Smoke production for plywood as a function of ventilation factor from Saito [31]

#### 14. Estimation of Flame Spread Rates

After an unwanted fire has started flames spread away from the point of origin. The rate of flame spread,  $V_f$ , is affected by several environmental factors and the thermophysical/thermochemical properties of the materials. For solids of thickness  $> 1$  mm Eq. (53) Quintiere and Harkleroad [32] illustrate some of these variables.

##### Solids

$$V_f \propto \frac{(T_f - T_{ig})^2}{k\rho c(T_{ig} - T_s)^2} \quad (53)$$

where  $T_f$  - is the flame temperature which depends on available oxygen

$T_{ig}$  - is the ignition temperature

$T_s$  - is the upstream surface temperature resulting from an external heat flux.

Figure B19 schematically depicts the plume spread phenomena.

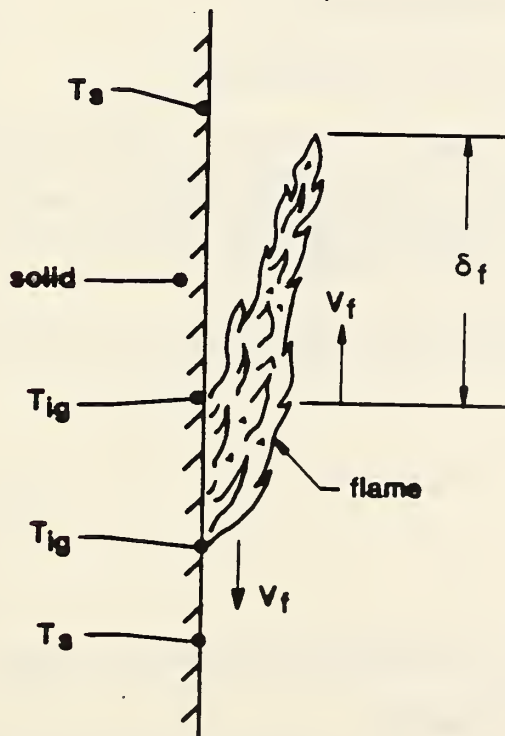


Figure B19. Sketch of flame spread model.

The relationship shown above can be converted into an estimate of downward flame spread rate using,

Flame Spread Opposed to Flow (downward)

$$V_f \approx \frac{\phi}{k\rho c(T_{ig} - T_s)^2} \quad (54)$$

where

$$\phi = V_a (k\rho c)_g (T_f - T_{ig})^2 \quad (55)$$

and

$$V_a = \frac{\left(\frac{k}{\rho c}\right)_g (T_f - T_\infty)^{1/3}}{T_\infty} \quad \text{opposed flow characteristic gas velocity under natural convection conditions} \quad (56)$$

- where
- $k_g$  = thermal conductivity of gas phase
  - $\rho_g$  = specific heat of gas
  - $c_g$  = specific heat of gas
  - $g$  = gravitational acceleration ( $9.8 \text{ m/s}^2$ )
  - $T_f$  = adiabatic flame temperature
  - $T_\infty$  = ambient and initial temperature

It has been found for a wide range of materials that  $\phi$  generally ranges between 1 and 15  $(\text{kW})^2/\text{m}^3$ ;  $T_{ig}$ , ranges between 250 and 600°C; and  $k\rho c$  ranges between 0.01 and 1.0  $(\text{kW}/\text{m}^2\text{K})^2\text{s}$  [32]. These are to be considered pseudo-properties valid for Eq. (54) under opposed flow natural convection flame spread in vertical orientation.

For upward flame travel, flame spread rate can be described by:

Upward Flame Spread

$$V_f \approx \frac{(\dot{q}''_f)^2 \delta_f}{k\rho c (T_{ig} - T_s)^2} \quad (57)$$

where  $\dot{q}''_f$  = heat transfer per unit time and per unit area

and  $\delta_f$  = flame extension length

Practical applications of Eq. (57) have not been developed, and general methods for predicting  $\dot{q}''_f$  and  $\delta_f$  do not exist.

## 15. Flame Spread Over Liquids

Glassman [33] reports on recent research efforts and theories for flame spread over liquids. As is shown in Figure B20, there are basically two different regimes for fires on liquids. One regime relates to flame spread which is controlled by gas phase phenomena when the bulk liquid temperature ( $T_L$ ) reaches its flash point or, for sustained burning, its fire point temperature  $T_f$ . The other regime occurs when the bulk liquid temperature is below its fire point temperature. This slower flame spread phenomena depends on the evaporation of the liquid to sustain and control the process. As the liquid temperature rises above the fire point temperature to  $T_{LSt}$ , a stoichiometric fuel-air mixture is formed near the surface, and consequently flame spread occurs in the gas phase. This rate of flame spread is related to the bulk liquid temperature and its surface tension.

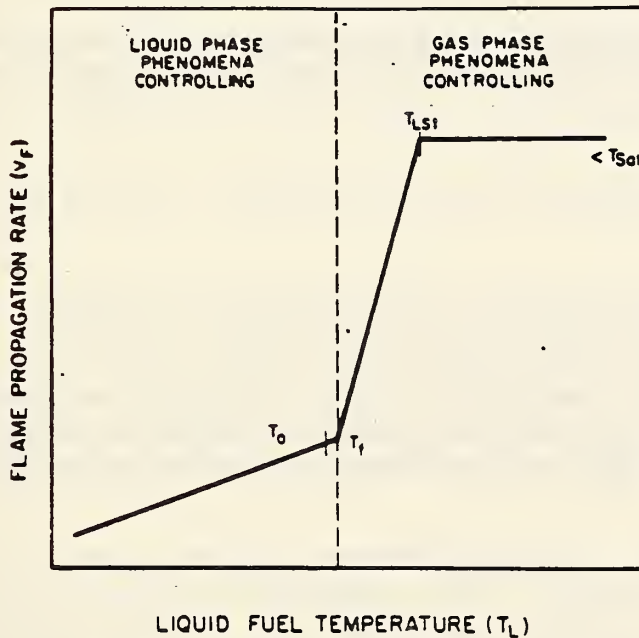


Figure B20. Schematic of the flame spreading rate as a function of the liquid temperature of the fuel [33].

A report by Williams [34] gives a qualitative formula for the flame spread rate,  $V_f$ , on liquid fuels.

$$V_f = \frac{\sigma'}{\mu_\ell} \frac{\mu_\ell^2 \ell}{\rho_\ell \sigma'}^{1/3} \quad (58)$$

where  $\sigma'$  = gradient in surface tension

$$\sigma' = \frac{d\sigma}{dT} (T_{1g} - T_o) / \ell \quad (59)$$

$T_{ig}$  = liquid ignition temperature

$T_0$  = initial liquid temperature

$\ell$  = length characteristic forward flame heat transfer to the liquid

$\mu_\ell$  = liquid viscosity

$\rho_\ell$  = liquid density

The application of this equation to practical problem solving is not straightforward since  $\ell$  depends on the heat transfer characteristics of the particular problem. Referral to references [33,34] will give some further background and insight on potential applications.

### 16. Fully Developed Fire Burn Time

Once a fire has started and has become fully developed, it is of interest to be able to estimate the duration of burning. This can be easily estimated by

$$t_b \approx \frac{m_f}{\dot{m}_f} \quad (60)$$

or

$$m_f = \int_0^{t_b} \dot{m}_f dt \quad (61)$$

where  $m_f$  is the mass of fuel available to burn (vaporize) and  $\dot{m}_f$  is the burning (vaporization) rate of the fuel under the specified environmental conditions. The value for  $\dot{m}_f$  can be estimated using the equations located in section 2.

### 17. Conclusion

To conclude this paper, it would be appropriate to use the techniques presented to make estimates for the development of a hypothetical fire. An exercise of this type is presented in the "Example" which follows section 18.

This report has brought together a number of techniques developed by various researchers for evaluating the fire environment. These predictive methods can be useful in estimating many of the critical elements related to fire behavior and help provide a better understanding of this complex phenomenon. It should be remembered when using this report while making predictions that the results are only estimates. These estimates, which spring from the state-of-the-art, are meant to provide a reasonable approximation and in some cases just an order of magnitude for the particular elements under study. More accurate predictions typically involve more complex calculations using more powerful methods than a simple calculation. In many cases, additional research is needed to formulate new solutions, derive more data, and to develop more sophisticated fire models than currently exist. Nevertheless the approach presented here provides, in addition to its estimates, a conceptual framework for what we can do and what we must learn to do.

## 18. References

1. Delichatsios, M.A., Fire Growth Rates in Wood Cribs, Combustion and Flame, 27, 267-278 (1976).
2. Heskestad, G., Modeling of Enclosure Fires, 14th Symposium (International) on Combustion, The Combustion Institute, Pittsburgh, p. 1021, (1973).
3. Lawson, J.R., Walton, W.D., Twilley, W.H., Fire Performance of Furnishings as Measured in the NBS Furniture Calorimeter. Part I, National Bureau of Standards (U.S.) NBSIR 83-2787 (1983).
4. Babrauskas, V., Combustion of Mattresses Exposed to Flaming Ignition Sources - Part I. Full Scale Tests and Hazard Analysis, National Bureau of Standards, (U.S.), NBSIR 77-1290, (1977).
5. Orloff, L., Fire Growth on Polyurethane Foam, Modak, A.T., ed., Influence of Enclosures on Fire Growth, Volume II - Analysis, Tech. Report, FMRC J.I. OAOR3.BU, RC78-BT-24, Factory Mutual Research Corp., Norwood, MA (July 1978).
6. Modak, A.T., Croce, P.A., Plastic Pool Fires, Combustion and Flame, 30, 251-265, (1977).
7. Burgess, D.S., Grumer, J., Wolfhard, H.G., Burning Rates of Liquid Fuels in Large and Small Open Trays, International Symposium on the Use of Models in Fire Research, Publication 786 National Academy of Sciences, (November 1959).
8. Modak, A.T., Thermal Radiation from Pool Fires, Combustion and Flame, 29, 177-192 (1977).
9. McCaffrey, B.J., Purely Buoyant Diffusion Flames: Some Experimental Results, National Bureau of Standards, (U.S.) NBSIR 79-1910 (1979).
10. Zukoski, E. E., Kubota, T., Cetegen, B., Entrainment in Fire Plumes, Fire Safety Journal, 3, 107-121 (1980/81).
11. Hasemi, Y., Tokunaga, T., Modeling of Turbulent Diffusion Flames and Fire Plumes for the Analysis of Fire Growth, Fire Dynamics and Heat Transfer, The American Society of Mechanical Engineers, 21st National Heat Transfer Conference, HTD-Vol. 25, (1983).
12. You, H.Z., Faeth, G.M., Ceiling Heat Transfer During Fire Plume and Flame Impingement, Fire and Materials, Vol 3, (1979).
13. Zukoski, E.E., Development of a Stratified Ceiling Layer in the Early Stages of a Closed-Room Fire, Fire and Materials, Vol. 2, No. 2, (1978).
14. Quintiere, J.G., Birky, M., McDonald, F., Smith, G., An Analysis of Smoldering Fires in Closed Compartments and Their Hazard Due to Carbon Monoxide, Fire and Materials, Vol. 6, Nos. 3 and 4, (1982).

15. Quintiere, J.G., A Simple Correlation for Predicting Temperature in a Room Fire, National Bureau of Standards (U.S.), NBSIR 83-2712, (1983).
16. McCaffrey, B.J., Quintiere, J.G., Harkelroad, M.F., Estimating Room Temperatures and the Likelihood of Flashover Using Fire Test Data Correlations, Fire Technology, 17, 2, p. 98, (May 1981).
17. Steckler, K.D., Quintiere, J.G., Rinkinen, W.J., Flow Induced by Fire in a Compartment, Nineteenth Symposium (International) on Combustion, The Combustion Institute, pp. 913-920, (1982).
18. Quintiere, J.G., Steckler, K., Corley, D., An Assessment of Fire Induced Flows in Compartments, Fire Science and Technology, Vol. 4, No. 1, p. 1-14, (June 1984).
19. Kawagoe, K., Sekine, T., Estimation of Fire Temperature - Time Curve for Rooms, Ministry of Construction, Japanese Government, (June 1963).
20. Thomas, P.H., Bullen, M.L., Quintiere, J.G. and McCaffrey, B.J., Flashover and Instabilities in Fire Behavior, Combustion and Flame, 38, 159-171, (1980).
21. Thomas, P.H., Heselden, A.J.M., Law, M., Fully-Developed Compartment Fires -- Two Kinds of Behavior, Ministry of Technology and Fire Offices Committee, Fire Research Station, Borehamwood, England Technical Paper No. 18, (1967).
22. Zukoski, E.E., Kubota, T., Experimental Study of Environment and Heat Transfer In a Room Fire, Final Report, Grant NB82NADA3033, National Bureau of Standards, (U.S.), (July 1984).
23. Jones, W.W., Quintiere, J.G., Prediction of Corridor Smoke Filling by Zone Models, Combustion Science and Technology, Vol. 35, pp. 239-253, (1984).
24. Quintiere, J.G., Smoke Measurements: An Assessment of Correlations Between Laboratory and Full-Scale Experiments, Fire and Materials, Vol. 6, Nos. 3 and 4, (1982).
25. Babrauskas, V., Applications of Predictive Smoke Measurements, Journal of Fire and Flammability, Vol. 12, p. 51, (January 1981).
26. Tewarson, A., Physico-Chemical and Combustion/Pyrolysis Properties of Polymeric Materials, National Bureau of Standards (U.S.), NBS-GCR-80-295, (1980).
27. Rasbash, D.J., Smoke and Toxic Products Produced at Fires, Plastics Institute Transaction and Journal, pp. 55-61, (January 1967).
28. Jin, T., Visibility through Fire Smoke (Part 2), Report of the Fire Research Institute of Japan, Nos. 33, 31, (1971).
29. Lopez, E.L., Smoke Emission from Burning Cabin Materials and the Effect on Visibility in Wide-Bodied Jet Transports, Journal of Fire and Flammability, Vol. 6, (October 1975).

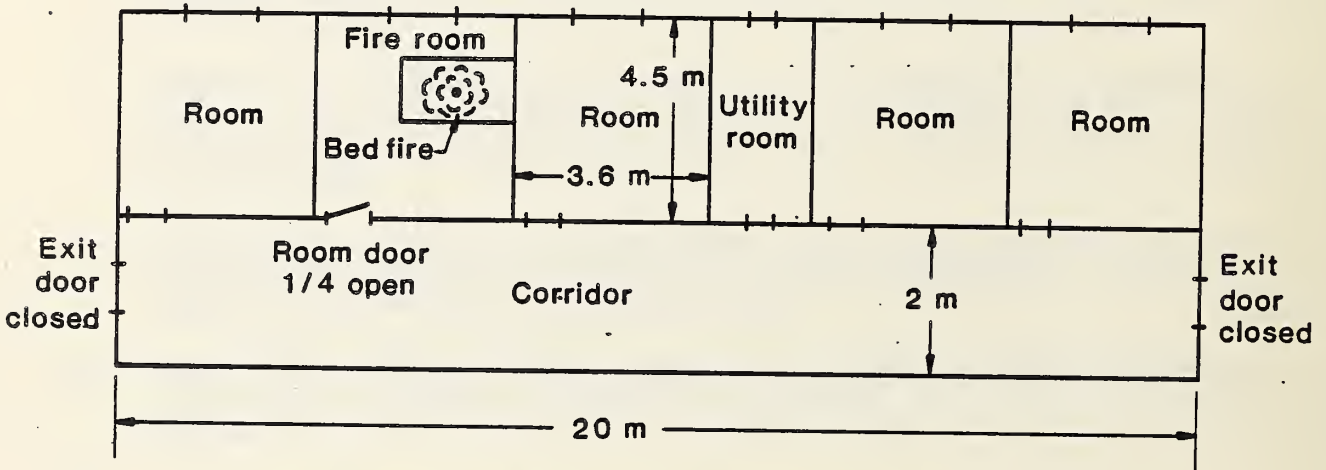
30. Seader, J.D., Ou, S.S., Correlation of the Smoking Tendency of Materials, Fire Research, 1, 3-9, (1977).
31. Saito, F., Smoke Generation from Building Materials, 15th Symposium (International) on Combustion, The Combustion Institute, 269 (1974).
32. Quintiere, J.G., Harkelroad, M., New Concepts for Measuring Flame Spread Properties, presented at Symposium on Application of Fire Science to Fire Engineering, ASTM, SFPE, (June 1984).
33. Glassman, I., Dryer, F.L., Flame Spreading Across Liquid Fuels, Fire Safety Journal, Vol. 3, Nos. 2-4, (January-March 1981).
34. Williams, F.A., Mechanisms of Fire Spread, Sixteenth Symposium (International) on Combustion, The Combustion Institute, 1281-1294, (1976).

## 19. EXAMPLE

This exercise is designed to provide an example of the use of the predictive methods presented in this report. It is intended as a hypothetical illustration and should not be construed as representative of the hazard associated with the particular items, materials and occupancy configuration selected. The first step in analyzing a fire scenario is to define the problem in terms of information required by the relevant predictive formulae.

### Problem:

The fire takes place in a hotel room. A fire starts from a cigarette lighter in the center of a bed with a polyurethane foam mattress. The room door is left 1/4 open as the occupant flees the room. Figure B21 shows the plan for the hotel section being studied.



Note: Ceiling height in rooms and corridors 2.4 m.  
All doors are closed except the fire door.

Figure E1. Room Fire Example.

### Analysis of Fire Growth and Consequences

In this section, the prediction methods presented earlier are used to calculate mass loss rate, heat release rate, flame height, ceiling heat flux, temperature rise, ventilation flow rate, visibility, smoke filling, and smoke transport for the sample problem. The data required to make these calculations are provided as well as the assumptions used to simplify the calculation process. Tables of predicted values are presented and selected results are shown graphically.

#### Mass Loss Rate

The first step in these predictions of fire growth and hazardous conditions is the determination of an expression for energy generation rate of the fire. Using Eq. (3) with  $\beta = 0$  yields the following expression for fuel mass loss rate.

$$\dot{m} = \alpha e^{\alpha t} \text{ where } \alpha = 0.03$$

The solution to this expression is shown in Table E1 and Figure E2 for times up to 250 s. Mass loss rates for times from 250 s to 300 s are calculated using the steady state burning formula for wood cribs:

$$\dot{m}_f = 0.09 W_o H_o^{3/2}$$

where  $W_o = 0.23$

$$H_o = 2$$

This represents the ventilation-limited fire case. It is employed at the time when the ratio of fuel mass loss rate to air flow rate to the room exceeds its stoichiometric ratio (8).

#### Heat Release Rate

Heat release rate was calculated using the equation:

$$\dot{Q} = \dot{m}\Delta H$$

where  $\Delta H = 15.7$  (kJ/g) for the polyurethane foam mattress in the example.

#### Radiant Flux

From the heat release rate the radiant heat transfer to a nearby surface can be calculated using Eq. (7). In this prediction, it is assumed that  $R_o$ , the distance from the heat source to the wall is 1.8 m. The  $\chi_r$  value for polyurethane foam in this example is 0.35. Both values for  $\dot{Q}$  and  $\dot{q}_o''(R_o)$  are presented in Table E1. The radiant flux  $\dot{q}_o''(R_o)$  as a function of time is shown in Figure E3.

#### Flame Height

The values for flame height,  $H_f$ , and ceiling flame impingement length,  $H_R$ , in Table E1 and Figure E4 were calculated using Eqs. (8) and (14), respectively. In Eq. (14), the value for  $H = 1.8$  m since the bed height is subtracted from the overall ceiling height, and  $D$  was selected as a constant of 0.5 m. (Although the fire is growing, it is not strongly dependent on  $D$ .)

#### Ceiling Heat Flux

Table E1 and Figure E3 also contain predictions for heat flux to the room's ceiling. These results were developed using Eq. (15b). The values for radiant flux derived from Eq. (7) were added to values from Eq. (15b) to predict the total heat flux to the ceiling. In this example radiation from the hot gas layer has not been included in the total heat flux to the ceiling. However, an upper limit for radiation to the ceiling from the hot gas layer can be estimated as  $\sigma T^4$  where  $\sigma$  is  $5.6697 \times 10^{-8} \text{ W/m}^2 - \text{K}^4$ .

## Temperature Rise

Predictions for gas temperature rise,  $\Delta T$ , in the room are presented in column 8 of Table E1. Also see Figure E5. These values were generated using Eq. (31), but before the various temperatures were calculated thermal penetration times,  $t_p$ , for the gypsum walls and plywood floors were determined. The following parameters were used in these calculations:

Gypsum wallboard (walls/ceiling)

$$t_p = 393 \text{ s}$$

$$\rho = 960 \text{ kg/m}^3$$

$$c = 1.1 \text{ kJ/(kg-K)}$$

$$k = 1.7 \times 10^{-4} \text{ kJ/(m-K)}$$

$$\delta = 0.0159 \text{ m}$$

Plywood (floor)

$$t_p = 711 \text{ s}$$

$$\rho = 540 \text{ kg/m}^3$$

$$c = 2.5 \text{ kJ/(kg-K)}$$

$$k = 1.2 \times 10^{-4} \text{ kJ/(m-K)}$$

$$\delta = 0.0159 \text{ m}$$

As a result of these calculations, it was found that values for  $h_k$  in Eq. (31) would be determined using  $\sqrt{k\rho c/t}$  where  $t \leq t_p$ . At this point, it is important to note that new values for  $h_k$  are calculated with each new time in the prediction of  $\Delta T$ . For  $t \leq t_p$ ,  $h_k$  was calculated by

$$h_k = \frac{A_1 h_{k,1} + A_2 h_{k,2}}{A}$$

where

$$A_1 = 55.08 \text{ m}^2 \text{ area for walls and ceilings}$$

$$A_2 = 16.2 \text{ m}^2 \text{ area for floor}$$

$$A = 71.28 \text{ m}^2 \text{ total}$$

and  $h_{k,1}$  and  $h_{k,2}$  correspond to the gypsum board and plywood respectively.

When extended calculations are made for  $t > t_p$  for either the walls and ceiling or floor,  $k/\delta$  should be substituted into the above equation. For

$\Delta T$  calculations at times greater than the point of flashover, Eq.(41) was used. Values for the parameter in Eq. (31 and 41) are as follows:

$$g = 9.8 \text{ m/s}^2$$

$$c_p = 1.046 \text{ kJ/(kg-K)}$$

$$\rho_o = 1.25 \text{ kg/m}^3$$

$$T_o = 293 \text{ K}$$

$$A_o = 0.46 \text{ m}^2$$

$$H_o = 2 \text{ m}$$

#### Ventilation Flow Rate

Since both  $\dot{Q}$  and  $\Delta T$  are now available, ventilation flow rate is calculated. In this procedure, Eqs. (32, 33, 34 and 35) are used to make the predictions. For times down to 220 s where  $\psi \leq 1$ ,  $y_2 = 0.5$  was used in the calculation. For  $\psi > 1$ , Eq. (33) was used to calculate an estimated value of  $y_2$ . This was done by substituting the preceding result of  $\dot{m}_1$  into the equation. The values of  $M_o$  and  $\dot{m}_o$  were determined using Eqs. (32 and 34), and  $\dot{m}_1$  results were found with Eq. (35). The values used in this calculation were as follows:

$$\rho_a = 1.25 \text{ kg/m}^3$$

$$g = 9.8 \text{ m/s}^2$$

$$W_o = 0.23 \text{ m}$$

$$H_o = 2 \text{ m}$$

It can be seen in Table E1 and Figure E6 that the ventilation starts to drop off at about 220 s and then starts to rise again. The 220 s point is where the estimated value for  $y_2$  was started, and it is continued until the ventilation limit condition is reached at a time between 250 and 255 s. At this point and beyond, the  $\dot{m}_f$  value is based on steady state enclosure ventilation limited formula, and the calculation for  $\dot{m}_1$  was stopped.

#### Corridor Visibility

The last column in Table E1 consists of predictions of visibility,  $L_v$ , in the corridor. Also see Figure E7. The equation used in this prediction was as follows:

$$L_v = \frac{k_v V}{\alpha x} \int_0^t \dot{m} dt$$

where

$$k_v = 2$$

$$V = (\text{Width})(\text{length})(\text{height}) \text{ of corridor} \\ (2\text{m}) \quad (20\text{m}) \quad (2.4\text{m})$$

and

$$\int_0^t \dot{m} dt = \int_0^t \alpha e^{\alpha t} dt = e^{\alpha t} - 1 \Big|_0^t \text{ for mattress}$$

$$\alpha = 3300 \text{ m}^2/\text{kg}$$

$$x = 0.3 \text{ g smoke particulates/g fuel}$$

These predictions show that visibility would be about 0.1 m when flashover (based on  $\Delta T = 500^\circ\text{C}$ ) occurs. (It should be noted that this calculation assumes a well-mixed gas state in the corridor. But this does not occur until 181s approximately. So use of the formulae before this time will over estimate the visibility by the ratio of corridor volume to actual smoke layer volume.

#### Smoke Filling

Two other tables are presented in this example. Table E2 is a listing of various room smoke filling times based on different steady state heat release rates. Equation (23b) was used to calculate these values. The following values were used in these calculations:

$$\alpha = 1/5.4$$

$$\rho_\infty = 1.25 \text{ kg/m}^3$$

$$T_\infty = 293 \text{ K}$$

$$c_p = 1.046 \text{ kJ/kg-k}$$

$$g = 9.8 \text{ m/s}^2$$

$$H = 2.4 \text{ m}$$

$$s = 16.2 \text{ m}^2$$

These results suggest that combustion products begin to leave the room i.e., the layer is just below the door soffit ( $H = 1.99 \text{ m}$ ) at about 10 to 35 s.

Table E3 contains additional predictions which provides an order of events for the fire growth example. Smoke filling time for the room was taken from Table E2, and visibility in the corridor was taken from Table E1. The value for smoke filling time in the corridor was generated using Eqs. (45, 46, and 48). Parameter values used in this calculation were as follows:

$$\rho_a = 1.24 \text{ kg/m}^3$$

$$g = 9.8 \text{ m/s}^2$$

$$H_c = 2.32 \text{ m}$$

$$\dot{Q} = 100 \text{ kW}$$

$$L_c = 1.046 \text{ kJ/kg-K}$$

$$T_a = 293 \text{ K}$$

$$\tau = 47$$

$$A = 40 \text{ m}^2$$

The time for the occurrence of flashover and the ventilation limit time was taken from Table E1. The time for flashover is based on a 500°C temperature rise, and the ventilation limit is based on the effective fuel-air mass ratio where

$$\gamma = \frac{\Delta H_{\text{air}}}{\Delta H_{\text{fuel}}} = \frac{3.03 \text{ kJ/g air}}{15.7 \text{ kJ/g fuel}} = 0.193 \text{ g fuel/g air}$$

This mass ratio was compared with fuel and air values contained in Table E1.

### Smoke Transport

The predictions at the bottom of Table E3 were developed using Eq. (42) where

$\rho_c$  was selected to correspond to the room temperature (T) so that

$$\frac{\rho_a - \rho_c}{\rho_a} = 1 - \frac{T_a}{T}$$

Parameters used in this calculation were as follows:

$$g = 9.8 \text{ m/s}^2$$

$$T_a = 293 \text{ K}$$

$$T = 303 \text{ K}$$

$$H = 2.4 \text{ m}$$

Smoke transport times to the corridor ends were calculated using Eq. (43). Center line distances from the hotel room door were 4.2 m and 15.8 m respectively for the near and far ends of the corridor.

Thus a chronology of significant events and the magnitude of physical fire effects have been estimated for this scenario. It's accuracy is at least good to an order of magnitude and more exact assessments of accuracy must be based on the assumptions and support literature for each of the formulas used.

Table E1. Fire Growth Predictions

| $t$<br>(s) | $\dot{m}_f$<br>(g/s) | $\dot{Q}$<br>(kW)              | $\dot{q}_o''$ ( $R_o$ )<br>(kW/m <sup>2</sup> ) | $H_f$<br>(m) | $H_R$<br>(m) | $\dot{q}''(0)$<br>(kW/m <sup>2</sup> ) | $\Delta T$<br>(°C) | $\dot{m}_1$<br>(kg/s) | Corridor<br>$L_v$<br>(m) |
|------------|----------------------|--------------------------------|---|--------------|--------------|--|--------------------|-----------------------|--------------------------|
| 0          | 0.00                 | 0.0                            | -   | -            | -            | -                                      | -                  | -                     | -                        |
| 10         | 0.04                 | 0.6                            | -   | -            | -            | -                                      | -                  | -                     | -                        |
| 20         | 0.05                 | 0.8                            | -   | -            | -            | -                                      | -                  | -                     | -                        |
| 30         | 0.07                 | 1.1                            | -   | -            | -            | -                                      | -                  | -                     | -                        |
| 40         | 0.10                 | 1.6                            | -   | 0.28         | -            | 0.11                                   | 1                  | 0.034                 | 83.6                     |
| 45         | 0.12                 | 1.9                            | -   | 0.29         | -            | 0.12                                   | 7                  | 0.090                 | 67.9                     |
| 50         | 0.13                 | 2.0                            | -   | 0.30         | -            | 0.13                                   | 8                  | 0.095                 | 55.7                     |
| 55         | 0.16                 | 2.5                            | -   | 0.33         | -            | 0.15                                   | 9                  | 0.101                 | 46.1                     |
| 60         | 0.18                 | 2.8                            | -   | 0.35         | -            | 0.17                                   | 10                 | 0.106                 | 38.4                     |
| 65         | 0.21                 | 3.3                            | -   | 0.37         | -            | 0.19                                   | 11                 | 0.111                 | 32.1                     |
| 70         | 0.24                 | 3.8                            | -   | 0.39         | -            | 0.22                                   | 12                 | 0.115                 | 27.1                     |
| 75         | 0.28                 | 4.4                            | -   | 0.42         | -            | 0.24                                   | 14                 | 0.124                 | 22.8                     |
| 80         | 0.33                 | 5.2                            | -   | 0.44         | -            | 0.28                                   | 15                 | 0.128                 | 19.3                     |
| 85         | 0.38                 | 6.0                            | -   | 0.47         | -            | 0.32                                   | 17                 | 0.135                 | 16.4                     |
| 90         | 0.45                 | 7.1                            | -   | 0.50         | -            | 0.36                                   | 19                 | 0.142                 | 14.0                     |
| 95         | 0.52                 | 8.2                            | -   | 0.53         | -            | 0.41                                   | 21                 | 0.149                 | 11.9                     |
| 100        | 0.60                 | 9.4                            | -   | 0.56         | -            | 0.46                                   | 24                 | 0.157                 | 10.2                     |
| 105        | 0.70                 | 11.0                           | 0.09  | 0.60         | -            | 0.52                                   | 27                 | 0.164                 | 8.7                      |
| 110        | 0.81                 | 12.7                           | 0.11  | 0.64         | -            | 0.59                                   | 29                 | 0.169                 | 7.4                      |
| 115        | 0.94                 | 14.8                           | 0.13  | 0.68         | -            | 0.67                                   | 33                 | 0.178                 | 6.4                      |
| 120        | 1.10                 | 17.3                           | 0.15  | 0.72         | -            | 0.76                                   | 37                 | 0.186                 | 5.4                      |
| 125        | 1.28                 | 20.1                           | 0.17  | 0.76         | -            | 0.87                                   | 41                 | 0.194                 | 4.7                      |
| 130        | 1.48                 | 23.2                           | 0.20  | 0.81         | -            | 0.98                                   | 45                 | 0.200                 | 4.0                      |
| 135        | 1.72                 | 27.0                           | 0.23  | 0.86         | -            | 1.11                                   | 50                 | 0.208                 | 3.4                      |
| 140        | 2.00                 | 31.4                           | 0.27  | 0.91         | -            | 1.26                                   | 56                 | 0.216                 | 3.0                      |
| 145        | 2.32                 | 36.4                           | 0.31  | 0.97         | -            | 1.42                                   | 62                 | 0.223                 | 2.5                      |
| 150        | 2.70                 | 42.4                           | 0.36  | 1.03         | -            | 1.61                                   | 69                 | 0.231                 | 2.2                      |
| 155        | 3.14                 | 49.3                           | 0.42  | 1.09         | -            | 1.83                                   | 77                 | 0.238                 | 1.9                      |
| 160        | 3.65                 | 57.3                           | 0.49  | 1.16         | -            | 2.07                                   | 86                 | 0.245                 | 1.6                      |
| 165        | 4.24                 | 66.6                           | 0.57  | 1.23         | -            | 2.35                                   | 95                 | 0.251                 | 1.4                      |
| 170        | 4.92                 | 77.2                           | 0.66  | 1.31         | -            | 2.66                                   | 106                | 0.257                 | 1.2                      |
| 175        | 5.72                 | 89.8                           | 0.77  | 1.39         | -            | 3.01                                   | 117                | 0.263                 | 1.0                      |
| 180        | 6.64                 | 104.2                          | 0.90  | 1.48         | -            | 3.41                                   | 130                | 0.267                 | 0.9                      |
| 185        | 7.72                 | 121.2                          | 1.04  | 1.57         | -            | 3.87                                   | 145                | 0.272                 | 0.8                      |
| 190        | 8.97                 | 140.8                          | 1.21  | 1.66         | -            | 4.39                                   | 161                | 0.275                 | 0.7                      |
| 195        | 10.42                | 163.6                          | 1.41  | 1.77         | -            | 4.97                                   | 178                | 0.278                 | 0.6                      |
| 200        | 12.10                | 190.0                          | 1.63  | 1.88         | 0.07         | 5.63                                   | 198                | 0.279                 | 0.5                      |
| 205        | 14.06                | 220.7                          | 1.90  | 1.99         | 0.10         | 6.38                                   | 219                | 0.280                 | 0.41                     |
| 210        | 16.34                | 256.5                          | 2.20  | 2.12         | 0.25         | 7.23                                   | 243                | 0.279                 | 0.36                     |
| 215        | 18.98                | 298.0                          | 2.56  | 2.25         | 0.34         | 8.19                                   | 270                | 0.278                 | 0.31                     |
| 220        | 22.05                | 346.2                          | 2.98  | 2.38         | 0.42         | 9.28                                   | 300                | 0.288                 | 0.26                     |
| 225        | 25.62                | 402.2                          | 3.46  | 2.53         | 0.52         | 10.52                                  | 332                | 0.293                 | 0.23                     |
| 230        | 29.77                | 467.4                          | 4.02  | 2.69         | 0.62         | 11.92                                  | 369                | 0.297                 | 0.20                     |
| 235        | 34.59                | 543.1                          | 4.67  | 2.86         | 0.73         | 13.51                                  | 409                | 0.300                 | 0.17                     |
| 240        | 40.18                | 630.8                          | 5.42  | 3.03         | 0.83         | 15.30                                  | 453                | 0.301                 | 0.14                     |
| 245        | 46.69                | 733.0                          | 6.31  | 3.22         | 0.94         | 17.34                                  | 503                | 0.301                 | 0.12                     |
| 250        | 54.24                | 851.6                          | 7.32  | 3.42         | 1.06         | 19.65                                  | 558                | 0.300                 | 0.11                     |
| 255        | 58.55                | Steady state wood crib burning |   |              |              |  | 630                |                       |                          |
| 260        | 58.55                |                                |   |              |              |  | 632                |                       |                          |
| 265        | 58.55                |                                |   |              |              |  | 634                |                       |                          |
| 270        | 58.55                |                                |   |              |              |  | 636                |                       |                          |
| 275        | 58.55                |                                |   |              |              |  | 638                |                       |                          |
| 280        | 58.55                |                                |   |              |              |  | 640                |                       |                          |
| 285        | 58.55                |                                |   |              |              |  | 642                |                       |                          |
| 290        | 58.55                |                                |   |              |              |  | 644                |                       |                          |
| 295        | 58.55                |                                |   |              |              |  | 646                |                       |                          |
| 300        | 58.55                |                                |   |              |              |  | 648                |                       |                          |

Table E2. Room Smoke Filling Time Predictions, Steady State Fires

| Time (s) | Heat Release Rate 0.5 kW<br>Smoke layer height (m) | Heat Release Rate 1.0 kW<br>Smoke layer height (m) | Heat Release Rate 10 kW<br>Smoke layer height (m) | Heat Release Rate 100 kW<br>Smoke layer height (m) |
|----------|--|--|---|--|
| 0        | 0.00   | 0.00   | 0.00  | 0.00   |
| 2        | 2.38   | 2.37   | 2.34  | 2.27   |
| 4        | 2.35   | 2.34   | 2.28  | 2.15   |
| 6        | 2.33   | 2.32   | 2.22  | 2.04   |
| 8        | 2.31   | 2.29   | 2.17  | 1.95   |
| 10       | 2.29   | 2.26   | 2.12  |  |
| 12       | 2.27   | 2.24   | 2.07  | Note: 1.99(m)                                      |
| 14       | 2.25   | 2.21   | 2.02  | Reached  |
| 16       | 2.23   | 2.19   | 1.97  | @ 7(s)   |
| 18       | 2.21   | 2.16   |   |  |
| 20       | 2.19   | 2.14   | Note: 1.99(m)                                     |  |
| 22       | 2.17   | 2.11   | Reached   |  |
| 24       | 2.15   | 2.09   | @ 15(s)   |  |
| 26       | 2.13   | 2.07   |   |  |
| 28       | 2.11   | 2.04   |   |  |
| 30       | 2.09   | 2.02   |   |  |
| 32       | 2.07   | 2.00   |   |  |
| 34       | 2.06   | 1.98   |   |  |
| 36       | 2.04   |  |   |  |
| 38       | 2.02   | Note: 1.99(m)                                      |   |  |
| 40       | 2.00   | Reached  |   |  |
| 42       | 1.99   | @ 33(s)  |   |  |

Table E3. Summary of Critical Event Predictions

| Event  | Time (s) | Velocity (m/s) |
|--|----------|----------------|
| Smoke filling of room                        | -10-35   |                |
| Visibility of 1(m) in corridor               | -175     |                |
| Smoke filling of corridor                    | -181     |                |
| Occurrence of flashover                      | -245     |                |
| Ventilation limit in room                    | -250     |                |
| Smoke front velocity with $\Delta T$ of 10°C |          | 0.44           |
| Smoke transport time to near end of corridor | - 9.5    |                |
| Smoke transport time to far end of corridor  | -35.9    |                |

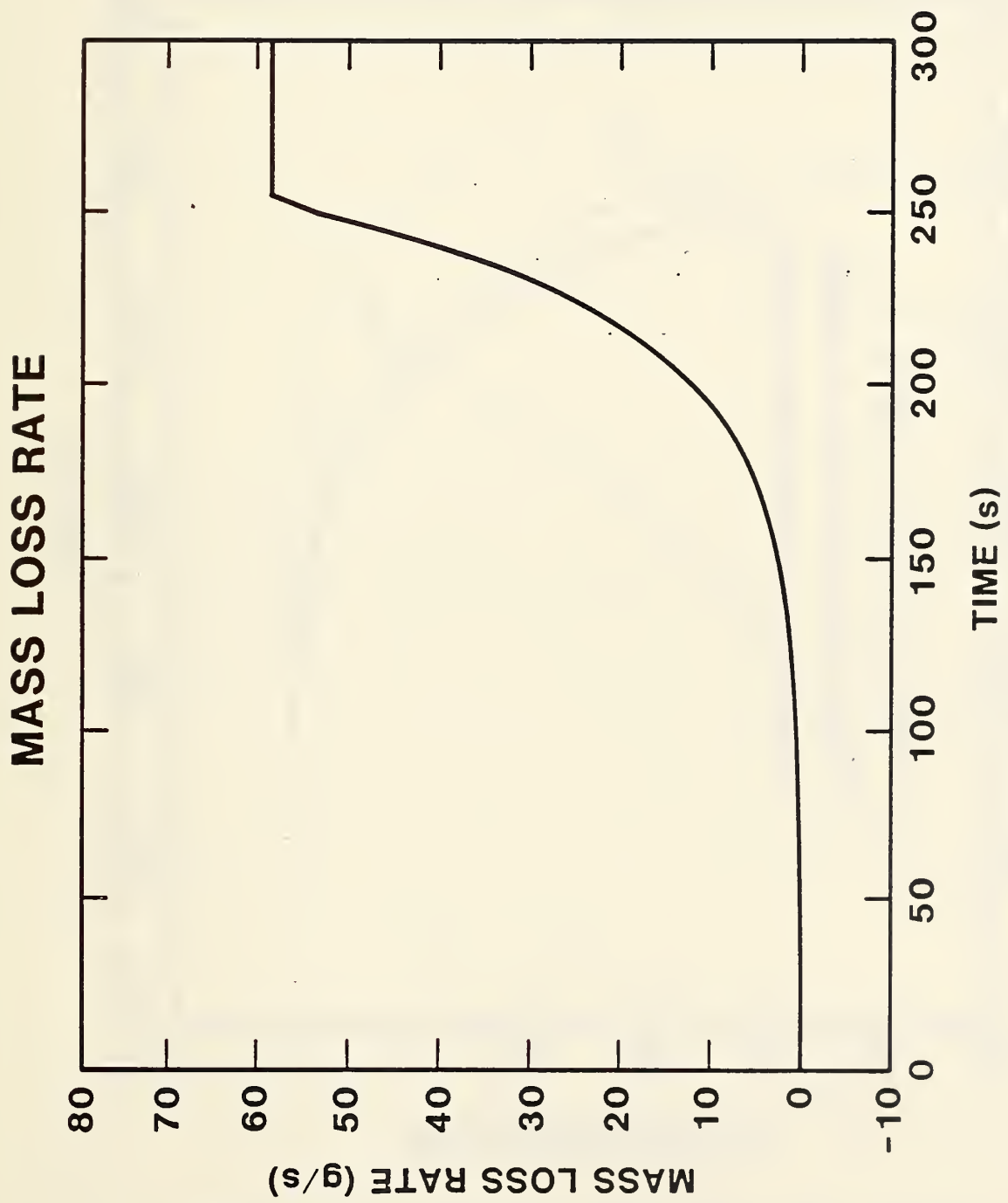


Figure E2. Mass Loss Rate for Fire Growth Example.

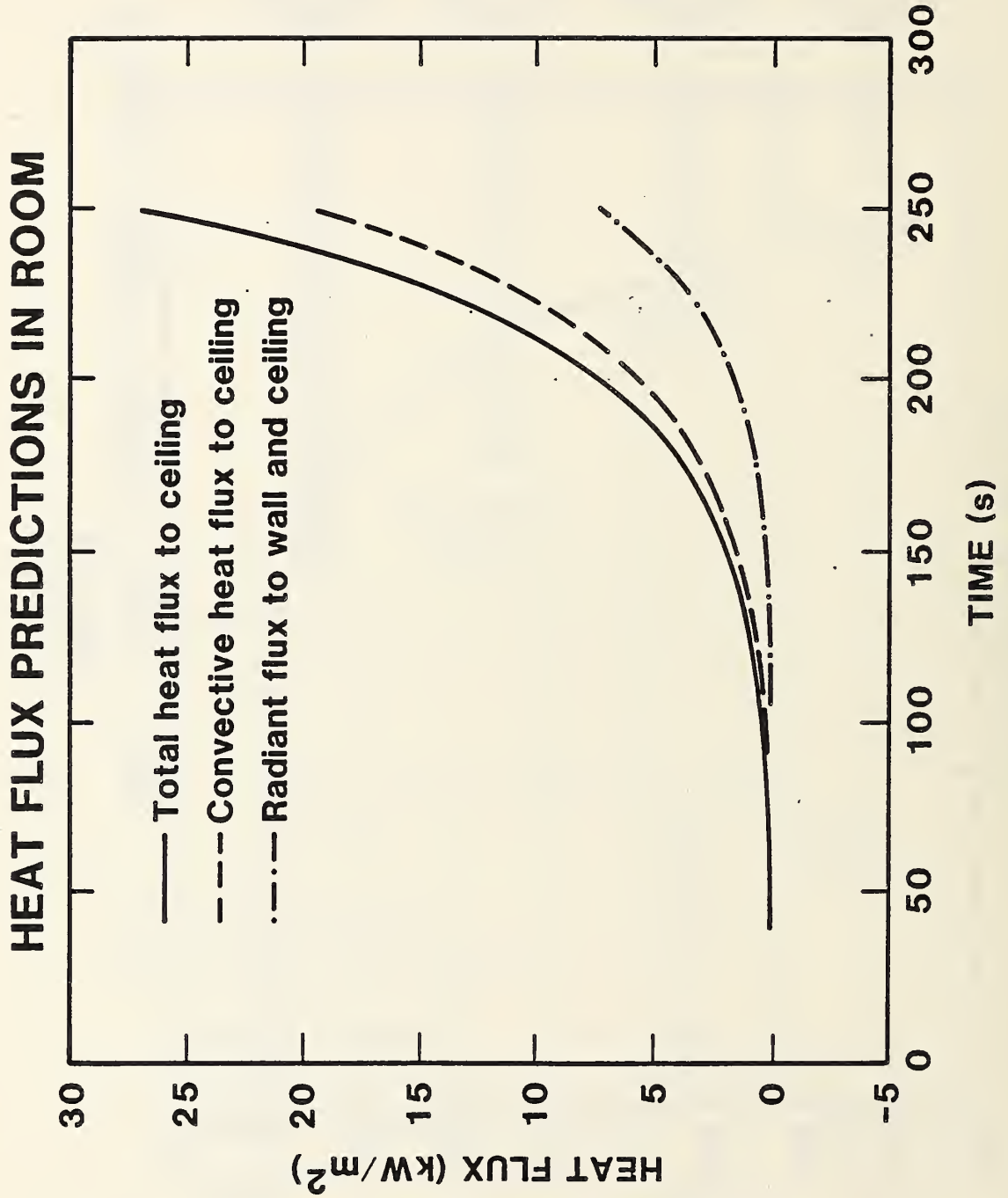


Figure E3. Heat Flux Predictions in Room for Fire Growth Example.

# FLAME HEIGHT AND EXTENSION ACROSS CEILING

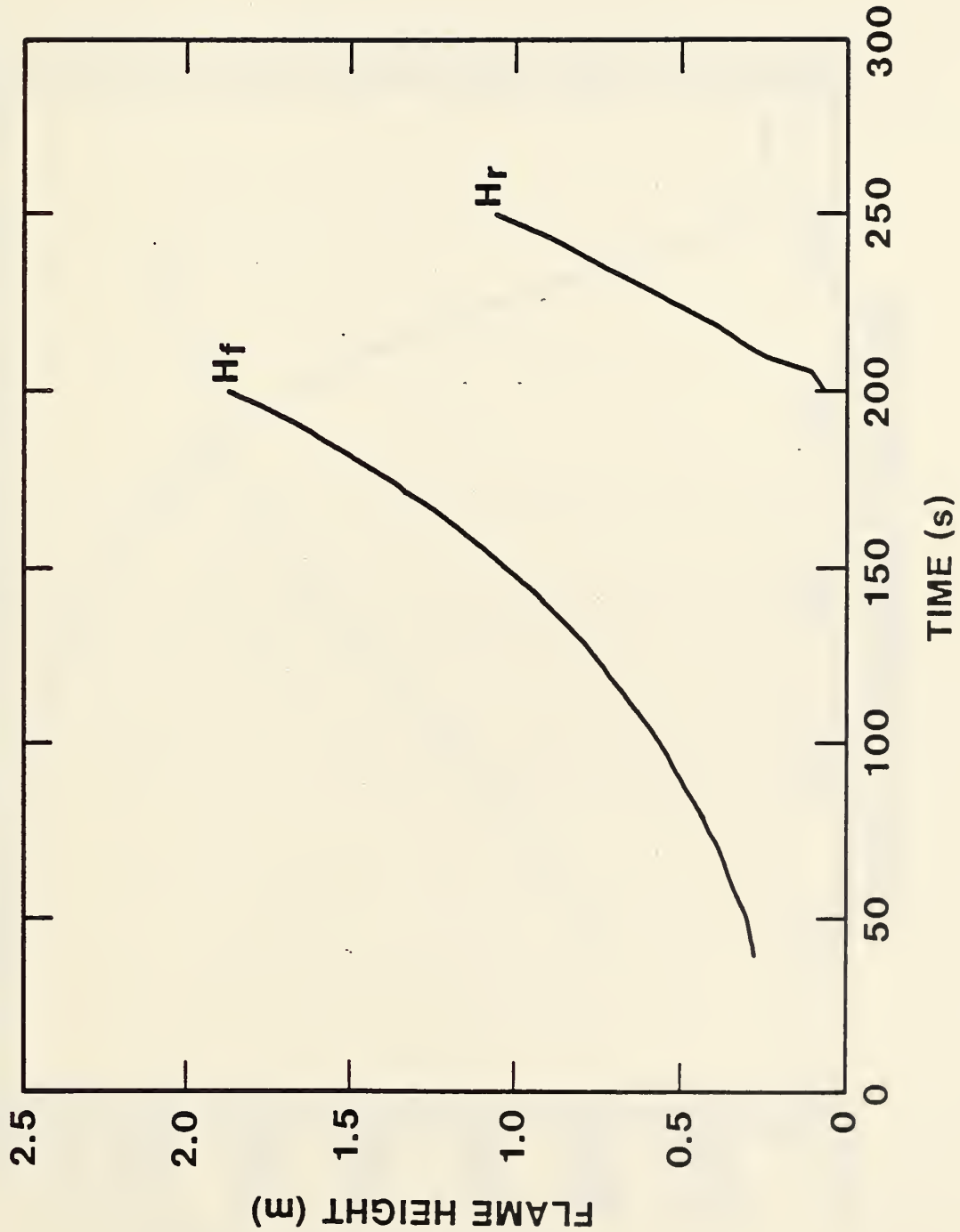


Figure E4. Flame Height and Extension Across Ceiling for Fire Growth Example.

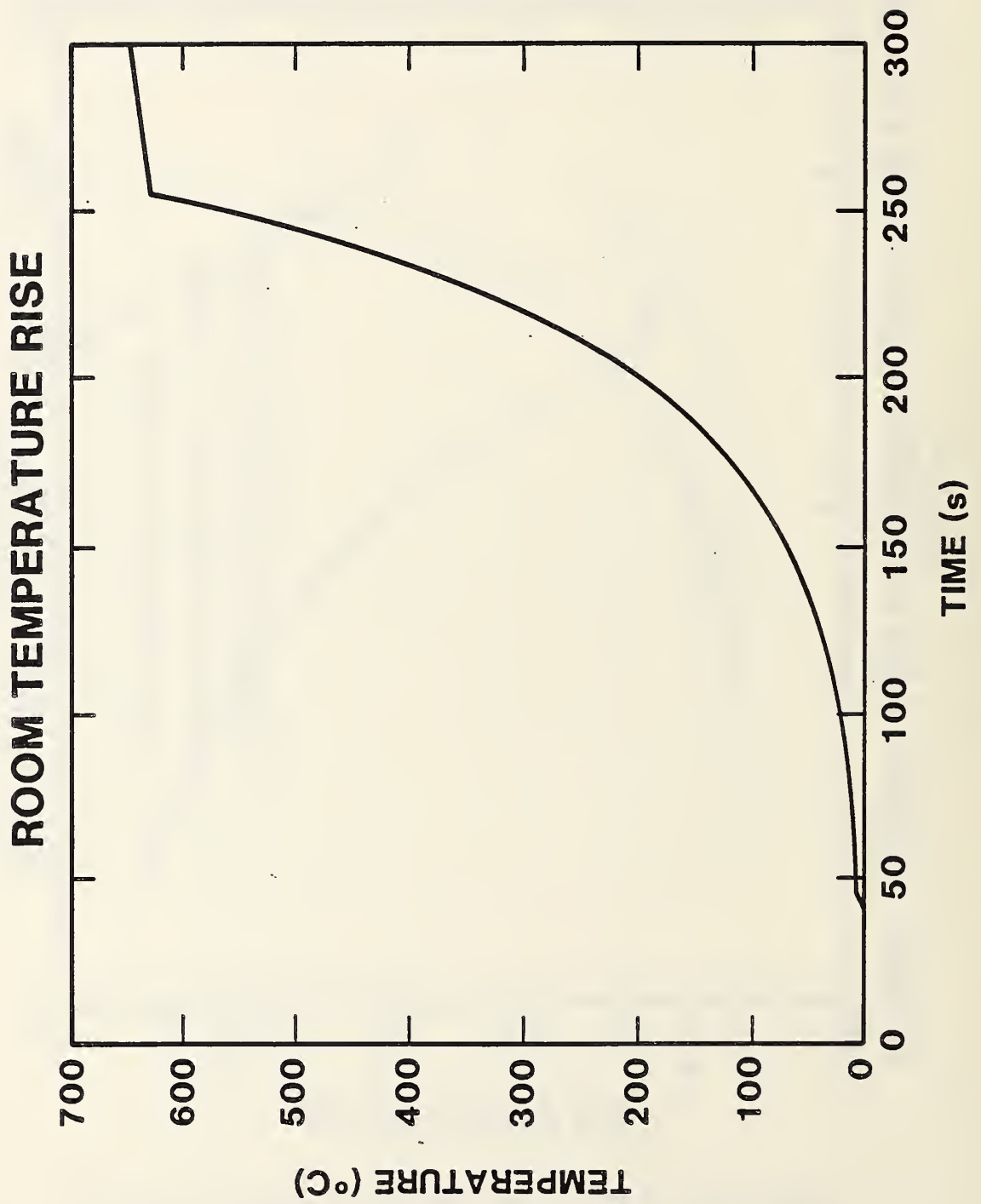


Figure E5. Room Temperature Rise for Fire Growth Example.

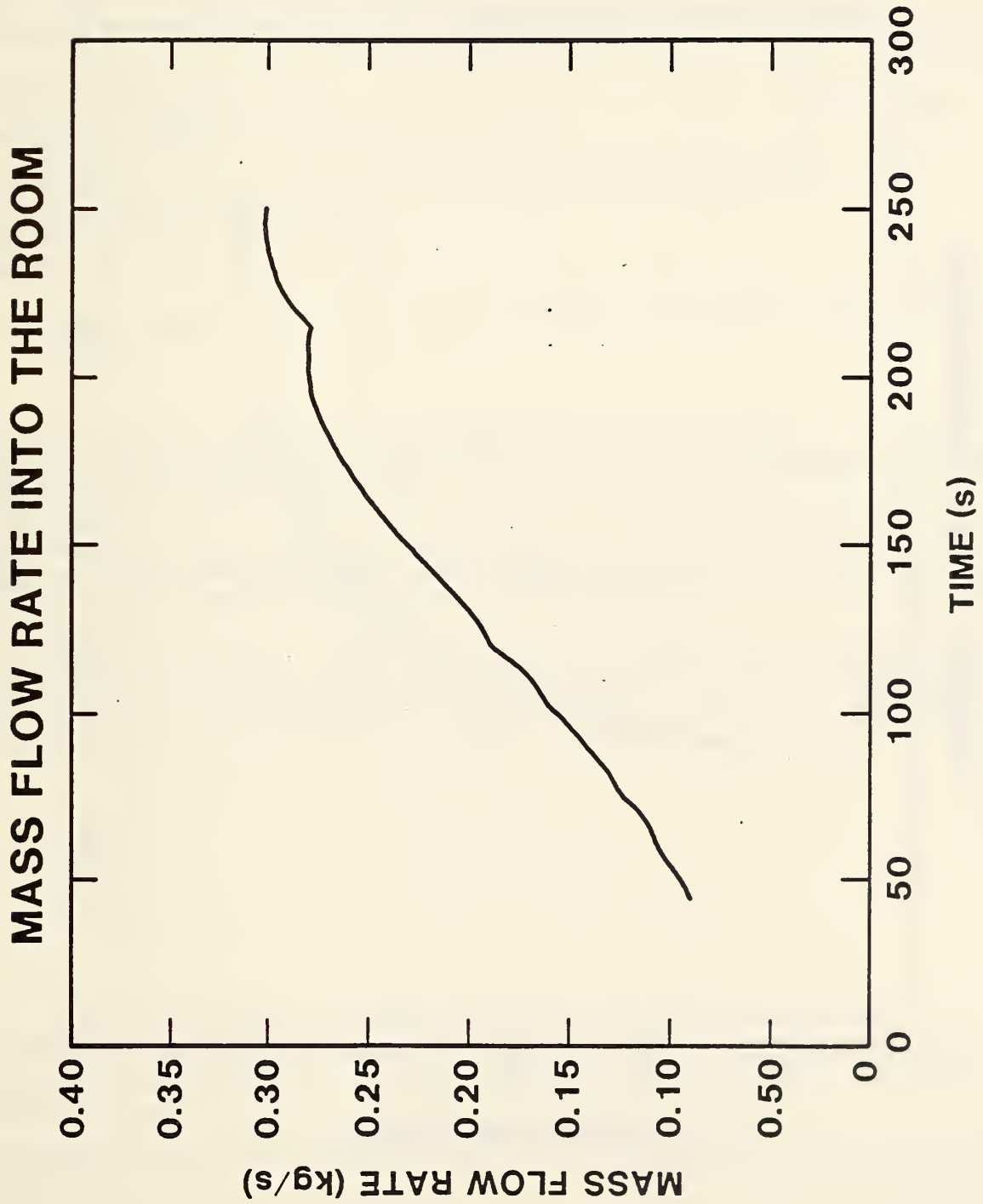


Figure E6. Mass Flow Rate into the Room for Fire Growth Example.

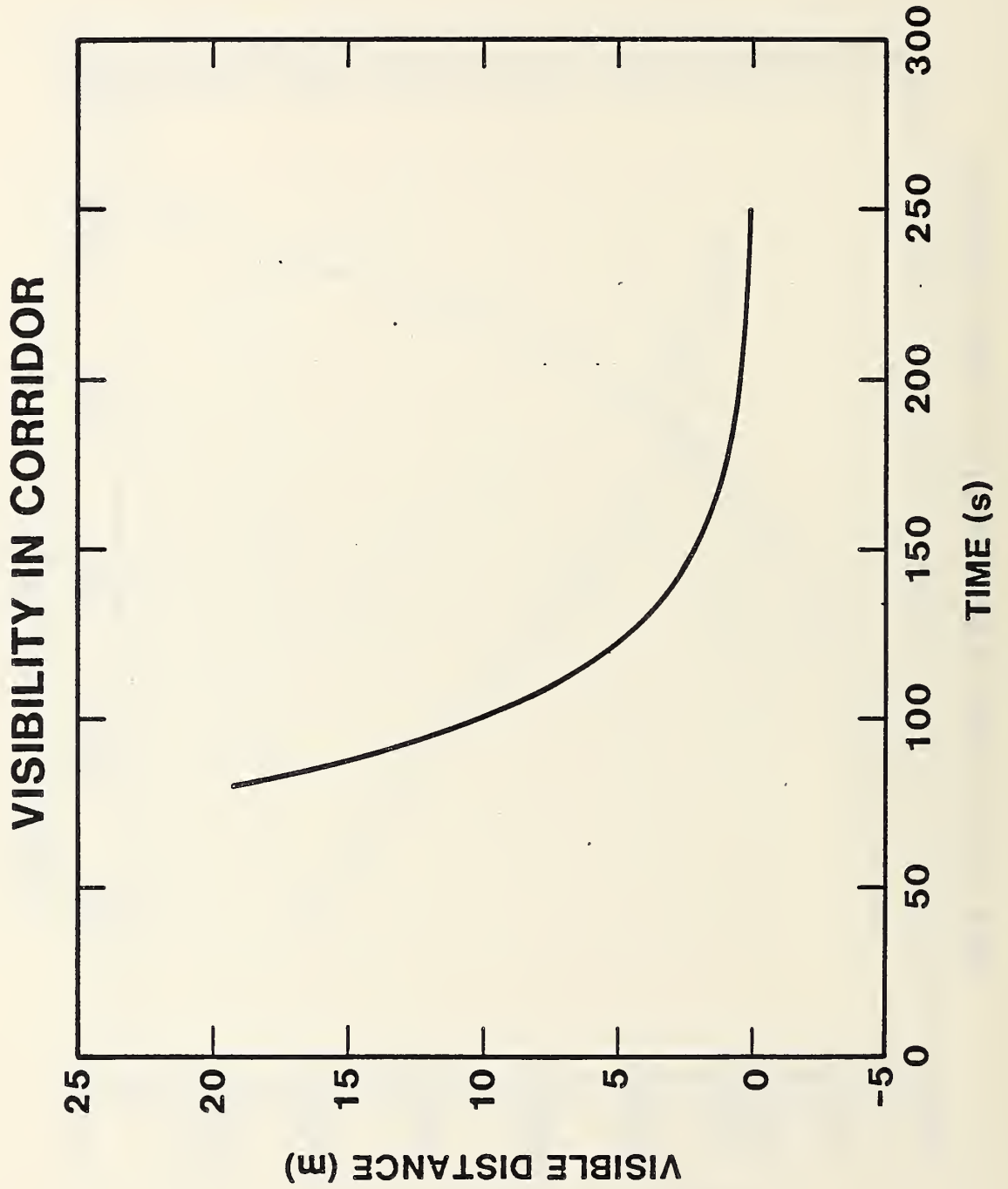


Figure E7. Visibility in Corridor for Fire Growth Example.

|  |  |   |   |
|--|--|---|---|
| U.S. DEPT. OF COMM.<br><b>BIBLIOGRAPHIC DATA SHEET</b><br><i>(See instructions)</i>  | <b>1. PUBLICATION OR REPORT NO.</b><br>NBSIR-85/3159 | <b>2. Performing Organ. Report No.</b>    | <b>3. Publication Date</b><br>June 1985       |
| <b>4. TITLE AND SUBTITLE</b><br>FIRE GROWTH IN COMBAT SHIPS  |  |   |   |
| <b>5. AUTHOR(S)</b><br>J. Quintiere, H. Baum and R. Lawson   |  |   |   |
| <b>6. PERFORMING ORGANIZATION</b> <i>(If joint or other than NBS, see instructions)</i><br><br><b>NATIONAL BUREAU OF STANDARDS</b><br><b>DEPARTMENT OF COMMERCE</b><br><del>WASHINGTON, D.C. 20234</del> Gaithersburg, MD 20899  |  | <b>7. Contract/Grant No.</b>              | <b>8. Type of Report &amp; Period Covered</b> |
| <b>9. SPONSORING ORGANIZATION NAME AND COMPLETE ADDRESS</b> <i>(Street, City, State, ZIP)</i><br>U.S. David Taylor Naval Ship<br>Research and Development Center<br>Washington, D.C.   |  |   |   |
| <b>10. SUPPLEMENTARY NOTES</b><br><br><input type="checkbox"/> Document describes a computer program; SF-185, FIPS Software Summary, is attached.  |  |   |   |
| <b>11. ABSTRACT</b> <i>(A 200-word or less factual summary of most significant information. If document includes a significant bibliography or literature survey, mention it here)</i><br><br>A discussion of fire phenomenology pertaining to ships is presented. It draws on background from ship fires, combat ship construction characteristics and scientific knowledge developed for building fires.<br><br>Its immediate goal is to assess the prospect of developing a deterministic (physics) model for ship fire growth as initiated by explosive weapon effects. A specific analysis of vented explosion flows is given as well as a procedure for computing fire growth phenomena from formulae. |  |   |   |
| <b>12. KEY WORDS</b> <i>(Six to twelve entries; alphabetical order; capitalize only proper names; and separate key words by semicolons)</i><br>Computation; explosions; fire damage; fire growth; fire models; room fires; shipboard fires.  |  |   |   |
| <b>13. AVAILABILITY</b><br><br><input checked="" type="checkbox"/> Unlimited<br><input type="checkbox"/> For Official Distribution. Do Not Release to NTIS<br><input type="checkbox"/> Order From Superintendent of Documents, U.S. Government Printing Office, Washington, D.C. 20402.<br><br><input checked="" type="checkbox"/> Order From National Technical Information Service (NTIS), Springfield, VA. 22161  |  | <b>14. NO. OF PRINTED PAGES</b><br><br>98 | <b>15. Price</b><br><br>\$11.50               |









